Design of the subsurface of land reclamations for freshwater storage and recovery
A new view on land reclamations

van Ginkel, Marloes

Citation (APA)
van Ginkel, M. (2019). *Design of the subsurface of land reclamations for freshwater storage and recovery: A new view on land reclamations*. [Dissertation (TU Delft), Delft University of Technology]. https://doi.org/10.4233/uuid:af7008fb-c8e2-42d4-b9da-c077366e59ac

Important note
To cite this publication, please use the final published version (if applicable).
Please check the document version above.

DESIGN OF THE SUBSURFACE OF LAND RECLAMATIONS FOR FRESHWATER STORAGE AND RECOVERY

A NEW VIEW ON LAND RECLAMATIONS

Dit proefschrift is goedgekeurd door de promotor:
Prof.dr.ir. T.N. Olsthoorn

Samenstelling promotiecommissie:

Rector Magnificus,	voorzitter
Prof.dr.ir. T.N. Olsthoorn	Technische Universiteit Delft, *promotor*

Onafhankelijke leden:

Prof.dr.ir. T.J. Heimovaara	Technische Universiteit Delft
Prof.dr.ir. S.N. Jonkman	Technische Universiteit Delft
Prof.dr.ir. C. van Rhee	Technische Universiteit Delft
Prof.dr.ir. L.C. Rietveld	Technische Universiteit Delft
Prof.dr. R.J. Schotting	Universiteit Utrecht
Dr. G. Houben	Bundesanstalt fur Geowissenschaften und Rohstoffe, Duitsland
Prof.dr.ir. H.H.G. Savenije	Technische Universiteit Delft, *reservelid*

SAMENVATTING

Tegenwoordig woont al meer dan de helft van de wereldbevolking in dichtbevolkte steden langs de kust en die steden groeien maar door. Dit zal ongetwijfeld leiden tot een toenemend aantal landaanwinningen in zee voor stadsuitbreidingen, industriële- of recreatiedoeleinden, havens en vliegvelden, zoals we dat nu al zien gebeuren. Voor de ontwikkeling van de leefomgeving op die landaanwinningen is zoet water een belangrijk aspect. Het grondwater is zout, in elk geval als het nieuwe land net is aangelegd, en zoet water kan niet altijd van het vasteland worden aangevoerd, omdat in veel megasteden al een zoetwatertekort dreigt als gevolg van verstedelijking en klimaatverandering. Daarom is ontzilting voor de meeste landaanwinningen het enige alternatief voor de watervoorziening, maar dit is duur en verbruikt veel energie.

In dit proefschrift is onderzocht hoe de ondergrond van landaanwinningen kan worden aangelegd, ingericht en gebruikt voor het vasthouden en terugwinnen van zoet water. Door de ondergrond te gebruiken om regenwater op te vangen en vast te houden, gezuiverd afvalwater opnieuw te gebruiken en zoetwatervoorraden aan te leggen, wordt de landaanwinning minder afhankelijk van wateraanvoer van het vasteland of van ontzilting. En dat is zeker in het licht van duurzaamheid en klimaatadaptatie belangrijk.

In de ondergrond van landaanwinningen is veel ruimte beschikbaar. Ondergrondse berging is aantrekkelijk vanwege het minimale ruimtebeslag aan maaiveld en omdat het onderhoudsvrij is, want in de bodem blijft de temperatuur constant en zijn er geen algen en insecten die het water kunnen vervuilen. Bovendien kan zoet grondwater het nieuwe land op een natuurlijke manier vergroenen, als het bereikbaar is voor planten en bomen. Deze voordelen zorgen ervoor dat ondergrondse zoetwaterberging de robuustheid van de watervoorziening en de kwaliteit van de leefomgeving op deze nieuwe landen in potentie versterkt.

Grondwater in landaanwinningen staat in direct contact met de zee en is daardoor in principe zout. Van nature kan in sommige eilanden en duingebieden een ondergrondse zoetwaterbel drijvend op het zoute grondwater ontstaan. De natuurlijke ontwikkeling van zo'n zoetwaterlens kost echter vele tientallen jaren en vraagt om een constante zoetwater aanvulling. Zoet water kan ook op een kunstmatige manier door middel van putten in een zout watervoerend pakket worden gepompt, tijdelijk geborgen en later teruggewonnen. Deze opslagtechniek wordt bijvoorbeeld toegepast door de

drinkwaterbedrijven in de Nederlandse duinen en door de tuinbouw in het Westland.

Natuurlijk is de terugwinbaarheid van het zoete water essentieel voor de haalbaarheid van ondergrondse berging. In de bodem komt het zoete water onvermijdelijk in contact met zout grondwater en het is de uitdaging om te voorkomen dat het zoete water door menging met zout water en opdrijven als gevolg van het dichtheidsverschil tussen zoet en zout water niet meer terugwinbaar is.

In de praktijk en de wetenschappelijke literatuur wordt de terugwinbaarheid van zoet water in zout grondwater tot nu toe gestuurd door operationele factoren, zoals het geïnjecteerde en teruggewonnen volume, putlocaties en -configuraties, onttrekkingsdebiet en opslagtijd. De fysische eigenschappen van het watervoerende pakket, die ook de terugwinbaarheid beïnvloeden, zoals porositeit, doorlatendheid en dikte van het watervoerend pakket, worden als vaststaand gezien. Nieuw voor landaanwinningen ten opzichte van natuurlijke ondergrond, is dat de fysische eigenschappen onderdeel uitmaken van het ontwerp van de landaanwinning. Daardoor ontstaan mogelijkheden om menging en opdrijven beter in de hand te houden en zo een hogere terugwinbaarheid te halen.

In dit proefschrift is onderzocht hoe de ondergrond van landaanwinningen kan worden ontworpen, ingericht en gebruikt voor het vasthouden en terugwinnen van zoet water. Ten eerste zijn een drietal concepten ontwikkeld om de menging en het opdrijven van zoet water in een zout watervoerend pakket beter in de hand te houden, namelijk:
1. De eigenschappen van kunstmatig aangelegde watervoerende pakketten waarmee menging, opdrijven en voorkeursstroming worden beperkt;
2. Ondergrondse verticale barrières van een beperkte diepte, waardoor het zoetwatervolume zich niet in horizontale richting kan uitspreiden en de voorraad zich sneller kan opbouwen;
3. Zoutwateronttrekking van onder de zoetwatervoorraad, waarmee het opdrijven van het zoetwatervolume wordt gecompenseerd.

Ten tweede is inzicht verkregen in de heterogeniteit en doorlatendheid van vijf landaanwinningen die door middel van de wereldwijd meest toegepaste plaatsingsmethoden zijn aangelegd, namelijk: dumpen, rainbowen en walpersen.

Met behulp van een numeriek model werd een terugwinbaarheid van 65% in de eerste opslag-terugwin-cyclus oplopend tot 90% in volgende cycli berekend als zoet water wordt opgeslagen en teruggewonnen uit een deel van een zout watervoerend pakket dat wordt afgeschermd door ondergrondse barrières. Zonder ondergrondse barrières, kan de terugwinbaarheid worden verhoogd als het zout watervoerend pakket is opgebouwd uit dunne horizontale lagen. In beide gevallen is het verstandig om horizontale of verticale putten en putfilters en infiltratiebedden mee te nemen bij de aanleg van het nieuwe land, omdat je dan werk met werk kan maken.

Een praktische manier om de terugwinwaarheid van zoet water in een zout watervoerend pakket te optimaliseren, is door het te combineren met de onttrekking van zout grondwater van onder het opgeslagen zoet water. Deze manier is vooral handig als er ook zout water voor ontzilting nodig is. Met behulp van een numeriek model werd voor deze opslagmethode een terugwinbaarheid van 70% in de eerste opslag-terugwin cyclus oplopend tot 80% in volgende cycli berekend.

De landaanwinningen Maasvlakte II in Nederland, Palm Jumeirah in Dubai, de haven van Hong Kong en de vliegvelden van Singapore en Hong Kong zijn aangelegd door een combinatie van dumpen, rainbowen en walpersen. Uit de analyse in dit proefschrift blijkt dat al deze plaatsingsmethoden tot een bepaalde mate van heterogeniteit leiden door verschillen in de segregatie van de zandkorrels per plaatsingsmethode, waardoor de doorlatendheid van landaanwinningen niet constant is. De segregatie varieert ook binnen een plaatsingsmethode; dit komt door locatie specifieke omstandigheden, zoals de sedimentatiediepte, de korrelverdeling en de hoekigheid van de korrels. Hoewel landaanwinningen dus niet homogeen zijn, blijkt uit de analyse dat de bodemopbouw van nieuw land wel veel voorspelbaarder is dan van natuurlijke bodems, en bovendien komen verstorende kleilaagjes niet voor, omdat alleen maar zand wordt toegepast.

De conclusie van dit proefschrift is dat landaanwinningen die zijn gemaakt van zand door middel van dumpen, rainbowen en walpersen geschikt zijn voor het vasthouden en terugwinnen van zoet water en dat menging en opdrijven van zoet water in zout watervoerende pakketten in de hand kan worden gehouden door middel van ondergrondse barrières en horizontale gelaagdheid en door combinatie met zoutwater onttrekking van onder de zoetwatervoorraad.

In toekomstige landaanwinningen kunnen verschillende uitkomsten van deze studie worden gecombineerd; vooral de combinatie van berging tussen ondergrondse barrières en zoutwater onttrekking van onder de zoetwater voorraad lijkt een relatief eenvoudige manier om een goed terugwinbare voorraad zoet water in nieuwe landaanwinningen te ontwikkelen. Het groeiende aantal landaanwinningen dat wereldwijd wordt aangelegd om de verstedelijking en economische ontwikkeling in kustgebieden op te vangen, waarvoor een robuuste zoetwatervoorziening moet worden gewaarborgd, maakt de resultaten van dit proefschrift breed toepasbaar.

SUMMARY

Today, more than half of the world's population already lives in densely populated megacities along coasts and these cities are still growing. This will undoubtedly lead to an increasing number of seaward expansions for residential, industrial and recreational development, ports and airports, which we already see happening today. Fresh water is an important aspect for the development of such new lands, because groundwater is saline, at least initially, and fresh water cannot always be supplied from the mainland, simply because many coastal megacities already suffer from increasing freshwater shortages due to urbanisation and ongoing climate change. This leaves desalination as only alternative for the freshwater supply of most land reclamations, but this technique is expensive and highly energy consuming.

This thesis examines how the subsurface of land reclamations can be optimally designed, created and operated for the storage and recovery of fresh water. The land reclamation becomes less dependent on supply from the mainland or desalination when rainwater in collected and retained, waste water is treated and reused, and freshwater storage capacity is build up on the new land. This is profoundly important in the light of sustainability and climate adaptation.

A lot of space is freely available in the subsurface of land reclamations. The almost zero footprint above ground and its conserving qualities both with respect to evaporation and water quality make subsurface storage of fresh water attractive. Moreover, fresh groundwater, if accessible to plants and trees, will immediately enhance the image of the new land in a natural way. All these benefits ensure that subsurface freshwater storage and recovery potentially increases the robustness of the water supply and the quality of life on these new lands.

Groundwater in land reclamations is directly connected to the sea and is, therefore, saline. In oceanic islands and dune areas, a subsurface freshwater lens floating on saline groundwater can develop in a natural way. The natural development of such a freshwater lens, however, takes many decades and requires a constant inflow of fresh water. Fresh water can also be infiltrated and recovered in saline aquifers by means of groundwater wells. This technique is e.g. applied by the Dutch drinking water companies as well as by agri- and horticulturists.

The feasibility of subsurface freshwater storage and recovery requires a high freshwater recovery efficiency, which is at risk because the injected fresh water will inevitably come into contact with saline groundwater present in the subsurface of the land reclamation. The challenge is to prevent that the freshwater recovery efficiency is impacted by mixing with salt water and by buoyancy caused by the density difference between fresh and salt water.

In practice as well as in scientific literature, the recovery of fresh water in saline groundwater has always been controlled by operational factors, such as injected and recovered volume, location of injection and recovery wells, recharge rates and storage duration. However, the physical properties of the aquifer that also influence the recovery efficiency, like porosity, hydraulic conductivity and aquifer thickness, have always been considered as fixed and site-specific. New for land reclamations compared to natural soils is that these physical properties become part of the design of land reclamations, and, therefore, this creates opportunities to better manage mixing and buoyancy to reach high recovery efficiencies.

This thesis examines the design, creation and operation of the subsurface of land reclamations for freshwater storage and recovery. Firstly, three concepts have been identified that allow managing the mixing and density stratification of a freshwater volume in saline aquifers. These are:
1. The properties of these man-made aquifers that reduce mixing and density stratification;
2. Vertical flow barriers of limited depth that prevent the volume of fresh water from expanding radially, speeding up the formation of the freshwater stock;
3. Saltwater extraction from below the freshwater stock, which prevents the freshwater volume from floating up by counteracting buoyancy.

Secondly, insight has been given in the internal structure of the porous media and its hydraulic properties of five land reclamations that were constructed by the most commonly applied placement methods, i.e., bottom dumping, rainbowing and pipeline discharge.

Numerical modelling showed that freshwater recovery rates are on the order of 65% in the first storage-recovery cycle, rising to as much as 90% in subsequent cycles when fresh water is stored and recovered from a saline aquifer bounded by installed vertical flow barriers. Without flow barriers, the freshwater recovery efficiency may be raised when creating an aquifer with horizontal layering. In both cases, the storage and recovery can be fine-tuned by horizontal or vertical wells and infiltration beds and it is recommended to include those wells and infiltration beds when constructing the new land.

A practical way to achieve high freshwater recovery efficiency in a saline aquifer is to combine it with saltwater extraction from below the stored fresh water. This method is especially useful if salt water for desalination is also required. Numerical calculations suggest that freshwater recovery rates of up to 70% are then achievable in the first cycle increasing to 80% in subsequent ones.

The land reclamations Maasvlakte II in the Netherlands, Palm Jumeirah in Dubai, and the airports of Singapore and Hong Kong have been constructed by a combination of bottom dumping, rainbowing and pipeline discharge. It was found that all placement methods lead to some degree of heterogeneity, so that the hydraulic conductivity is not uniform in new lands constructed by these placement methods. This is a consequence of the extent of segregation of grains pertaining to each placement method. Segregation also varies within a specific placement method due to its characteristics and site-specific circumstances such as settling depth, grain-size distribution and angularity resulting from grain type. Even though heterogeneity exists in land reclamations, it is shown that it is still more predictable than that of natural soils and, moreover, disturbances, such as clay layers, do not occur because only sand is used.

The conclusion of this dissertation is that land reclamations constructed of sand by bottom dumping, rainbowing and pipeline discharge are generally suitable for subsurface storage and recovery of fresh water and that the mixing and density stratification of fresh water stored in saline aquifers can successfully be controlled by the application of flow barriers or the construction of horizontal layering in the soil structure, and by combination of freshwater storage with saltwater extraction during operation.

Several outcomes of this study can be combined in future land reclamations; especially the combination of freshwater storage between flow barriers and salt water extraction from below the stored volume seems a relatively simple way to develop a recoverable freshwater volume in future land reclamations. The increasing number of land reclamations that result from the ongoing worldwide urbanisation of coastal areas, for which a robust freshwater supply must be guaranteed, make the results of this thesis widely applicable.

CONTENTS

CHAPTER 1 INTRODUCTION

1.1 Rationale

Over recent decades, land reclamations have been constructed worldwide. This thesis examines how the subsurface of land reclamations can be designed, created and operated for the storage and recovery of fresh water. Land reclamations are defined in this thesis as man-made artificial islands constructed in the coastal zone by bringing together large volumes of sand dredged from the seafloor (Figure 1). The most well-known examples are probably Palm Jumeirah and the islands of the World Archipelago in Dubai, the United Arab Emirates.

Today, half of the world's cities with more than one million people are sited in coastal areas (United Nations 2010) and these coastal megacities exhibit high rates of population growth and urbanisation (Neumann et al. 2015; Merkens et al. 2016) so that they are constantly expanding. Population growth, urbanisation and economic development put high pressure on the available space in these megacities and options for urban expansion in the hinterland have mostly already been used. Therefore, there is a growing tendency for urban expansion in seaward direction by means of land reclamation. Examples are Changi airport in Singapore (Malaysia), Eko Atlantic in the city of Lagos (Nigeria), Chek Lap Kok airport in Hong Kong (China), Maasvlakte II in the Port of Rotterdam (the Netherlands), and those that are currently under construction in Jakarta Bay (Indonesia) and planned in Manilla (the Philippines). In coming years, more coastal megacities will undoubtedly expand by means of land reclamation for residential, industrial and recreational development, ports and airports.

Figure 1: Schematisation of a land reclamation.

Fresh water is an important aspect for the development of land reclamations in the ocean. Freshwater demand on these new lands includes water for domestic and industrial purposes, flora and fauna, irrigation, dry bulk dust prevention or even the periodic testing of firefighting facilities. Because land reclamations are constructed in the ocean, there is no fresh water available and the groundwater is as saline as seawater, at least immediately following construction. Therefore, fresh water is mainly supplied by pipelines from the mainland or by desalination of seawater. The proportion of natural water resources on land reclamations, such as rainwater and fresh groundwater, often remains limited over time. This is because buildings and paved infrastructure typically cover a high percentage of land, which limits groundwater recharge and rainwater harvesting, even on reclamations in moderate or tropical climates with considerable rainfall.

However, freshwater cannot always be supplied from the mainland due to an already high and continuously growing pressure on available freshwater resources in the hinterland. Over-exploitation on the mainland has already led to severe depletion of groundwater resources due to which many coastal megacities struggle with soil subsidence caused by dehydration of soft clay and peat soils. In addition, the rivers that pass these cities are generally so polluted that they do not qualify as source of drinking water. Even if water resources on the mainland are sufficient now, water shortages will likely arise in the future because of climate change (IPCC 2013) causing temperature increase, sea level rise, longer periods of drought and more intense rainfall that makes this resource harder to capture.

This leaves seawater desalination as only alternative for the freshwater supply of most land reclamations. It is reliable from the perspective that it makes land reclamations self-supporting; i.e., not dependent on supply from the mainland. The downside, however, is that it is very costly to build and operate desalination plants, and that they require high amounts of energy while the disposal of brine and chemical waste are other complications. Furthermore, operation is complex in polluted environments.

The drawbacks of both piped and desalinated water can be overcome by collecting and retaining rainwater, reusing treated wastewater and creating freshwater storage capacity on the new land. Moreover, such storage is essential to counter emergency situations and balances out fluctuations in demand and supply as well as in energy consumption. Storage capacity can be

achieved by aboveground storage tanks, or by underground storage in which fresh water is injected and recovered by groundwater wells. The latter is known as Aquifer Storage Recovery (ASR, Pyne 1995) or Managed Aquifer Recharge (Dillon et al. 2006) and promises potential for land reclamations.

The possibilities for storage above ground are minimal, due to the high land prices and the high costs involved with aboveground storage tanks. Subsurface storage, on the other hand, has a minimal footprint above ground and utilizes the large space that is available in the subsurface of the land reclamation. In addition, these systems only require little maintenance and they do not harbour mosquitos or cause algae blooms and the water has a constant temperature in the absence of evaporation and sunlight (e.g., Pyne 1995; Dillon et al. 2006). If the fresh groundwater table is shallow, subsurface freshwater storage and recovery also forms a 'natural' freshwater resource for vegetation and thus becomes an alternative for drip irrigation. Considering these advantages, subsurface freshwater storage and recovery, therefore, has great potential to add value to the robustness of the water supply and the quality of life on land reclamations.

In oceanic islands and dune areas, a freshwater lens can develop in a natural way by the combination of the density difference between fresh and salt water, gravity and Darcy's Law. Badon Ghijben (1889) and Herzberg (1901) were the first to describe the physics of a freshwater lens (Figure 2).
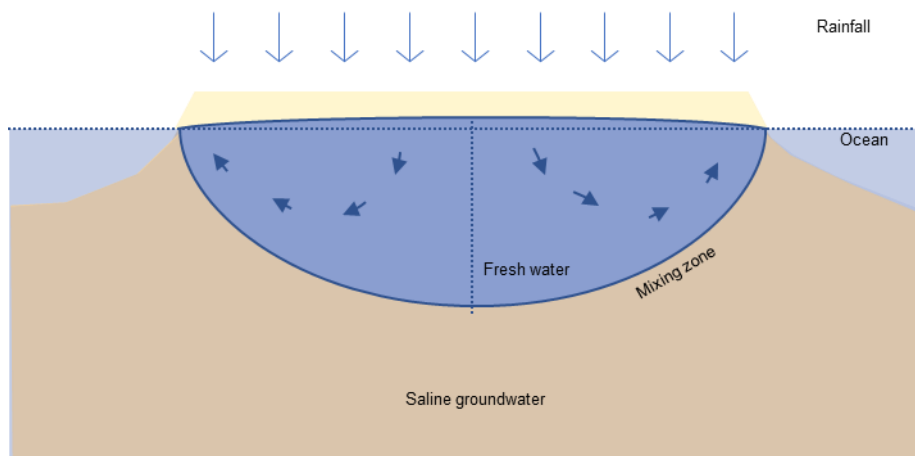

Figure 2: A freshwater lens in an oceanic island under natural conditions.

The so-called Ghijben-Herzberg principle (e.g., Bear 1979) describes the position of the interface between fresh and saline groundwater. It states that the depth of the fresh-salt interface below mean sea level is about 40 times the piezometric head with respect to mean sea level, for normal ocean water having a density of 1025 kg/m^3. The natural development of a freshwater lens takes many decades and requires a constant inflow of fresh water. Fresh water can also be infiltrated and recovered in saline aquifers by means of groundwater wells.

In reclaimed lands below sea level, so-called polders, shallow rainwater lenses can develop during the rainy season (De Louw et al. 2011; Eeman et al. 2011; Eeman et al. 2012; De Louw et al. 2013). Such shallow rainwater lenses are local miniatures of Badon-Ghijben Herzberg lenses due to continuous upward seepage of saline water into the polder. This dissertation only looked at reclaimed islands because of their much larger potential subsurface freshwater storage capacity with respect to polders.

The freshwater recovery efficiency is considered critical to the feasibility of subsurface freshwater storage and recovery. The injected fresh water will inevitably come into contact with saline groundwater in the land reclamation. One aspect is its mixture with salt water and the second aspect is how its flow is influenced by the denser salt water. The lower density fresh water is forced to the top of the aquifer where it spreads out in a layer that becomes too thin to recover (Figure 3). Mixing and density stratification can both negatively influence the recovery efficiency, defined as the ratio between injected and recovered fresh water (e.g., Lowry and Anderson 2006; Ward et al. 2007; Bakker 2010).

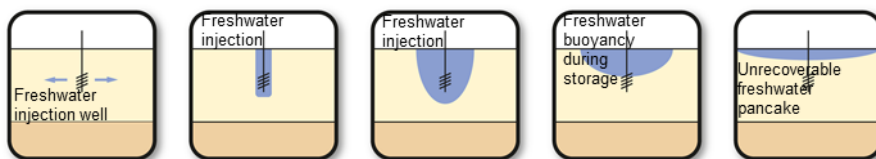Figure 3: Density stratification of a volume of fresh water injected in a saline aquifer over time; the freshwater volume floats up to the top of the aquifer and spreads out.

The recovery efficiency is controlled by the physical properties of the aquifer, well design and operation. In practice as well as in the scientific literature, the physical properties of potential storage-recovery sites, like porosity, hydraulic

conductivity and aquifer thickness, are so far regarded as fixed, predefined, site-specific conditions (e.g., Merritt 1986; Dillon et al. 2006; Lowry and Anderson 2006; Misut and Voss 2007). The steering parameters to control the recovery efficiency are then limited to operational factors, such as injected and recovered volume, location of injection and recovery wells, recharge rates and storage duration (e.g., Pyne 1995; Maliva and Missimer 2010; Zuurbier et al. 2014; Ward et al. 2009; Bakker 2010). However, the physical limitations can be overcome for subsurface freshwater storage and recovery in land reclamations.

Land reclamations are designed from scratch, which implies that the properties of the new aquifer are part of the design and construction and can, therefore, be optimized to control mixing and density stratification of subsurface freshwater storage and recovery, at least to some extent. As such, specific sediment types and placement techniques can be selected and applied to obtain the desired porosity, hydraulic conductivity and layering. Subsurface structures can also be incorporated to better manage mixing and density stratification and facilitate recovery. It is expected that taking advantage of the possibilities of such an a priori design will result in significant higher recovery efficiencies as compared to an ASR in a natural aquifer of similar salinity, thickness and average grain size.

1.2 Aim and method

Worldwide, land reclamations are constructed for the urban expansion of coastal megacities and freshwater supply plays an important role in their sustainable development, especially in the light of climate change and depletion of natural water resources in the hinterland. It is expected that these new lands in the ocean are suitable for subsurface freshwater storage and recovery and that the design from scratch and construction offer opportunities to not only manage mixing and buoyancy operationally, but also create physical properties of the subsurface to reach high recovery efficiencies.

This thesis, therefore, examines how the subsurface of land reclamations can be optimally designed, created and operated for freshwater storage and recovery. However promising, the incorporation of subsurface freshwater storage and recovery has not yet been considered in the design of land reclamations.

This is partly due to lack of knowledge about the optimal aquifer properties for freshwater storage and recovery in a saline environment. Therefore, three concepts have been identified in this thesis that allow managing the mixing and density stratification occurring along with freshwater storage and recovery in saline aquifers. These are:

1. The properties of these man-made aquifers that reduce mixing and buoyancy and preferential flow (Chapter 2).
2. Vertical flow barriers of limited depth that prevent the volume of fresh water from expanding radially, speeding up the formation of the freshwater stock (Figure 4, Chapter 3).
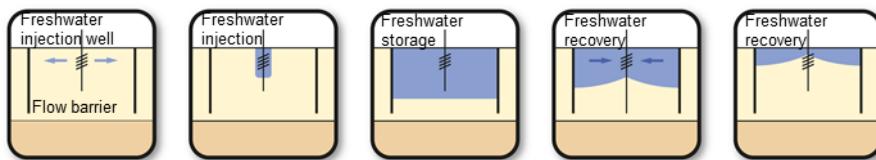
Figure 4: Schematisation of freshwater storage and recovery between flow barriers in a saline aquifer.

3. Saltwater extraction from below the freshwater stock, which prevents the freshwater volume from floating up by counteracting buoyancy (Figure 5, Chapter 4).
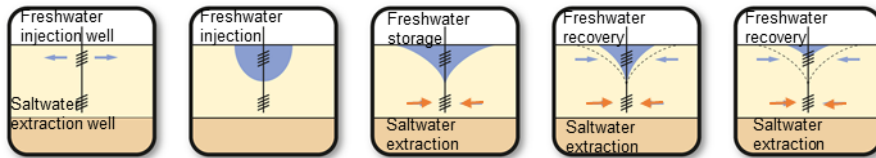
Figure 5: Schematisation of freshwater storage and recovery in combination with a saltwater extraction well.

A second reason why subsurface freshwater storage and recovery has not yet been considered in the design of land reclamations is because little is known about the aquifer properties that can be created. Dredging techniques have been studied intensively (e.g., Mastbergen and Bezuijen 1988, Sladen and Hewitt 1989; Lee et al. 1999; Lee 2001; Chang et al. 2006; Lees et al. 2012; Van 't Hoff and Van der Kolff 2012), but these studies have mainly focused on geotechnical aspects that are related to bearing capacity and risk of liquefaction while properties such as hydraulic conductivity have not yet been considered in detail.

In the hydrological studies considering the increase of the freshwater volume under adjacent old land caused by land reclamations in Hong Kong, China and along the Dutch North Sea coast (the *Zandmotor*), Jiao et al. (2001; 2006) and Huizer et al. (2017), for instance, applied a constant porosity and conductivity for the land reclamation. Only Chua et al. (2007) specifically addressed the hydraulic properties of a land reclamation in Singapore.

Average conductivity values may be sufficient to determine external hydrological effects of land reclamations. However, more detailed information is required if land reclamations are to be considered for water storage as part of their freshwater supply. Therefore, Chapter 5 of this thesis provides insight in the internal structure of the porous media and its hydraulic properties of different land reclamations that were constructed by bottom dumping, rainbowing and pipeline discharge.

Lastly, the design and construction of land reclamations has hitherto been completely separated from that of the water supply required for the future development of these new lands. Dredging engineers have always focused on meeting the geotechnical requirements that are related to bearing capacity and risk of liquefaction for the lowest costs of construction, without responsibility for later water supply; water engineers who appear later, then have to deal with the land as it was constructed. This thesis, therefore, tries to close the gap between dredging and water engineers to achieve a more sustainable water supply on future land reclamations using their subsurface for freshwater storage and recovery.

1.3 Outline

The flow chart in Figure 6 depicts the structure of this thesis and the research questions that are discussed in the subsequent chapters. The following paragraphs provide an overview of the subsequent chapters.

Chapter 2 provides an overview of the aquifer properties influencing the recovery efficiency of fresh water stored in saline aquifers. Based on this review, Chapter 2 presents the properties of man-made saline aquifers that reduce mixing, buoyancy and preferential flow by discussing three designs: 1) a storage system completely separated from its environment, 2) a partly open system bounded by flow barriers, and 3) an open system in an aquifer with high vertical anisotropy.
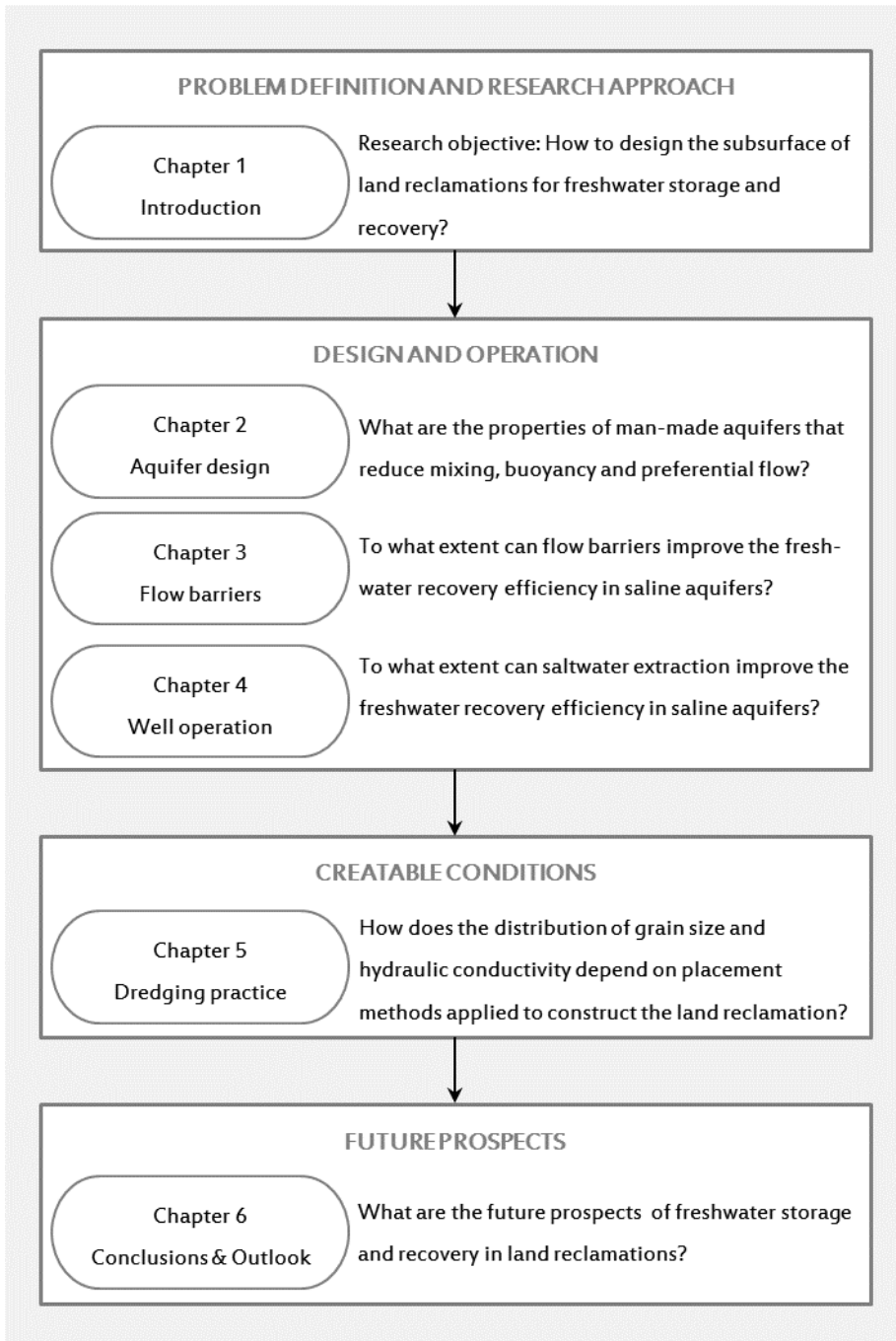
Figure 6: Thesis structure.

As shown in Chapter 2, flow barriers that partly penetrate a saline aquifer have a positive influence on the recovery efficiency, as they prevent a volume of fresh water stored between these barriers from expanding radially. Chapter 3 provides insight in how flow barriers influence groundwater flow within the storage zone and mixing between fresh and saline water. Chapter 3 presents the results of a sand-tank experiment and numerical modelling (SEAWAT in the *mfLab* environment) aimed at quantifying the effect that flow barriers have on the groundwater flow and on mixing between fresh and saline water for different phases of storage and recovery.

One operational paradigm to keep a volume of fresh water stored in a saline aquifer in place is by continuous saltwater extraction from below the stored volume of fresh water. Chapter 4 provides insight in the required saltwater extraction from below the freshwater stock to prevent the freshwater volume from floating up by counteracting buoyancy for different phases of storage and recovery. In Chapter 4, an analytical solution is derived that quantifies the required saltwater discharge to keep a given volume of fresh water in place. Numerical modelling (SEAWAT in the *mfLab* environment) is applied to determine how much fresh water can be recovered.

While the previous chapters focused on preferable design and operational conditions for freshwater storage and recovery in land reclamations, Chapter 5 focuses on what is creatable within current dredging practice. This chapter presents an overview of the most commonly applied placement methods: 1) bottom dumping, 2) rainbowing and 3) pipeline discharge. The distributions of grain sizes and resulting hydraulic conductivities are derived for each placement method and are subsequently validated by comparison with semi-variograms of cone-penetration tests from five existing land reclamations: Maasvlakte II (Rotterdam, the Netherlands), Palm Jumeirah (Dubai, the United Arab Emirates), Changi Airport (Singapore, Malaysia), Chep Lap Kok and West Kowloon (both in Hong Kong, China).

Chapter 6 concludes that land reclamations constructed of sand by bottom dumping, rainbowing and pipeline discharge are generally suitable for subsurface storage and recovery of fresh water and that, next to the operations, also flow barriers and horizontal layering in the soil structure can be applied in the construction of land reclamations to better manage mixing and buoyancy and so reach high recovery efficiencies. Chapter 6 discusses the implications and further research perspectives. The dissertation concludes with the

prospects for future land reclamations in which various outcomes of this thesis can be combined to support the freshwater supply through subsurface storage and recovery.

CHAPTER 2 AQUIFER DESIGN FOR FRESHWATER STORAGE AND RECOVERY IN LAND RECLAMATIONS

2.1 Chapter introduction

As was explained in the Introduction, the purpose of this thesis is to examine how the subsurface of land reclamations can be optimally used for freshwater storage and recovery, by evaluating the physical properties and operational parameters that are preferable for freshwater storage and recovery in saline aquifers. As a first step, this chapter qualitatively explores the preferable aquifer conditions that reduce mixing, buoyancy and preferential flow of freshwater stored and recovered in a saline aquifer.

While freshwater storage and recovery is nowadays widely applied in saline aquifers for seasonal or emergency water storage, one would expect a lot of thought to be devoted to what the preferable aquifer conditions are. As Section 2.2 explains, however, this appears not to be the case. The most relevant research determining preferable aquifer conditions for freshwater storage and recovery focused on the influence of aquifer properties on the recovery efficiency of wells, but not on optimal conditions in general. Section 2.2 provides an overview of the general outcomes of these studies and presents the rationale for the study. Three artificial aquifer designs are discussed in the following sections. Considering what optimal conditions for freshwater storage and recovery would be, one might initially think of a storage system completely separated from its environment. Section 2.3, however, lists several drawbacks of a completely separated storage system. Alternative aquifer designs are presented in Sections 2.4 and 2.5: a partly open system bounded by flow barriers (Section 2.4) and an open system with high vertical anisotropy (Section 2.5). Based on the discussion of the three artificial aquifer designs, the general requirements of the subsurface for freshwater storage and recovery in saline environment are presented in Section 2.6.

2.2 The influence of aquifer properties on the freshwater recovery efficiency

Artificial recharge of water to an aquifer for later recovery and use, otherwise known as artificial storage and recovery (ASR; Pyne 1995), is nowadays widely applied for seasonal or emergency water storage. Therefore, one would expect a lot of thought to be devoted to what the optimal aquifer conditions for ASR would be, but this does not appear to be the case.

In some situations, local hydrogeology may impact the selection of ASR sites; however, according to Pyne (1995), this is the exception rather than the rule since ASR wells are usually located where they provide the greatest benefit to the water utility or agency. This location is often near the supply area to reduce the costs and time of transportation. At that specific site, one deals with the existing local hydrogeology through well design and construction (e.g., Maliva and Missimer 2010; Zuurbier et al. 2014) and operation (Ward et al. 2009; Bakker 2010). The screening tool of Bakker (2010) is applied in Chapter 3 to assess the recovery potential of a freshwater storage system.

In line with Pyne's field experience, Lowry and Anderson (2006) distinguished physical properties of the aquifer and operational factors that control the recovery efficiency of ASR. Properties like porosity, hydraulic conductivity, aquifer thickness and density of native water, as well as quality, are regarded as predefined site-specific conditions, while operational factors such as injected volume, location of injection and recovery wells, recharge and recovery rates and storage duration, can be changed at the wellhead by the operator to optimize the ASR system.

The most relevant research determining optimal aquifer conditions for ASR focused on the influence of aquifer properties on the recovery efficiency of ASR wells. These studies are, firstly, comparisons between ASR sites, such as the studies executed by e.g., Merritt (1986), Dillon et al. (2006), Lowry and Anderson (2006) and Misut and Voss (2007). On the other hand, there are theoretical considerations regarding dimensionless parameter groups in analytical solutions, as described by e.g., Esmail and Kimbler (1967), Ward et al. (2007, 2008, 2009) and Bakker (2010). The general outcomes of these studies indicate that porosity, hydraulic conductivity, vertical anisotropy, dispersivity, density of native water versus that of the injected water, and the thickness of the aquifer all influence the recovery efficiency. This makes sense

because these aquifer properties determine the degree of the underlying recovery efficiency processes of mixing and density stratification.

The question of which aquifer conditions are preferable for ASR is usually not relevant in practice because the costs of the required earth displacement and construction works are so high that they generally outweigh the economic benefits of ASR systems. However, the situation is different in the case of land reclamations that are currently being constructed worldwide. Aquifers are, in fact, created in these projects and their conditions can be optimized for specific ASR applications. Specific sediment types may be chosen, and different dredging techniques can be applied to create the optimal aquifer conditions for recharge and recovery in terms of porosity, conductivity, anisotropy, and dispersivity to control mixing processes and density stratification.

Three artificial aquifer designs are discussed in this chapter. The aim is to make readers aware that aquifers are created while constructing land reclamations and that this provides opportunities for ASR. This perspective may change the way we look at the optimal hydraulic properties of land reclamations.

2.3 Artificial aquifer design 1: Complete separation of the storage zone from its environment

Considering what optimal conditions for ASR would be, one might initially think of a design as presented in Figure 7 in which the stored water is completely separated from the surrounding groundwater system. In artificial aquifer design 1, vertical walls of impermeable material such as clay or sheet piles along the storage zone and a confining layer at the bottom prevent interaction with lower quality ambient water or water with a different density. Water infiltrates at the top and seeps through the storage zone. The water is recovered through horizontal wells from a layer of gravel at the bottom. This layer has a relatively high hydraulic conductivity, thus allowing an evenly distributed lowering of the water table, which results in a relatively quick recovery, also from the outer regions of the storage zone.

On further consideration, however, the continuous alteration between anaerobic and aerobic conditions could well result in internal contamination of e.g., iron and manganese precipitates resulting in clogging. Whether these reactions will occur in practice, is highly dependent on the aquifer material and

nutrients in the injection water. The wells at the bottom of the storage zone are also practically inaccessible for maintenance and replacement. Finally, the design is expected to be costly and it will be difficult to completely guarantee that the vertical walls and the confining layer at the bottom will be sufficiently impermeable. Seepage of poor-quality water through the impervious walls could pollute the stored water with little chance to clean it other than complete replacement of the fill.
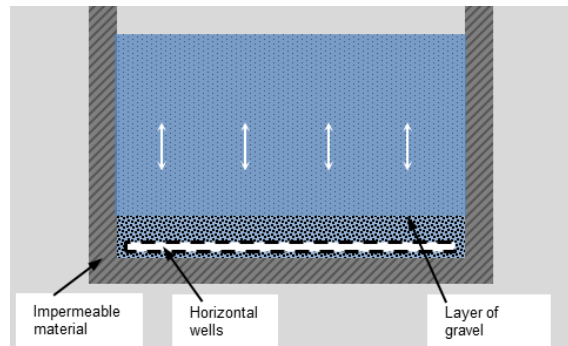
Figure 7: Artificial aquifer design 1: the storage zone is completely separated from the surrounding groundwater system through vertical walls and a confining bottom layer.

It thus appears that complete separation of the storage zone from its environment is not as optimal as perhaps initially thought. Solutions to clogging are, firstly, the prevention of alternating anaerobic and aerobic conditions, secondly, the choice of aquifer material and the separation of different sediment types, and, thirdly, regular flushing of the system. The latter requires the stored water to be in open communication with the surrounding groundwater system. The construction of a partly open ASR system will be simpler and cheaper compared to artificial aquifer design 1. However, the injected water will inevitably come into contact with native groundwater, which is generally saline water in land reclamations. Mixing and density stratification will occur, and the question arises as to how the aquifer should be designed such that injected water can be kept both in place and separated from ambient water. In the remainder of this chapter, that question is discussed with the help of two potential artificial aquifer designs.

2.4 Artificial aquifer design 2: Partly open system bounded by flow barriers

Consider an unconfined saline aquifer of which a certain part is surrounded by vertical impermeable walls that partly penetrate the aquifer (Figure 8). When fresh water is infiltrated between the flow barriers, the density difference between the two water types causes the lighter freshwater to float on top of denser saline groundwater; the mixing zone separates the two fluids. Usually, the problem with fresh water injected into aquifers containing denser salt water is that the fresh water volume tends to float upward to the top of the aquifer and spreads out, where it is impossible to recover at a later stage. In artificial aquifer design 2, the flow barriers obstruct the fresh water volume from expanding radially. Such walls were already suggested by e.g., Anwar (1983) and Luyun et al. (2011) as a measure to prevent salt water intrusion in coastal aquifers.

The interface between injected fresh water and native saline water will gradually turn into a transition zone between the two water types (e.g., Esmail and Kimbler 1967; Verruijt 1971). The amount of mixing is theoretically controlled by the longitudinal and transverse dispersivities, and the flow velocity, as well as molecular diffusion. Dispersivity increases significantly with the heterogeneity of the aquifer material. The storage zone should, thus, consist of homogeneous fine sand to minimize mixing.
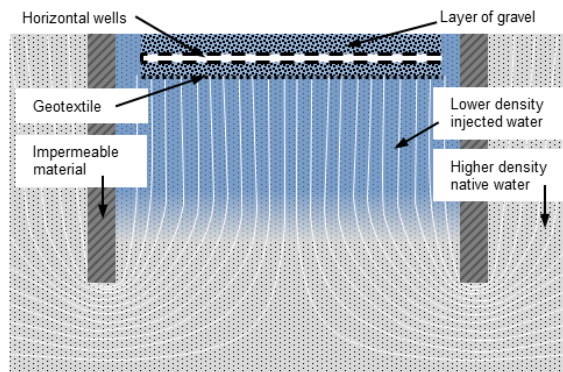

Figure 8: Artificial aquifer design 2: ASR in a saline aquifer bounded by partly penetrating impermeable walls (the *white lines* indicate *stream lines* during injection and recovery).

Conditions should be such that fresh water can be recovered quickly with the interface staying more or less horizontal. Fresh water is, therefore, preferably recovered by horizontal wells at the top of the aquifer. Horizontal wells in a layer of gravel at the top of the aquifer ensure small head gradients during recovery, thus minimizing saltwater upconing. The thickness of the layer of gravel and the required recovery rates should be balanced to decrease the risk of wells running dry. A geotextile between the layer of gravel and the underlying sand prevents fines from being washed into the gravel layer, where they might otherwise cause clogging. During pumping, the vertical flow velocity will unevenly be distributed over the width of the storage zone. Especially notice that the flow rates will be considerably higher along the edges than in the middle due to contraction of stream lines below the flow barrier (Figure 8). The fluctuations in flow velocity may be counteracted by spatially adjusting the grain size of the sediment within the storage area. While the required grain-size distribution can readily be modelled, methods to actually realize this have yet to be researched and developed.

The placement of material during dredging works may not be as accurate as theoretically desired, potentially causing unexpected and unknown spatial variations in the characteristics of the artificial aquifer. This could result in preferential flow paths or flow zones, which may substantially affect flow and mixing (e.g., Fiori and Jankovic 2012; Dagan et al. 2013) and may lead to advection-induced vertical fingering. The layer of gravel at the top should preferably be constructed after the in situ hydraulic distribution of the lower layer has been determined, so that the properties of the gravel layer can be tailored to compensate for spatial variations of the conductivity in the underlying sand. Effective in situ spatial hydraulic conductivity testing is another technology to be developed.

Leakage through the enclosing walls may occur due to construction errors and phenomena such as rabbit holes and wormholes, cracks caused by uneven settlement, and desiccation of clays. While during storage periods the density difference between fresh water and the surrounding saline groundwater would force outward leakage, inflow of saline groundwater would occur during recovery, when the head in the storage zone is low. Some leaked-in saline water may, thus, be present after a recovery period, which fortunately tends to sink downward during storage periods due to its higher density. This process may be enhanced by active flushing.

2.5 Artificial aquifer design 3: Open system with high vertical anisotropy

Artificial aquifer design 3 may be preferred where the ocean floor consists of clay, as is often the case in deltas and coastal areas (Figure 9). This clay restricts the depth of the storage zone (Tijs 2014). In such shallow and extended artificial aquifers, fresh water is best injected and recovered by multiple fully penetrating wells. When using such systems of individual wells, the size of the stored volume associated with each well is limited by the time required to inject and extract the water. Artificial aquifer design 3 is, therefore, restricted to relatively small storage volumes per well.
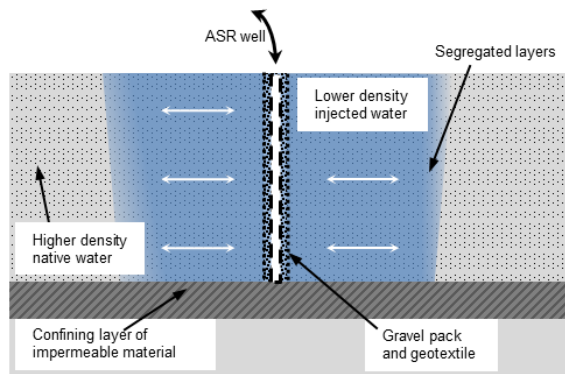

Figure 9: Artificial aquifer design 3: ASR in a saline aquifer with segregated layers.

An initial vertical interface between two fluids with different densities, as it develops after a vertical ASR-well starts injecting, will rotate as has often been demonstrated, e.g., Bakker et al. (2004) and Van Ginkel et al. (2014). As time passes, the two fluids stratify with the denser fluid spreading along the bottom and the lighter fluid accumulating along the top of the aquifer. It is desirable to limit buoyancy-induced flow as much as possible to prevent this density stratification. Ideally, the interface would remain vertical. This requires only horizontal flow, i.e., zero vertical flow. In any case, the vertical anisotropy should be as large as possible. Kumar and Kimbler (1970) and Ward et al. (2008) already mentioned that layering improves the recovery efficiency where the individual layers have identical properties and there is no cross flow between them.

The segregation of coarser and finer particles that always occurs during submerged settling of dredged material may be exploited and optimized to obtain such desired aquifer properties. This requires a layer-after-layer build-

up of the aquifer where small layers of sand must be distributed evenly over the entire width of the storage zone and then left sufficient time to settle. Although this technique is more time consuming and therefore more expensive than regular dredging, it is often applied on clayey ocean floors for geotechnical reasons.

Artificial aquifer design 3 consists of many thin layers, each with a grain size that varies from coarse to fine vertically. The design inevitably risks entrainment of fines into the well, which may cause all kind of problems such as clogging, braising of pump impellers and damage of the aquifer itself by loss of particles. The design of the gravel pack and screen slot thus requires special attention and a geotextile around the gravel pack of each well may be required to prevent fines from being washed into the gravel pack and the well.

2.6 Conclusions

Three artificial aquifer designs that reduce mixing, buoyancy and preferential flow occurring along with freshwater storage and recovery in saline aquifers have been discussed. It was shown that complete separation of the storage zone from its saline environment is not as optimal as perhaps initially thought. More dynamic (partly) open freshwater storage systems provide the opportunity to regularly flush the system to prevent internal contamination. As a result of (partly) open freshwater storage systems, the injected fresh water will come into contact with saline groundwater and mixing and density stratification will occur. These processes generally have a negative impact on the recovery efficiency.

It was shown that the density-induced buoyancy of fresh water in saline aquifers can be used for freshwater storage and recovery when it is combined with flow barriers. In that case, the aquifer properties can be improved by incorporation of (horizontal) wells, geotextile and a gravel bed in construction works. Chapter 3 further quantifies the effect of flow barriers on the freshwater recovery efficiency. In case land reclamations are constructed by means of many thin sandy layers, the vertical anisotropy of these artificial aquifers in combination with multiple fully-penetrating wells prevents density stratification. Under such circumstances, the design of the gravel pack and screen slot require special attention and a geotextile around each well may be required to prevent entrainment of fines into the well.

CHAPTER 3 FRESHWATER STORAGE AND RECOVERY BETWEEN FLOW BARRIERS IN A SALINE AQUIFER

3.1 Chapter introduction

As was shown in the previous chapter, flow barriers that partly penetrate a saline aquifer have a positive influence on the freshwater recovery efficiency, as they prevent a volume of fresh water stored between these barriers from expanding radially. It is not exactly known, however, how flow barriers influence groundwater flow within the storage zone and mixing between fresh and saline water. In this chapter, the effect that flow barriers have on the groundwater flow and on mixing between fresh and saline water are examined for different phases of storage and recovery, using a sand tank experiment and numerical modelling.

Section 3.2 consolidates current scientific knowledge about flow barriers in saline aquifers and presents the rationale for the study. Section 3.3 describes the theoretical setup of the problem and quantifies the effect of flow barriers on the freshwater recovery efficiency compared to freshwater storage and recovery without barriers. Section 3.4 presents the setup and the results of the sand tank experiment. The results in Section 3.5 and Section 3.6 show that the groundwater flow is unevenly distributed over the width of the storage zone during pumping. Section 3.7 analyses the thickness of the mixing zone during injection, storage and recovery. Section 3.8 shows that the recovery efficiency declines for increasing ratio between the width and depth of the flow barriers and for increasing ratio between the depth of the flow barriers and the thickness of the aquifer. Leakage through gaps in the enclosing walls reduces the recovery efficiency (Section 3.9). As an optimization of the storage principle, Section 3.10 shows how a gravel layer at the bottom of the storage zone, which may be added to land reclamations, results in more uniform vertical head gradients in the storage zone, which enhances the recovery efficiency. So far, injection and recovery were simulated as uniform fluxes along the top of the storage zone. In practice, injection and recovery may be realized by a head difference between the storage zone and the aquifer. Section 3.11 compares the two injection and recovery methods: constant flux and constant head.

3.2 Flow barriers in saline aquifers

Artificial recharge of fresh water for later recovery and use, known as aquifer storage and recovery (ASR; Pyne 1995), is increasingly applied for temporal water storage. ASR in brackish or saline aquifers appears hydrologically feasible as was already shown by Cederstrom (1947). However, the problem with fresh water injected into aquifers containing denser salt water is that the fresh water tends to float upward to the top of the aquifer and spread out over the denser salt water, where it is impossible to recover at a later stage. Several researchers have demonstrated the negative effect of density induced buoyancy on the recovery-efficiency of ASR (e.g. Esmail and Kimbler 1967; Kumar and Kimbler 1970; Merritt 1986; Ward et al. 2007, 2008, 2009; Bakker 2010), where the recovery efficiency is defined as the ratio between injected and recovered fresh water (e.g. Lowry and Anderson 2006). The negative influence of density induced buoyancy on the recovery efficiency is most severe for small-scale ASR (e.g., Ward 2007, 2009; Bakker 2010; Van Ginkel et al. 2014). Small-scale ASR is defined as the ratio of injected volumes with respect to the third power of the thickness of the aquifer.

While most scholars studied the buoyancy phenomenon analytically or numerically, only few of them have looked at solutions to overcome this problem for small-scale ASR. At an ASR site in Marathon, Florida, a trickle flow was maintained during the storage period to counteract buoyancy (Pyne 1995). Maliva et al. (2006) proposed well design optimizations, such as one-way valves, inflatable packers, or additional partially penetrating wells as a solution. In line with these well optimizations, Zuurbier et al. (2014) tested a skimming technique consisting of multiple partially penetrating wells and reached recovery efficiencies on the order of 60% at a small-scale ASR system. Comparable recovery rates were found in numerical simulations by Van Ginkel et al. (2014), who presented an operational paradigm that combines ASR with salt water extraction from below the freshwater zone. The study of Zuurbier et al. (2015) demonstrated the potential benefits of horizontal wells on the recovery efficiency of ASR in coastal areas by numerical simulation.

In one of their recovery approaches, Van Ginkel et al. (2014) showed by a numerical simulation that flow barriers at a limited distance around the ASR well increase the recovery efficiency. Flow barriers are vertical walls constructed of sheet piles, clay, or other types of impermeable material. It was argued that salt water extraction from below the freshwater zone is not

required if small-scale ASR in saline aquifers is combined with vertical walls, because the vertical walls obstruct the floating fresh water from flowing sideways (Van Ginkel 2015). Flow barriers have not been applied to the authors' knowledge in practical ASR in saline aquifers to this date. Fresh water can be recovered by a network of drains or shallow or horizontal wells. The vertical walls are similar to flow barriers applied to reduce salt water intrusion in coastal aquifers. Anwar (1983) described how partially penetrating barriers across the flow direction modify the flow field and can increase the yield of fresh groundwater resources in unconfined coastal aquifers. Luyun et al. (2011) performed laboratory scale experiments and numerical simulations to determine the effects of the location and penetration depth of flow barriers on seawater intrusion control and Kaleris and Ziogas (2013) showed the protective effect of flow barriers on groundwater extractions near the coast.

The objective of this chapter is to investigate the flow dynamics and recovery efficiency of small-scale ASR in saline aquifers when combined with surrounding flow barriers. First, the recovery efficiency is computed for several ASR systems to quantify the effect of combining ASR with flow barriers. Second, a laboratory experiment was carried out to examine the behaviour of a fresh water volume injected between flow barriers in a saline aquifer during injection, storage and recovery. Third, simulations were performed to examine the effect of aquifer properties and flow barrier settings on the recovery efficiency. It was finally investigated if the recovery efficiency could be increased by a layer of gravel below the storage zone.

3.3 Theoretical setup of the problem

Consider ASR between two vertical walls in a vertical cross section (Figure 10). A Cartesian x,y coordinate system is adopted with the y-axis pointing vertically upward. The aquifer thickness is H [L], the length of the cross section is $2L$ [L], and vertical flow barriers with a penetration depth D [L] are located a distance $2B$ [L] apart. The aquifer is initially filled with saltwater of density ρ_s [M/L^3]. Uniform recharge P [L/T] is applied between the walls to simulate drains or shallow or horizontal ASR wells on top of the aquifer. The hydraulic conductivity of the aquifer k [L/T] is homogeneous and isotropic. The effective porosity of the aquifer is n [-]. The cross section is symmetric across the y axis, so that only the positive x domain is considered in this paper.
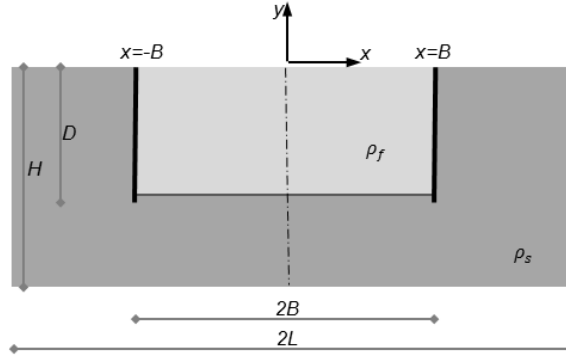
Figure 10: Problem setup: cross-section through an ASR system between two vertical walls.

Systems with and without flow barriers were simulated with SEAWAT (Langevin et al. 2008) in the mfLab environment. Simulations were performed in brackish aquifers (ρ_S=1005 kg/m^3, 5,000 mg/L total dissolved solids (TDS)) and saline aquifers (ρ_s=1025 kg/m^3, 42,000 mg/L TDS). The geometry and aquifer data are given in Table 1. Boundary conditions are an impermeable top boundary for $x>B$, a constant head of 0 m at $x=L$, different boundary conditions along the top of the storage zone during ASR operation, as discussed in the next paragraph, and no flow along all other boundaries. Elastic storage was neglected. The total variation diminishing (TVD) scheme was used to solve the solute transport equation.

Table 1	
Geometry and aquifer data	
Parameter	Value
H: Aquifer thickness (m)	30
D: Depth of the barrier (m)	15
L: Length of the model (m)	250
B: Width of the barrier (m)	30
ρ_f: Density fresh water (kg/m3)	1000
ρ_s: Density salt water (kg/m3)	1005 and 1025
k: Hydraulic conductivity (m/d)	10
n: Porosity (-)	0.35
P: Recharge (mm/d)	9 and 35
$\Delta x, \Delta y$: Grid size (m)	0.2
α_L: Longitudinal dispersivity (m)	0.1
α_T: Transversal dispersivity (m)	0.01
D_d: Molecular diffusion (cm^2/d)	$1 \cdot 10^{-5}$

The ASR process was repeated for five cycles. The duration of a cycle was one calendar year. One cycle was divided into four periods: an injection period of 3 months with a constant injection rate P along the top of the storage zone, a storage period of 3 months, a recovery period with a constant recovery rate P along the top of the storage zone until the average extracted concentration reached the international drinking water standard of 500 mg/L TDS (maximum 3 months), and an idle period until the year was complete. Simulations were performed for two different injection and recovery rates of P=9 mm/d and P=35 mm/d. The recovery efficiency μ is defined as the ratio between injected volume V_i and recovered volume V_r during a cycle:

$$\mu = \frac{V_r}{V_i} \tag{1}$$

Results for the recovery efficiency for P=9 mm/d are shown in Figure 11a. The computed recovery efficiency in the first cycle from a brackish aquifer was 50% and from a saline aquifer 35% for the cases with barriers compared to zero for the cases without barriers. The recovery efficiency increased in subsequent cycles, till 97% in the fifth cycle in a brackish aquifer and 89% in a saline aquifer for the cases with barriers compared to 50% in a brackish aquifer and 5% in a saline aquifer for the cases without barriers. The increase in recovery efficiency in successive cycles is consistent with earlier ASR studies (e.g. Kumar and Kimbler 1970; Merritt 1986; Pyne 1995; Ward et al. 2007; Bakker 2010).
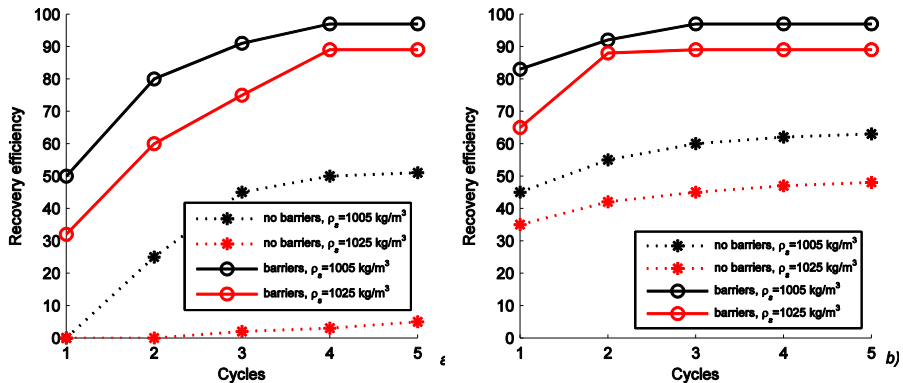

Figure 11: Calculated recovery efficiency in successive cycles for regular ASR and ASR combined with flow barriers: a) P=9 mm/d, b) P=35 mm/d. Black lines are brackish aquifers (ρ_s=1005 kg/m^3) and red lines are saline aquifers (ρ_s=1025 kg/m^3).

Results for P=35 mm/d are shown in Figure 11b. The recovery efficiency without barriers is 45% in a brackish aquifer and 35% in a saline aquifer in the first cycle for this larger injection and recovery rate. The recovery efficiencies for the cases with flow barriers are doubled those of the cases without flow barriers. Fresh water reached the bottom of the flow barriers in the third cycle and fresh water escaped underneath the barriers in subsequent cycles, which made this water unrecoverable so that the recovery efficiency did not increase beyond cycle 4.

The examples in Figure 11 show that the flow barriers lead to significantly improved recovery efficiencies for small-scale ASR systems. In these examples, one set of values was used for the hydraulic conductivity and thickness of the aquifer, width and depth of the flow barriers, and pumping rate. To investigate the flow dynamics further, a laboratory experiment was performed, and numerical simulations were conducted to study the effect of density difference, hydraulic conductivity and thickness of the aquifer, width and depth of the flow barriers and pumping rate.

3.4 Physical model

3.4.1 Setup laboratory experiment

Physical models are important tools to gain information about fresh and salt water interaction and flow dynamics (e.g. Pennink 1915; Stoeckl and Houben 2012; Luyun et al. 2011). A physical experiment was conducted for the right half of the symmetric flow system (Des Tombe et al. 2011). The experimental setup consisted of an acrylic box of L=100 cm, H=17 cm, and 10 cm width (Figure 12). The main section of the box was packed with glass beads with a diameter of 400-600 µm. The hydraulic conductivity of the glass beads was measured with a Darcy experiment. The hydraulic conductivity was 220 m/d and the porosity was 0.38. An acrylic screen of D=12 cm at B=35 cm functioned as a flow barrier. A saltwater reservoir at the right-hand boundary of the box was separated from the main section by a screen with an opening of 1 cm above the box's bottom. The head in the saltwater reservoir was maintained at 1 cm above the glass beads bed by a peristaltic inlet/outlet pump in the saltwater reservoir.
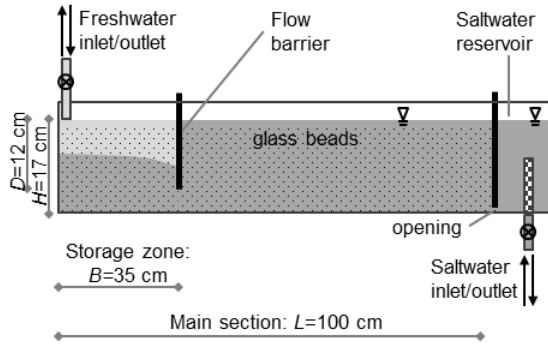
Figure 12: Schematic representation of the experimental setup.

Tap water was used as fresh water and was dyed with a yellow fluorescent tracer (fluorescein sodium salt) at a concentration of 8 mg/l to visualize the different water types. UV illumination was used to improve the contrast. It was assumed that the effect of the tracer on the viscosity of the fluid was negligible. Table salt at a concentration of 100 g/L was dissolved in tap water to prepare salt water. Water density was measured with a hydrometer. Freshwater density was ρ_f=1004 kg/m^3 and saltwater density ρ_s=1075 kg/m^3. The box was initially filled with salt water via tubes at the bottom of the box. Beads were packed in layers under fully saturated conditions to prevent air entrapment and were compressed after each layer was placed, similar to Luyun et al. (2011).

3.4.2 Experimental results

Fresh water was injected by an inlet pump at 1 cm above the glass beads bed in the upper left-hand corner of the storage zone at a rate of 15 ml/min to establish a freshwater injection layer across the top of the storage zone. Injection stopped as soon as fluorescent tracer started to flow underneath the vertical wall. This occurred after 75 minutes. The experimental results are shown in Figure 13 which depicts the water in the storage zone between the left part of the experimental setup (corresponding to the centre of the storage zone in Figure 12) and the barrier on the right. The bottom of the freshwater zone rotated in the direction of the bottom of the flow barrier during injection (Figure 13a). The inlet pump caused the washout of some glass beads in the upper left-hand corner of the storage zone, which resulted in the dark green colour in the upper left-hand corner of the figures. The injection period was followed by a storage period in which no water was injected or extracted. The freshwater zone rotated to a horizontal position in 1240 minutes. The results at the end of the storage period are shown in Figure 13b.

After the storage period, fresh water was recovered by the outlet pump in the upper left-hand corner of the storage zone at a rate of 15 mL/min. Recovery stopped as soon as the extracted freshwater concentration exceeded the Dutch drinking water standard of 150 mg/L. This occurred after 48 minutes, resulting in a recovery efficiency of 64%. Figure 13c shows the position of the freshwater zone after 30 minutes recovery. The freshwater zone rotated in the direction of the top of the flow barrier (Figure 13c). The inclined position of the bottom of the freshwater zone caused saltwater upconing along the flow barrier before all fresh water was recovered from the storage zone.

Uranine becomes brighter green in lower concentrations providing an indication of the thickness of the mixing zone between fresh and saline water, highlighted by the dashed white lines in Figure 13. It is noted that uranine has a light sensitivity and that UV illumination may have led to a decrease in concentration during the experiment; its extent was not assessed. The thickness of the mixing zone changed during the experiment (Figure 13). A noticeable feature of the results in Figure 13 is the widening of the mixing zone near the flow barrier during injection and the narrowing of the mixing zone at the same location during recovery.

The experimental results illustrate that the shape of the freshwater zone and the thickness of the mixing zone are influenced by the spatial variation of the flow rate in the storage zone. A large inclination of the bottom of the freshwater zone may result in leakage of fresh water under the flow barrier during injection, before the total storage capacity is reached, or saltwater upconing during recovery, before all fresh water is recovered, both decreasing the recovery efficiency.
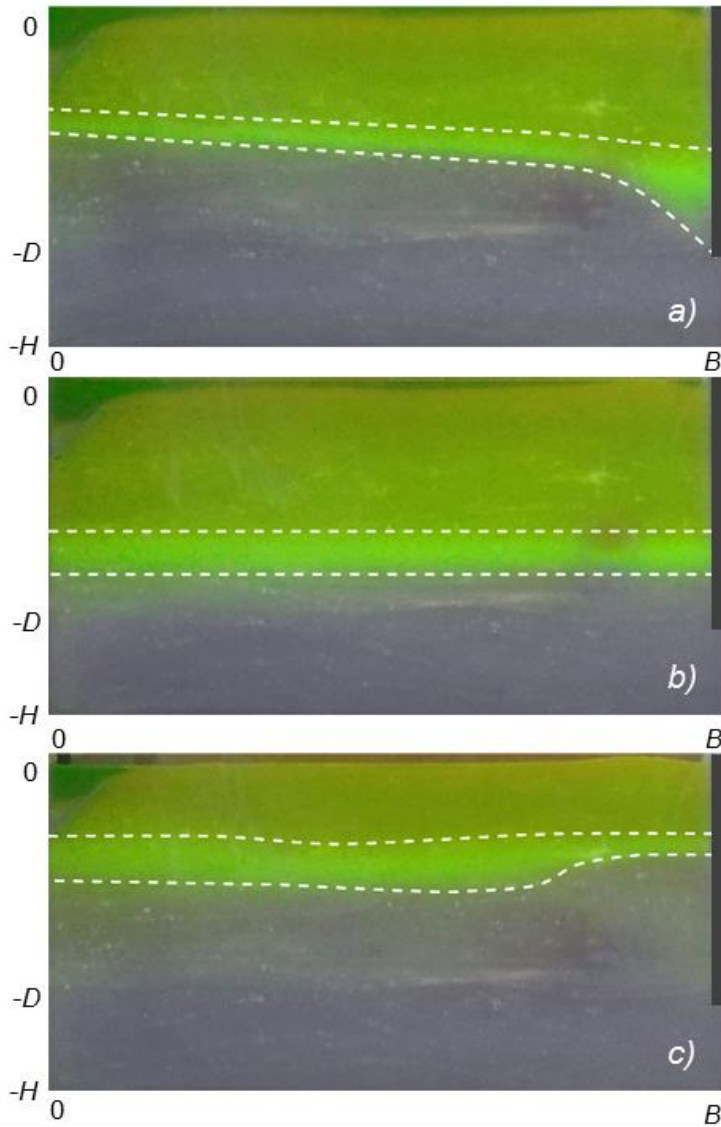
Figure 13: Freshwater zone (green) in the storage zone (between $x=0$ and $x=B$): a) end of injection (75 minutes), b) end of storage (1315 minutes), c) during recovery (1345 minutes). The dashed white lines indicate the thickness of the mixing zone between fresh water and salt water.

3.4.3 Comparison between the physical and numerical model

The physical experiment was simulated with SEAWAT. The discretization was $\Delta x=\Delta y=1$ cm. Boundary conditions are an impermeable top boundary for $x>B$, a constant head of 1 cm at $(x,y)=(L, H)$, different boundary conditions along the top of the storage zone, and no flow along all other boundaries. Longitudinal and transversal dispersivity were set to 0.1 cm and 0.01 cm, respectively, and molecular diffusion was $1 \cdot 10^{-5}$ cm^2/d. A uniform freshwater flux at a rate of 15 mL/min was applied along the top of the storage zone during injection.

The interface position in the storage zone at the end of the injection period is shown in Figure 14. The black curve indicates the centre of the mixing zone between fresh water and salt water of the physical model. The blue line is the 50% concentration contour line of SEAWAT. The SEAWAT results are in good agreement with those of the physical model. The red line is the 95% concentration contour as calculated by SEAWAT. This contour passed the bottom of the flow barrier at 75 minutes, similar to the first leakage of fluorescent tracer under the barrier as was observed in the experiment.
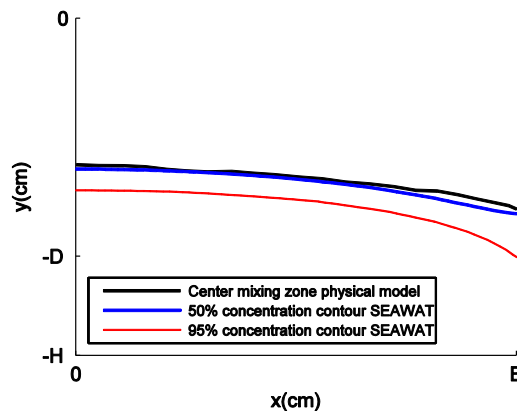

Figure 14: Measured interface position of the physical model (black line), the 50% concentration contour line and the 95% concentration contour line of SEAWAT at the end of the injection period.

The impermeable top boundary for $x>B$ in the numerical model was slightly different from the physical model boundary condition, where a fixed head was maintained at 1 cm above the glass beads bed. Figure 15 shows that there is no significant difference between the streamline patterns inside the storage zone for a fixed head boundary condition along the top for $x>B$ (red lines) or an impermeable top boundary (blue lines).
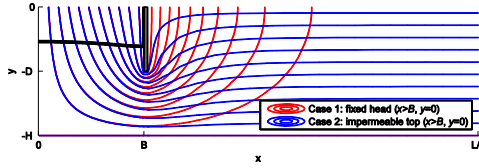
Figure 15: Streamlines ($\Delta\Psi$=0.10 m^2/d) during injection of fresh water in a saline aquifer for two cases. The black curve is the 50% concentration contour line. Note that the horizontal axis only runs to x=L/2.

3.5 Flow analysis during pumping and storage

SEAWAT was used to further investigate the flow and movement of the interface. The interface was defined as the 50% concentration contour line of SEAWAT and dispersion was excluded from the simulations by setting dispersivity and molecular diffusion to zero. Geometry and aquifer data are given in Table 2. The last column of Table 2 presents the range of aquifer parameters used for the sensitivity analysis.

Table 2		
Geometry and aquifer data		
Parameter	Base value	Range
H: Aquifer thickness (m)	30	-
D: Depth of the barrier (m)	15	-
L: Length of the model (m)	250	-
B: Width of the barrier (m)	30	-
ρ_f: Density freshwater (kg/m^3)	1000	-
ρ_s: Density saltwater (kg/m^3)	1025	1005-1025
k: Hydraulic conductivity (m/d)	10	1-20
n: Porosity (-)	0.35	-
P: Recharge (mm/d)	35	17-70
$\Delta x, \Delta y$: Grid size (m)	0.2	-
α_L: Longitudinal dispersivity (m)	0	-
α_T: Transversal dispersivity (m)	0	-
D_d: Molecular diffusion (cm^2/d)	0	-

The relationship between the specific discharge and the stream function for a divergent free flow is defined by the well-known relationships (e.g., Bear 1972):

$$q_x = -\frac{\partial \Psi}{\partial y} \qquad (2)$$

$$q_y = +\frac{\partial \Psi}{\partial x} \qquad (3)$$

Where Ψ is the stream function [L/T^2], x, y are spatial coordinates, and q_x and q_y are the components of the specific discharge vector. De Josselin De Jong (1960) showed that the stream function is a single valued and continuous function irrespective of the fluids involved. The stream function provides insight in the instantaneous flow field (snapshot in time) by means of its contours, the streamlines. The stream function is constant along a streamline and the difference in stream function values of two streamlines corresponds to the instantaneous discharge between these two streamlines in the cross section.

The streamlines during the injection of fresh water in a saline aquifer are shown in Figure 16a. The streamlines bend from the initial vertical position to horizontal below the flow barrier. The intensity of the discharge is highest at the bottom of the flow barrier where the streamlines are closest together. No flow occurs in the stagnation point at $(x,y)=(0,-H)$. The black curve indicates the position of the injection front at the end of the injection period. The injection front is inclined due to the higher flow velocity along the barrier compared to the centre of the storage zone.
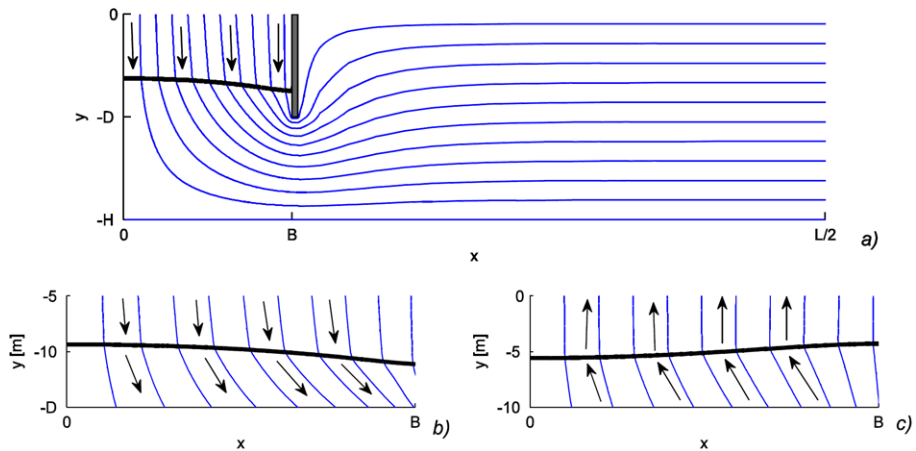

Figure 16: Streamlines ($\Delta\Psi$=0.10 m^2/d) a) during injection of fresh water in a saline aquifer; note that the horizontal axis only runs to $x=L/2$, b) detail of injection, and c) detail of recovery. The black curve represents the position of the interface and the black arrows indicate the flow direction.

If there is a density difference on either side of the injection front, a jump exists in the specific discharge component parallel to the interface, q_s (e.g., Bear 1972). This discontinuity in q_s along the interface represents a shear flow s that

equals the difference between the tangential components of the specific discharge vector across the interface (e.g., Bear 1972):

$$s = q_{t,s} - q_{t,f} = k \frac{\rho_s - \rho_f}{\rho_f} sin\alpha \qquad (4)$$

Where $q_{t,s}$ and $q_{t,f}$ are the components of the specific discharge vector tangential to the interface below and above the interface respectively, and α is the angle between the tangent to the interface and the positive x-axis. A shear flow always exists along an inclined interface that separates two fluids of different density. The component of the specific discharge normal to the interface, q_n, is continuous. The shear flow results in a change in direction and length of the specific discharge vector.

The discontinuous component of the specific discharge at the interface results in a kink in the streamlines at the interface. The kink in the streamlines is shown in the detailed representations of Figure 16b and Figure 16c that present the streamlines near the interface during injection and recovery, respectively. The shear flow increases with increasing slope of the interface (Eq. 4). Since the magnitude of the slope increases in x direction, the refraction of the streamlines at the interface is more pronounced for larger x (Figure 16).

The interface rotates to the stable position during the storage period. The black curve in Figure 17 indicates the position of the interface at the beginning of the storage period and the red line is the interface position at the end of the storage period. All flow during this period is caused by the density difference between the injected and native groundwater.
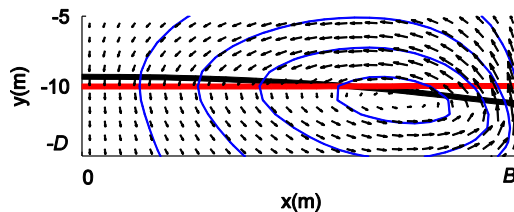

Figure 17: Streamlines (blue lines where $\Delta\Psi$=0.02 m²/d) and flow vectors at the beginning of the storage period. The black curve represents the position of the interface at the beginning and the red line at the end of the storage period.

3.6 Influence of aquifer properties and pumping rate

The effect of the density difference on the inclination of the interface is shown in Figure 18a. The black lines represent the position of the interface during injection at monthly time intervals in a saline aquifer with ρ_s=1025 kg/m³ and the red lines represent the same in a brackish aquifer with ρ_s=1005 kg/m³. A higher density difference between injected and native groundwater results in a less steep interface position. The shear flow is directly proportional to the density difference (Eq. 4) so that a larger density difference helps to flatten the interface.
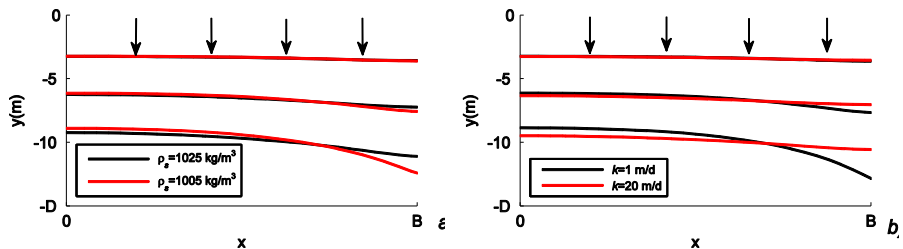

Figure 18: Interface position in the storage zone during injection at monthly intervals, comparison between a) saline (ρ_s=1025 kg/m³) and brackish aquifer (ρ_s=1005 kg/m³) with k=10 m/d and b) aquifers with hydraulic conductivity values of 1 m/d and 20 m/d, and ρ_s=1025 kg/m³.

The effect of different hydraulic conductivities is shown in Figure 18b where the black lines present the results for an aquifer with k=1m/d and the red lines for k=20 m/d. The shear flow is inversely proportional to the hydraulic conductivity (Eq. 4) so that higher conductivity values also flatten the interface, as is shown in Figure 18b. The same arguments apply to upconing during recovery, it being more severe when conductivities are smaller and when the salinity difference between the fluids is smaller.

The position of the interface between fresh water and salt water is also influenced by the pumping capacity. The black lines in Figure 19 present the position of the interface at 33%, 66% and 100% of injected volume for an injection rate of 70 mm/d and the red lines for 17 mm/d. The injection period was adjusted so that the total injected volume was similar in both cases. The inclination of the interface is higher for a larger injection rate. This is always the case when the density of the injection water is smaller than the density of the native groundwater.
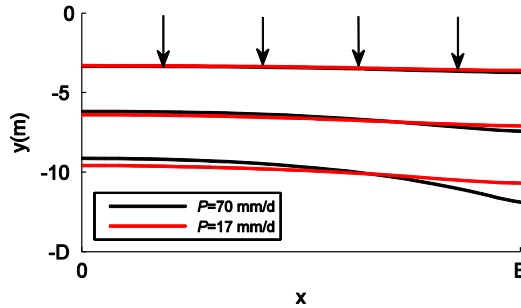
Figure 19: Interface position in the storage zone during injection of 33%, 66%, 100% of injection volume for two injection rates and ρ_s=1025 kg/m^3 and k=10 m/d.

3.7 Thickness mixing zone during pumping and storage

Eeman et al. (2010) showed that changes in fluid motion over time are important in the development of a freshwater lens and in the development of a mixing zone between this lens and upwelling saline water. This also applies to a freshwater volume between flow barriers in a saline aquifer. To simulate this behaviour, similar geometry and aquifer data were used as for the base case (Table 2), but longitudinal and transversal dispersivity were set to 0.1 m and 0.01 m, respectively, and molecular diffusion was set to 1·10^{-5} cm^2/d. Snapshots from the simulation are shown in Figure 20 for the first ASR cycle.

The width of the mixing zone is defined as the distance between the 95% concentration contours indicated by the pink lines in Figure 20. The mixing zone widens near the flow barrier during injection because the velocity increases in negative y direction. During recovery, the velocity decreases in upward direction thus narrowing the mixing zone at the same x location. This was also observed during the experiments (Figure 13).
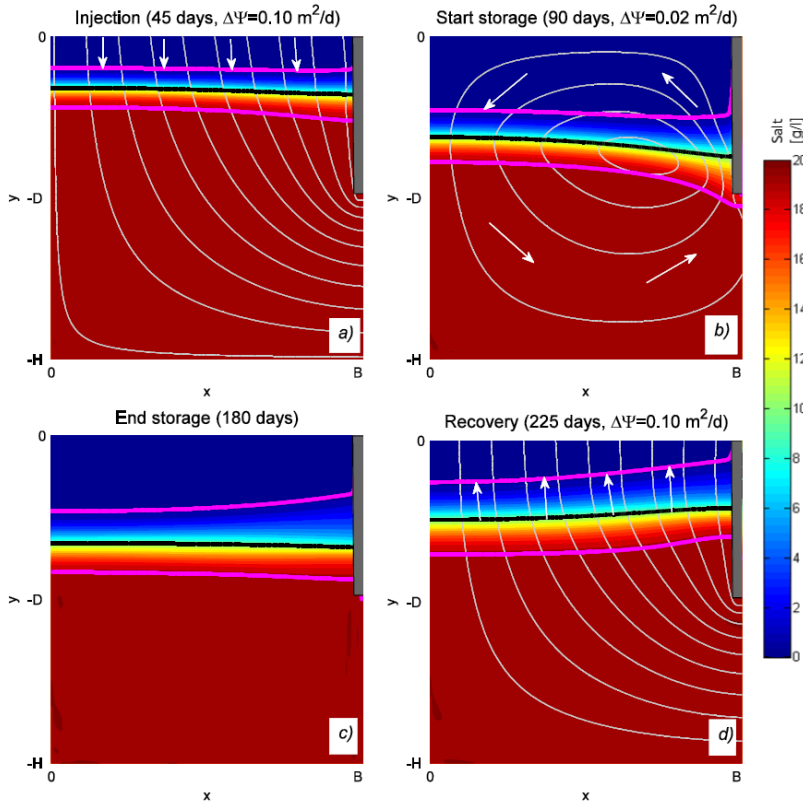
Figure 20: Flow simulation snapshots for a) injection, b) start storage, c) end storage, and d) recovery. The white lines are streamlines, the black curve is the 50% concentration contour line, and the pink lines are the 95% concentration contour lines.

3.8 Flow barrier settings

A larger distance between the flow barriers and a larger depth of the flow barriers increases the storage capacity, at least in theory. However, flow rates near and below the flow barrier are larger for a larger distance between the barriers, while the flow velocity in the centre stays the same. As a result, the inclination of the interface near the toe of the flow barrier increases for increasing ratios of the distance between the barriers and the depth of the barrier. Similarly, the flow rates in the opening under the flow barrier increase for increasing ratio between the depth of the barrier and the thickness of the aquifer. Also, leakage of fresh water underneath the barriers during injection occurs earlier for larger *B/D* and *D/H* ratios, and the recovery efficiency declines along with it.

The recovery efficiency is shown for five successive cycles for different ratios between the depth D of the barrier and the thickness of the aquifer H, and different ratios between the width B between the flow barriers and D (Figure 21). The highest recovery efficiency (on the order of 95% in the fifth cycle) is obtained for cases where the flow barriers penetrate a quarter of the thickness of the aquifer (D/H=0.25, black lines in Figure 21). Note that all three black lines (D/H=0.25) are on top of each other in Figure 21, as different B/D ratios have no influence on the recovery efficiency for these cases.
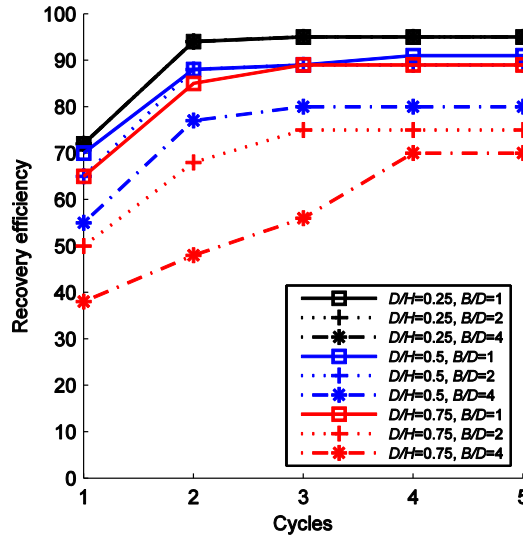

Figure 21: Calculated recovery efficiency in successive cycles for different flow barrier settings; width B between flow barriers, thickness H of the aquifer and depth D of the barriers. All three black lines are on top of each other.

For cases with D/H=0.5 (blue lines in Figure 21) the highest recovery efficiency is obtained for flow barriers where B/D=1 and B/D=2. For the case with a B/D ratio of 4, leakage underneath the barrier occurred in the first cycle after 50 days injection. The recovery efficiency of the first cycle was 55% for this case. Recovery efficiencies increased in subsequent cycles, until 80% in the third cycle, compared to 90% for the cases with a B/D ratio of 1 and 2.

Lowest recovery efficiencies were obtained for cases with D/H ratio=0.75 (red lines in Figure 21) in combination with a large width between the barriers. Leakage underneath the barrier during injection and upconing along the barrier during recovery resulted in a recovery efficiency of 40% in the first cycle, until 70% in the fifth cycle for this case.

3.9 Leakage through the walls

Leakage through the flow barriers may occur due to construction errors, cracks caused by uneven settlement, and desiccation of clays. The larger head in the freshwater storage zone compared to the surrounding saline aquifer forces outward leakage during injection and storage. This is illustrated in Figure 22 that shows snapshots for the simulation with an opening in the flow barrier at y=-5 m of 0.2 m height. The 2D model presents the conservative result that leakage occurs over the entire length of the flow barrier. In practice, the opening will be relatively small with respect to the length of the flow barrier.
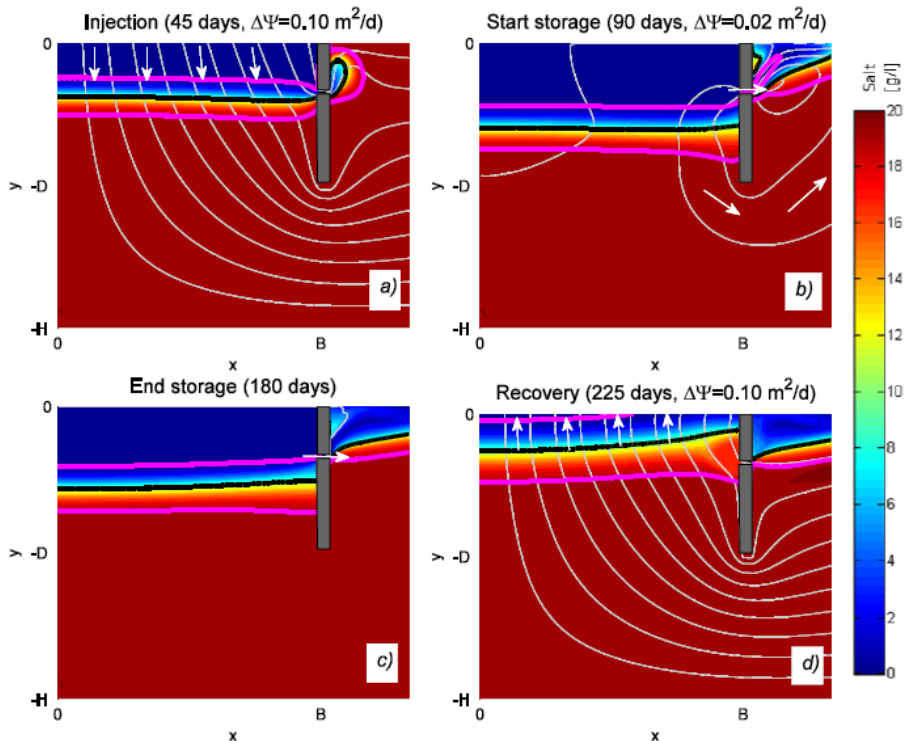

Figure 22: Flow simulation snapshots for a) injection, b) start storage, c) end of storage, and d) recovery with an opening in the flow barrier at y=-5 m. The white lines are streamlines, the black curve is the 50% concentration contour line and the pink lines are the 95% concentration contour lines.

The 500 mg/L contour line reached the opening after 60 days of injection. The outward flow of fresh water continued during the storage period until the head difference on both sides of the flow barrier became equal. Inflow of saline water occurred during recovery, when the head in the storage zone was low.

The recovery efficiency was 55%, a loss of 10% compared to the 65% without an opening in the flow barrier.

3.10 Gravel layer below the storage zone

The storage capacity can be increased by a layer of gravel below the storage zone. The high hydraulic conductivity of the gravel layer ensures relatively uniform head gradients in the storage zone, resulting in almost vertical flow, and reduction of the inclination of the interface. The construction of gravel layers may be feasible when constructing artificial aquifers such as in land reclamations. A storage zone with a gravel layer at the depth of the barriers was simulated. The results are shown in Figure 23.
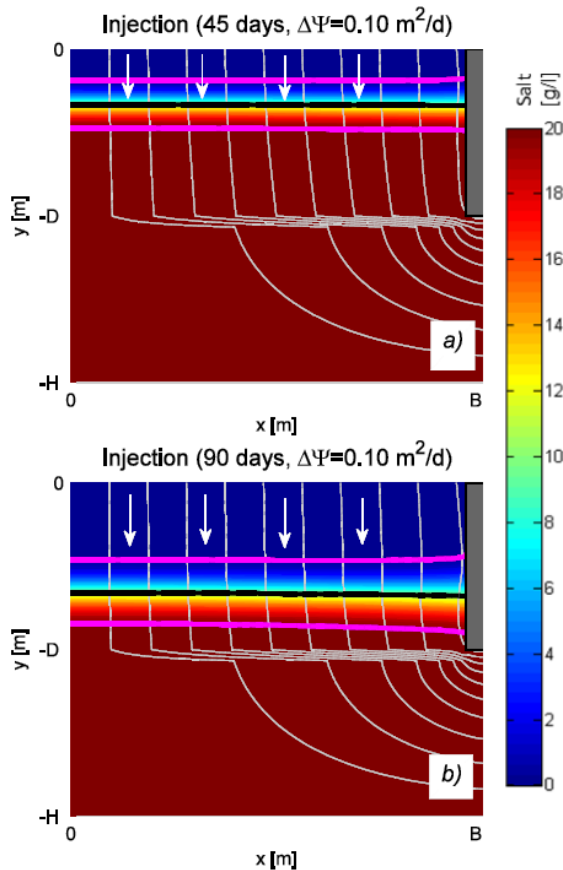

Figure 23: Flow simulation snapshots with a layer of gravel under the storage zone. The white lines are streamlines, the black curve is the 50% concentration contour line and the pink lines are the 95% concentration contour lines.

A layer of gravel of 1 m height with a hydraulic conductivity of 1000 m/d was located between $y=D$=-15 m and -16 m. The recovery efficiency of this simulation is 75%, 10% more than 65% efficiency without a gravel layer. This simulation was also performed for a layer of coarse sand with a hydraulic conductivity of 100 m/d resulting in a slightly lower recovery efficiency of 72%.

3.11 Injection by a constant head in the storage zone

So far, injection and recovery were simulated as uniform fluxes along the top of the storage zone. In practice, injection and recovery may be realized by a head difference between the storage zone and the aquifer. Consider an unconfined aquifer with geometry and aquifer data as presented in Table 2 with an initial head of 0 m and a constant head boundary of 0 m at L=2000 m. Storage changes are included in this simulation; the specific storage coefficient is $1 \cdot 10^5$ m^{-1} and the phreatic storage coefficient is 0.20. The head in the storage zone is raised to a constant head of 1.4 m and kept constant for an injection period of 3 months.

The phreatic surface during injection is shown in Figure 24a. The phreatic surface just outside the flow barrier is lower than the phreatic surface inside the storage zone due to the head loss of water flowing around the flow barrier. The freshwater head at the bottom of the flow barrier decreases through time, even though the phreatic surface inside the storage zone is fixed at 1.4 m. This is caused by the increase of fresh water, which is lighter than salt water.

If the storage zone is deep enough, fresh water injection with a fixed head will come to a halt in accordance with the Badon Ghijben Herzberg relation, which states that the maximum depth of the fresh water floating on top of saline water is equal to $y = h\rho_f/(\rho_s - \rho_f)$, where h is the phreatic surface in the storage zone above the water level in the surrounding saline aquifer. For h=1.4 m, ρ_f=1000 kg/m³, and ρ_s=1025 kg/m³, the maximum depth of the fresh water zone is y=-56 m, provided that the walls are that deep.
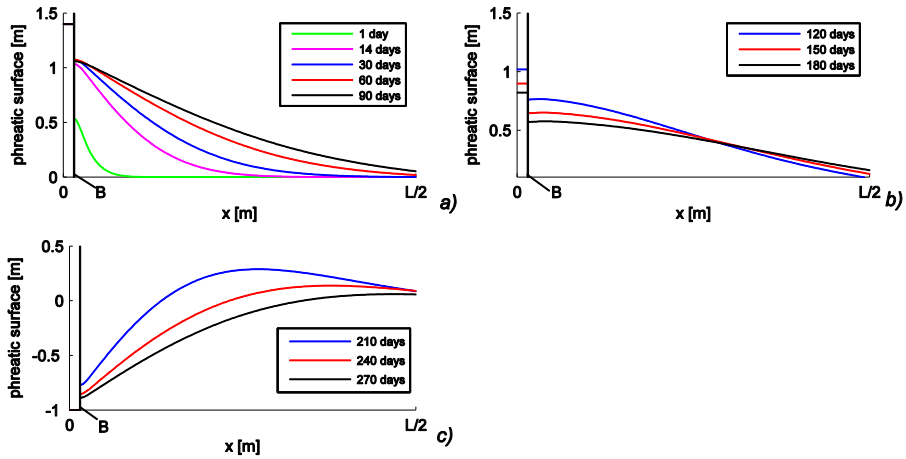
Figure 24: Phreatic surface during a) injection, b) storage and c) recovery for prescribed heads in the storage zone. Note that the horizontal axis only runs to $x=L/2$.

The injection period is followed by a storage period of 3 months without prescribed head in the storage zone. The phreatic surface recedes towards the initial value, but the storage period is too short to allow the phreatic surface to drop to 0 m. At the end of the storage period, the phreatic surface in the storage zone is 0.8 m (Figure 24b). The storage period is followed by a recovery period of 3 months in which the head in the storage zone is kept constant at -1 m. The phreatic surface during recovery is shown in Figure 24c.

The volume of injected water in the storage zone under fixed head conditions is compared to the volume under a constant and uniform injection/recovery rate (Figure 25). For the fixed head case, the injection rate is larger at the beginning of the injection period than at the end, but the total injection volume is similar to the case of constant, uniform injection. Similarly, recovery is much larger at the beginning of the recovery period. This could be modified by lowering the water level in the storage zone gradually during recovery.

The recovery efficiency for the first cycle under fixed head conditions is 48% compared to 65% under a constant and uniform injection/recovery rate. One of the reasons that the recovery efficiency under fixed head conditions is lower is that the relatively high recovery rate at the beginning of the recovery period results in quicker upconing of salt water along the flow barrier. Furthermore, the head in the storage zone is 1 m lower during recovery and the 500 mg/l concentration contour, therefore, reaches the recovery drains sooner.
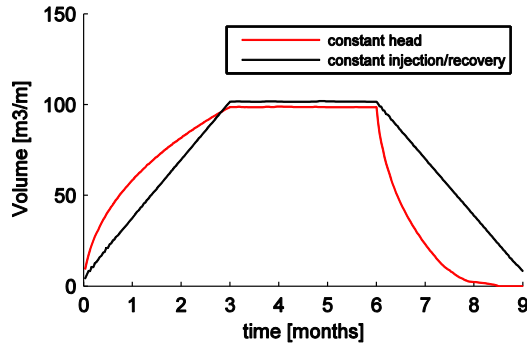
Figure 25: Injected water in the storage zone in one ASR cycle for constant heads and constant injection/recovery rates.

3.12 Conclusions

The recovery efficiency was investigated of small-scale ASR-systems in brackish and saline aquifers in combination with flow barriers. Recovery efficiencies of small-scale ASR-systems are generally so low that ASR is not a solution. The use of barriers increases the recovery efficiencies to acceptable levels for the cases investigated. Freshwater recoveries on the order of 65% in the first cycle and up to 90% in the following cycles were achieved for the studied configurations with constant flux while the recovery efficiency is somewhat lower for constant head.

The shear flow along the interface is proportional to the density difference between injected and native groundwater so that larger density differences reduce the inclination of the interface and increase the freshwater storage capacity. The shear flow is inversely proportional to the hydraulic conductivity so that higher conductivity values also flatten the interface. The inclination of the interface is smaller for lower pumping rates. The recovery efficiency declines for increasing ratio between the width and depth of the flow barriers and for increasing ratio between the depth of the flow barriers and the thickness of the aquifer. Leakage through gaps in the flow barriers reduces the recovery efficiency. A gravel layer at the bottom of the storage zone, which may be added to land reclamations, results in more uniform vertical head gradients in the storage zone, which enhances the recovery efficiency.

CHAPTER 4 FRESHWATER STORAGE RECOVERY IN COMBINATION WITH A SALTWATER EXTRACTION WELL

4.1 Chapter introduction

The previous chapters explained how the properties of the aquifer and flow barriers influence the recovery efficiency of a volume of fresh water stored in a saline aquifer. In addition to these physical properties of the aquifer, the recovery efficiency may also be affected by operational factors. In this chapter, a new operational paradigm is presented for freshwater storage and recovery in saline aquifers, which combines freshwater storage with saltwater extraction from below the stored volume of fresh water. The saltwater extraction counteracts the buoyancy due to the density difference between fresh and saline water, thus preventing the fresh water from floating up. Since freshwater storage is combined with saltwater extraction, the storage principle is especially useful in situations where the continuous flow of salt water can be used for desalination purposes. As an example, the operational paradigm is applied for the seasonal storage of fresh water produced by desalination plants in tourist resorts along the Egyptian Red Sea coast.

Section 4.2 provides background information related to the storage principle and presents the rationale for the study. Section 4.3 describes the theoretical setup of the problem. Section 4.4 presents an analytical Dupuit solution for the steady flow of salt water toward a well, with a volume of fresh water floating on top of the cone of depression. The required saltwater discharge to keep a volume of fresh water in place can be computed with this analytical solution. Numerical modelling (SEAWAT in the *mfLab* environment) is applied to determine how much fresh water can be recovered. Section 4.5 describes the numerical model setup. Three recovery approaches are examined in Section 4.6. Freshwater recovery rates in the order of 70% are achievable when salt water is extracted in high volumes (approach 1), flow barriers are applied (approach 2), or circular drains or shallow recovery wells are used (approach 3). The effect of ambient flow and interruptions of salt water pumping on the recovery efficiency are reported in Section 4.7.

4.2 Aquifer storage recovery in saline environment

Storage of water in an aquifer and subsequent extraction later is known as aquifer storage and recovery (ASR) (e.g., Pyne 1995). One of the primary concerns when evaluating the feasibility of ASR is recovery efficiency. The recovery efficiency is defined as the ratio between injected and recovered fresh water (e.g., Lowry and Anderson 2006; Ward et al. 2007; Bakker 2010). Cederstrom (1947) was the first to propose the concept of performing ASR in saline aquifers. Esmail and Kimbler (1967) and Kumar and Kimbler (1970) studied the storage of fresh water in saline aquifers by theoretical considerations and laboratory experiments and concluded that ASR in saline aquifers appears technically feasible. Merritt (1986) performed a numerical study to examine the hydrogeological, design, and management factors governing the recovery efficiency of fresh water stored in saline aquifers.

The problem with fresh water injected into aquifers containing denser salt water is that the injected fresh water tends to float upward to the top of the aquifer and spread out, where it is impossible to recover at a later stage. Research by Esmail and Kimbler (1967), Kumar and Kimbler (1970) and Merritt (1986) demonstrated the negative effect of buoyancy on the recovery efficiency of ASR in saline aquifers. In their theoretical mixed-convection analysis, Ward et al. (2007) demonstrated that with ASR in saline aquifers, the recovery efficiency is affected by ambient water density, the injection and recovery flow rates, storage duration, hydraulic conductivity, thickness of the aquifer, and dispersive mixing. This work was further expanded by Ward et al. (2008, 2009), who considered the effects of anisotropy and lateral flow on the performance of ASR systems in saline aquifers.
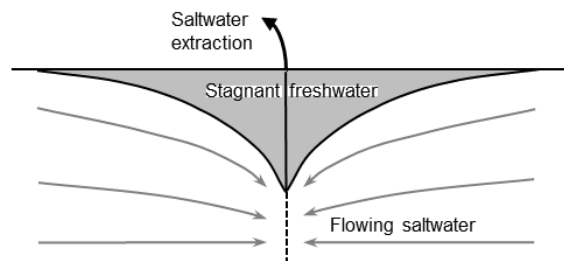

Figure 26: Freshwater storage in cone of depression of saltwater extraction well. The dark grey freshwater volume is trapped inside the cone of depression caused by the extracted salt water.

The objective of this chapter is to present a new operational paradigm for small-scale ASR in saline aquifers. It is proposed to combine freshwater storage with saltwater extraction from below the freshwater cone to increase the recovery efficiency of small-scale ASR in saline aquifers. The saltwater flow toward the well fixes the stored fresh water to the vicinity of the well, where it may be recovered later (Figure 26). This is similar to the technique of scavenger wells (Sufi et al. 1998; Aliewi et al. 2001; Asghar et al. 2002; Ali et al. 2004, Saeed and Ashraf 2005), but now with the objective to keep a fixed freshwater volume in place instead of maximizing the continuous extraction of fresh water. The method is especially useful in situations where the continuous flow of salt water can be used for desalination purposes, such as for many resorts along the Red Sea coast of Egypt, which inspired this method (van Ginkel et al. 2010).

4.3 Theoretical setup of the problem

Lack of fresh water is a central issue along the Egyptian Red Sea coast. The Egyptian Red Sea coastal area is virtually without recharge. Groundwater generally has a salinity that is equal to Red Sea water (salinity 42,000 mg/L). Aquifers consist of gravelly sand, with some limestone, and are directly connected to the sea. The thickness is several tens of meters and the hydraulic conductivity ranges from 10 to 50 m/d. Tourist resorts are continuously extracting saline groundwater and desalinate it by reverse osmosis. The freshwater demand of a resort varies seasonally between 1000 and 1500 m^3/d. Storage of fresh water may flatten out demand variations, thus potentially reducing the required reverse osmosis capacity.

Consider a regular ASR system for the seasonal storage of desalinated water along the Red Sea coast. The thickness of the aquifer is 20 m and the hydraulic conductivity is 30 m/d. The density of the native saline groundwater in the aquifer is 1030 kg/m^3. A volume of 10,000 m^3 of fresh water is injected over 3 months, followed by a storage period of 3 months. The recovery potential of this system is assessed with the screening tool of Bakker (2010). By considering Dupuit interface flow, Bakker (2010) shows that the recovery efficiency depends on a dimensionless parameter D, the relative lengths of the injection, storage and recovery phases, and the number of injection-storage-recovery cycles. The dimensionless parameter D is a function of the discharge of the well Q, the hydraulic conductivity K, the aquifer thickness H, and the dimensionless density difference:

$$D = \frac{Q}{K \upsilon H^2} \tag{5}$$

Where the dimensionless density difference is defined as:

$$\upsilon = (\rho_s - \rho_f)/\rho_f \tag{6}$$

For this example, the dimensionless parameter D is approximately 1 and based on Bakker's (2010) curves of recovery efficiency versus D the recovery efficiency is less than 5%. Therefore, a regular ASR system is not feasible in this setting. To increase the recovery efficiency of ASR systems under these circumstances, it is proposed to store and recover fresh water from the cone of depression of a saltwater extraction well, which is described in the remainder of this chapter.

4.4 Analytical solution

In this section, an analytical solution is derived for the steady flow of salt water toward a well with a volume of fresh water floating on top of the cone of depression. The analytical solution will be used to determine the required saltwater discharge for a given volume of fresh water. Consider steady radially symmetric flow of salt water toward a well in a homogeneous, horizontal, confined aquifer. Fresh water is in the storage phase and is stagnant. An interface separates fresh water with density ρ_f from salt water with density ρ_s. A cylindrical coordinate system is adopted with horizontal radial coordinate r and vertical coordinate z; the vertical datum is defined to be zero at the bottom of the aquifer and the horizontal datum is defined to be zero at the centre of the well. The elevation of the interface relative to the bottom of the aquifer as a function of r is written as $y(r)$ (Figure 27a).
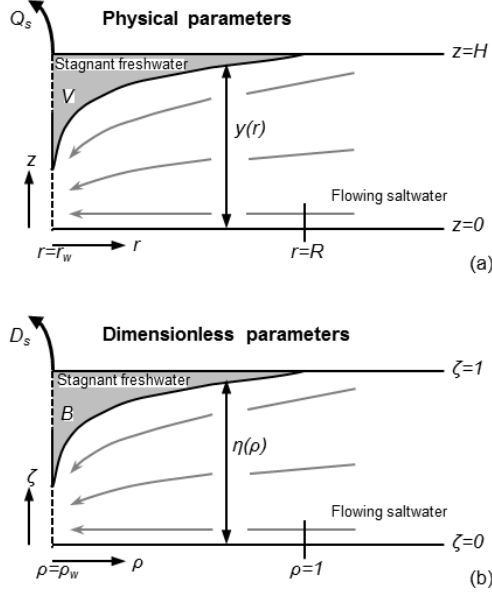
Figure 27: Radial interface flow problem definition in a) physical variables and b) dimensionless variables.

The Dupuit approximation is adopted, which means that resistance to vertical flow is neglected (e.g., Bakker 2010), and horizontal flow is uniformly distributed over the vertical. The total flow of salt water Q_s toward the well is constant at any distance r and may be written using Darcy's Law as:

$$Q_s = 2\pi r K y \frac{dh_s}{dr}, r < R \tag{7}$$

Where h_s is the saltwater head and R is the radius of the freshwater cone. The freshwater head in the fresh water zone is constant and equal to h_f. The freshwater pressure equals the salt water pressure anywhere along the interface:

$$\rho_f g\left(h_f - y\right) = \rho_s g(h_s - y) \tag{7}$$

So that the saltwater head can be written as:

$$h_s = \frac{\rho_f}{\rho_s} h_f + \frac{\rho_s - \rho_f}{\rho_s} y \tag{9}$$

The dimensionless density difference is defined as:

$$v_s = (\rho_s - \rho_f)/\rho_s \qquad (10)$$

Note the difference between the dimensionless density difference v_s used here and the density ratio v in Eq. 6 which is used in, e.g., Ward et al. (2007) and Bakker (2010). In contrast to regular ASR, the denominator in Eq. 10 is ρ_s instead of the usual ρ_f because the salt water is flowing rather than the fresh water.

Differentiation of Eq. 9 and using Eq. 10 gives:

$$\frac{dh_s}{dr} = v_s \frac{dy}{dr} \qquad (11)$$

Substitution of Eq. 10 for dh_s/dr in Eq. 7 gives:

$$Q_s = 2\pi r K v_s y \frac{dy}{dr} \qquad (12)$$

Eq. 12 may be integrated to obtain the elevation of the interface above the base of the aquifer:

$$\int y \, dy = \int \frac{Q_s}{2\pi K v_s} \frac{1}{r} dr + C \qquad (13)$$

Which gives:

$$y = \sqrt{H^2 + \frac{Q_s}{\pi K v_s} \ln \frac{r}{R}} \qquad (14)$$

Where the elevation of the interface relative to the bottom of the aquifer y is set equal to the thickness of the aquifer H at $r=R$. The volume V of the freshwater cone is calculated from the interface elevation as:

$$V = 2\pi n \int_{r_w}^{R} (H - y) r \, dr \qquad (15)$$

Where n is the porosity and r_w is the radius of the well.

Eq. 15 will be written in dimensionless form. Three dimensionless variables are introduced (Bakker 2010): The dimensionless radial coordinate σ, the dimensionless vertical coordinate ζ, and the dimensionless vertical position of the interface η (Figure 27b):

$$\sigma = \frac{r}{R}, \qquad \zeta = \frac{z}{H}, \qquad \eta = \frac{y}{H} \tag{16}$$

Two dimensionless parameters are introduced (Figure 27b): the dimensionless volume of the fresh water cone B:

$$B = \frac{V}{\pi H R^2 n} \tag{17}$$

And the dimensionless salt water discharge D_s:

$$D_s = \frac{Q_s}{K v_s H^2} \tag{18}$$

In contrast to Bakker's dimensionless parameter D (Eq. 5), which governs the freshwater flow in a regular ASR system, the subscript s for D_s and Q_s is used to indicate saltwater flow. Substitution of Eq. 14 for y in Eq. 15 and writing the volume of the freshwater cone in dimensionless form gives:

$$B = 2 \int_{\sigma_w}^{1} \left(1 - \sqrt{1 + \frac{D_s}{\pi} \ln\sigma} \right) \sigma d\sigma + C \tag{19}$$

Where σ_w is the dimensionless radius of the well:

$$\sigma_w = \frac{r_w}{R} \tag{20}$$

The result of the integral (Eq. 19) is:

$$B = \sqrt{\frac{D_s}{2\pi}} \mathrm{F}\left(\sqrt{\frac{2\pi}{D_s}}\right)$$

$$- \sigma_w^2 \left[\sqrt{\frac{D_s}{2\pi}} \mathrm{F}\left(\sqrt{ln\sigma_w^2 + \frac{2\pi}{D_s}}\right) - \sqrt{\frac{D_s}{\pi}} ln\sigma_w + 1 \right. \tag{21}$$

$$\left. + 1 \right]$$

Where F is the Dawson integral (Olver et al. 2010, formula 7.2.5).

The second term of Eq. 21 may be neglected because r_w<<R and therefore σ_w<<1. Hence, the relation between the dimensionless volume of the freshwater cone B and the dimensionless saltwater discharge D_s is:

$$B = \sqrt{\frac{D_s}{2\pi}} \mathrm{F}\left(\sqrt{\frac{2\pi}{D_s}}\right) \tag{22}$$

The dimensionless saltwater discharge D_s is plotted as a function of the dimensionless volume of the freshwater cone B in Figure 28 for a wide range of parameter values (Table 3). The required saltwater discharge to keep a specific freshwater volume in place can be determined from the graph in Figure 28 when the desired freshwater volume and the aquifer characteristics are known.

Table 3

Ranges of the physical parameters of the problem

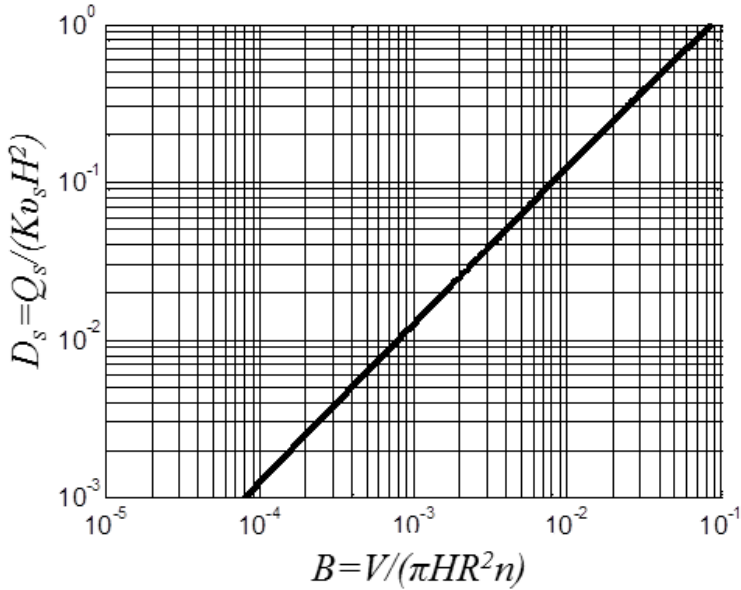| Parameter	Range
Saltwater discharge Q_s	100-1,000 m³/day
Hydraulic conductivity K	1-50 m/day
Aquifer thickness H	10-50 m
Dimensionless density difference υ_s	0.002-0.04
Effective porosity n	0.1-0.4
Volume of the freshwater cone V	5,000-100,000 m³
Radius of the freshwater cone R	50-500 m

Figure 28: Dimensionless saltwater discharge D_s as a function of the dimensionless volume of the freshwater cone B.

4.5 Numerical modelling

In the previous section, it was determined what saltwater extraction rate is needed to store a certain volume of fresh water. In the remainder of this chapter it will be studied how the fresh water can be recovered. The recovery efficiency and the system's behaviour are studied for three different recovery approaches with a numerical model.

The analytical solution (Eq. 22) is based on the approximation that fresh water and salt water are separated by an interface. In reality, there is a transition zone between the freshwater and saltwater zones, in which there is a gradual change in salinity and density. The dynamics of flow in the transition zone may be simulated with a numerical model for variable density groundwater flow and solute transport. The SEAWAT computer code (Langevin et al. 2008) is used in the *mfLab* environment (Olsthoorn 2013) in this study. A model is constructed for the situation along the Egyptian Red Sea coast. Model parameters are listed in Table 4. A freshwater volume of 10,000 m³ is stored within a cylinder with a radius of 120 m. For the given aquifer parameters, the value of the dimensionless volume B equals 0.03. The corresponding dimensionless saltwater discharge D_s equals 0.37 (Figure 28). This means that a saltwater

extraction of 130 m³/d is needed to store a freshwater volume of 10,000 m³ under these circumstances.

The ASR system is modelled as a radially symmetric system (Figure 27). The top and bottom of the model are no-flow boundaries, representing the impermeable confining layers above and below the aquifer. A constant-head boundary is defined as boundary condition at the edge of the model. Separate screens and a packer inside the casing are necessary to separate the fresh water and salt water. The freshwater injection and recovery screen is located at the upper 5 m of the aquifer; the saltwater extraction screen is located at the lower 5 m of the aquifer.

Table 4
Parameter values used for the numerical simulation

Parameter	Value
Hydraulic conductivity K	30 m/day
Aquifer thickness H	20 m
Effective porosity n	0.35
Radius of the freshwater cone R	120 m
Longitudinal dispersivity α_L	0.05 m
Transverse dispersivity α_T	0.005 m
Ambient water concentration C_a	42,000 mg/L
Injected water concentration C_i	0 mg/L
Constant head at boundary	0 m
Height of the model	20 m
Radius of the model	200 m
Cell height Δz	0.5 m
Cell width Δr	0.5-5 m
Injected freshwater volume V	10,000 m³
Time of injection, storage, recovery, idle	3 months

In SEAWAT, the preconditioned conjugate gradient (PCG) package is employed for the flow equation and the preconditioning method is Cholesky. The generalized conjugate gradient (GCG) package is used for the dispersion and source terms of the transport equation. The third-order total variation diminishing (TVD) scheme is used to solve the advection term.

4.6 Recovery approaches

Three recovery approaches are examined. In recovery approach 1, fresh water is injected and recovered by the same well. In recovery approach 2, fresh water is stored between vertical impermeable barriers. In recovery approach 3, fresh water is recovered with several circular recovery drains. Recovery is terminated when the average salinity in the well exceeds the Egyptian guideline for drinking water of 500 mg/L total dissolved solids (TDS). The process is

repeated for five cycles. The duration of a cycle is one calendar year. One cycle is divided into four periods: an injection period of 3 months, a storage period of 3 months, a recovery until drinking water standard is reached (maximum 3 months), and an idle period until the year is complete. The recovery efficiency μ is defined as the ratio between injected volume V_i and recovered volume V_r during a cycle:

$$\mu = \frac{V_r}{V_i} \tag{23}$$

4.6.1 Approach 1: Upper screen same well

In recovery approach 1, fresh water is recovered with the upper screen. First, the recovery efficiency is examined when the saltwater extraction is equal to the freshwater extraction during recovery: $Q_s = Q_f = 130$ m³/d. The steady-state position where fresh water is stagnant has not been reached after a storage period of 3 months. The radius of the freshwater cone after a storage period of 3 months is 60 m, which is approximately five times its height (12 m). During recovery, the interface rapidly rises to the upper screen. The toe of the interface reaches the bottom of the freshwater screen before much fresh water is recovered (Figure 29a).

The average salinity in the well reaches the threshold value after 5 d and fresh water recovery is terminated; the recovery efficiency is only 7%. The remaining fresh water is left behind in the aquifer during the idle period. The recovery efficiency increases in subsequent cycles, till 30% in the fifth cycle. Results for the recovery efficiency are shown in Figure 30. It is recalled that with regular ASR (i.e., no salt water extraction), the recovery efficiency is negligible, as discussed after Eq. 6 in Section 4.3.
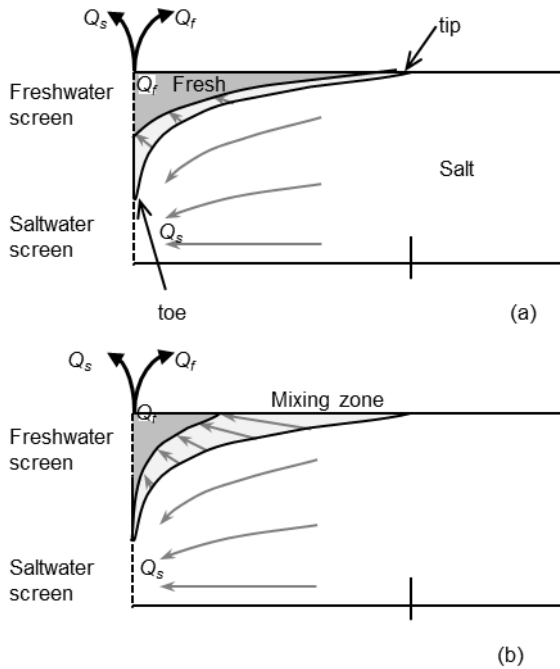
Figure 29: Schematization of fresh water and saltwater extraction using the same well a) if $Q_s=Q_f$ and b) if $Q_s>Q_f$ (vertical scale exaggerated).

More fresh water can be recovered by increasing the salt water extraction during freshwater recovery (Figure 29b). In practice, this might be done automatically based on an EC-sensor in the upper screen. Results for the recovery efficiency for $Q_s=2Q_f$ and $Q_s=10Q_f$ are shown in Figure 30. When $Q_s=2Q_f$ the recovery efficiency is 10% in the first cycle and 50% in the fifth cycle. When $Q_s=10Q_f$ the recovery efficiency is 60% in the first cycle and 70% in the fifth cycle. These results indicate that reasonable recovery efficiencies are feasible with recovery approach 1 when a large salt water extraction is used during freshwater recovery. This results in large saltwater volumes which might exceed the capacity of the desalination plant and need to be discharged. It is noted that the recovery efficiency is not a function of the values of Q_f and Q_s, but only of the ratio Q_f/Q_s.
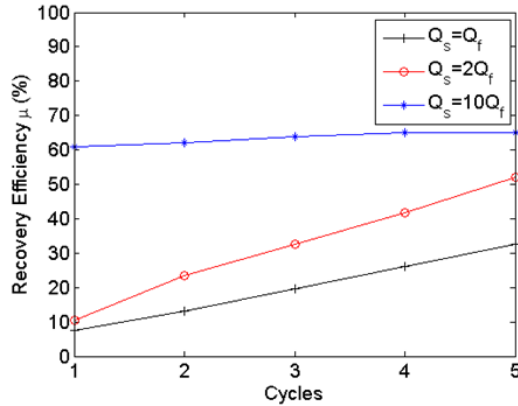
Figure 30: Recovery efficiency for different salt water extraction rates during recovery.

The SEAWAT results for cycle 1 with $Q_s = 2Q_f$ are shown in Figure 31.
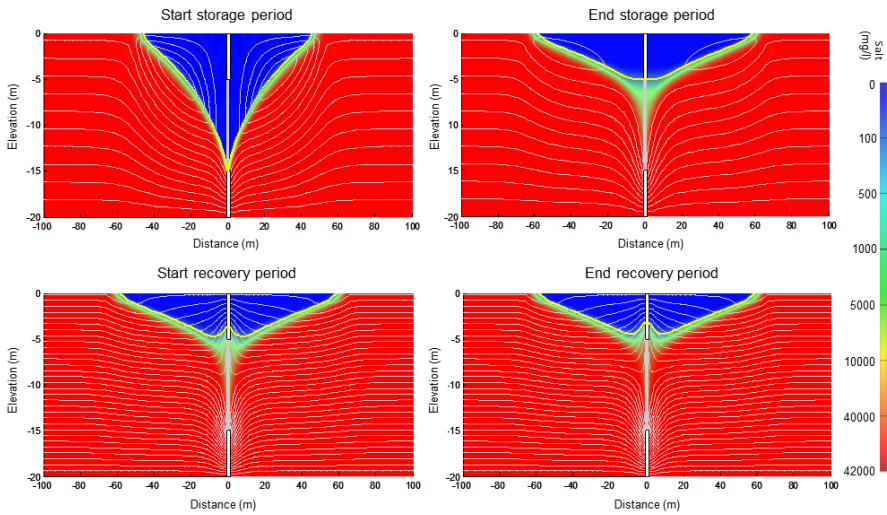

Figure 31: Flow simulation snapshots for different phases during cycle 1 with $Q_s=2Q_f$. The yellow line indicates the Egyptian guideline for drinking water (500 mg/L TDS), the white lines are instantaneous streamlines.

4.6.2 Approach 2: Upper screen same well and flow barriers

As described in the previous section, the radius of the freshwater cone is about five times its thickness after a storage period of 3 months. As a result, not much fresh water can be recovered without additional measures. In recovery approach 1, the recovery efficiency was increased by extracting more salt water during recovery. Another approach to increase the recovery efficiency is to limit the radius of the freshwater cone by means of subsurface impermeable barriers.

Subsurface impermeable barriers partly penetrate the aquifer at a limited distance from the well (Figure 32a) and obstruct the fresh water cone from expanding radially, resulting in a deeper location of the interface toe. The barriers may be constructed of sheet piles, clay, or other impermeable materials.

(a)

(b)
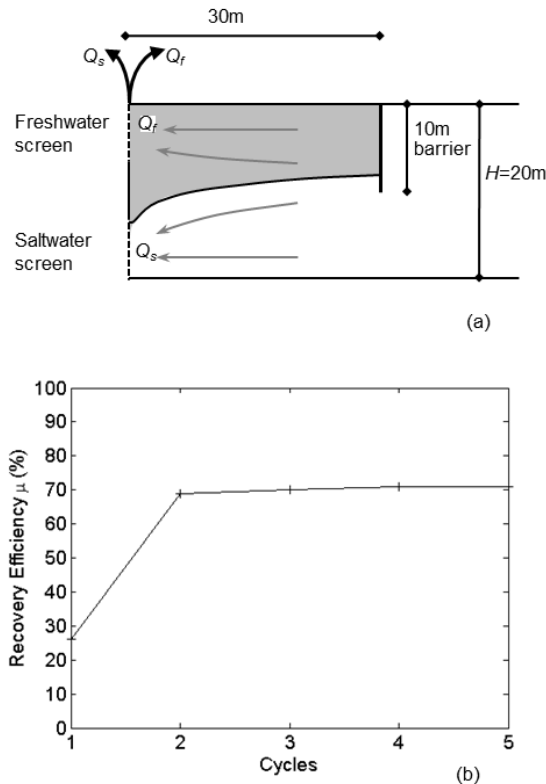
Figure 32: a) ASR system with vertical barriers and b) calculated recovery efficiency in successive cycles with $Q_s=Q_f=130$ m^3/d.

For this analysis, a barrier is placed at 30 m from the well, decreasing the radius of the cone during storage by a factor of two. The barrier extents to 10 m below the top of the aquifer. The saltwater extraction is equal to the freshwater extraction during recovery: $Q_s=Q_f=130$ m³/d. The recovery efficiency is 26% in the first cycle and increases to 70% in the second cycle but remains fairly constant thereafter (Figure 32b). This limit of 70% is due to the maximum storage volume between the barriers as defined by their radius and depth. Fresh water reaches the bottom of the barriers in the second cycle. Fresh water escapes underneath the barriers in subsequent cycles, which makes this water unrecoverable and the recovery efficiency does not increase in successive cycles. Leakage can be largely prevented when the optimal distance between the barriers and the depth of the barriers for an intended volume is determined by numerical modelling.

An advantage of recovery approach 2 is that saltwater extraction is not necessary during the storage phase. The model was run both with $Q_s=Q_f$ and without salt water extraction. The calculated recovery efficiency for recovery approach 2 with and without saltwater extraction during the storage phase is similar. Application of subsurface barriers in practice is restricted by the feasibility of construction and is, therefore, most attractive in shallow aquifers.

4.6.3 Approach 3: Circular recovery drains or shallow recovery wells

A third recovery approach is to extract fresh water over a larger areal extent of the freshwater cone by several circular recovery drains or shallow recovery wells as shown in Figure 33a.

As an example, four circular recovery drains are used with radii of 10, 20, 30, and 40 m surrounding the central well. Each recovery drain stops pumping as soon as the average salinity in the drain reaches the threshold value. The freshwater discharge is evenly distributed over the drains and the sum of all freshwater extractions $\sum Q_f=Q_s=130$ m³/d. The saltwater extraction is equal to the sum of the discharges of the recovery drains and decreases as recovery drains stop pumping. The recovery efficiency is 70% in the first cycle and increases to 80% in successive cycles (Figure 33b). This is just an example of a recovery approach that works reasonably well. Other configurations may work better. Optimization in terms of number and radii of the drains is beyond the scope of this study.
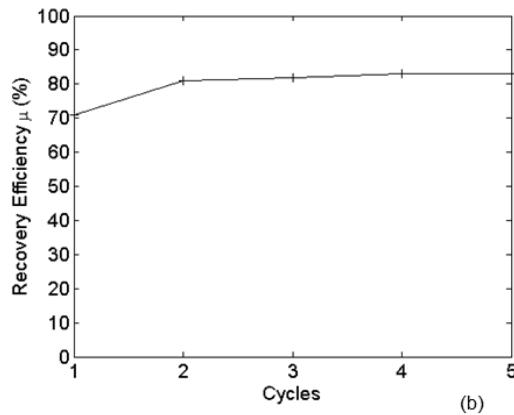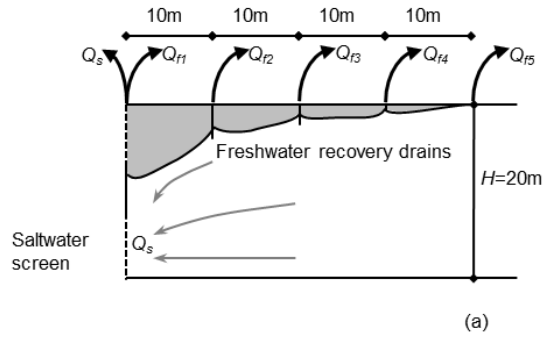
Figure 33: a) ASR system with multiple recovery drains and b) calculated recovery efficiency in successive cycles, $\sum Q_f = Q_s = 130$ m³/d.

4.7 Sensitivity analysis

4.7.1 Effect of ambient flow

Ward et al. (2009) studied the impact of ambient groundwater flow on the recovery efficiency of regular ASR systems in saline aquifers. They found that ambient groundwater flow causes a distorted, noncircular plume during the injection phase, lateral translation of the plume in the storage phase, and an asymmetrical capture zone in the recovery phase. The effect of ambient groundwater flow on the recovery efficiency of the proposed recovery approaches is examined next.

Consider recovery approach 1 with $Q_s = 2Q_f$. Results for the case without ambient groundwater flow are shown in Figure 30. Recovery efficiencies are calculated for cases with a background hydraulic gradient of respectively 1, 2,

and 5‰ and are compared with the results for the case without ambient groundwater flow. The recovery efficiency of these simulations is shown in Figure 34a. For hydraulic gradients of 1 or 2‰, a large portion of the stored volume remains around the well by the applied saltwater pumping, thus preventing the freshwater cone from drifting along with the ambient groundwater. The recovery efficiency decreases in the fifth cycle from 50% to 40% when a hydraulic gradient of 1‰ is applied compared to the situation without ambient groundwater flow. A hydraulic gradient of 2‰ results in a decrease in recovery efficiency in the fifth cycle from 50% to 30% compared to the situation without ambient groundwater flow. When a hydraulic gradient of 5‰ is applied, the stored volume drifts along with ambient groundwater and the recovery efficiency is zero.

The application of flow barriers around the well protects the freshwater cone from ambient groundwater flow. This is an advantage of recovery approach 2. The calculated recovery efficiencies for simulations with flow barriers and ambient groundwater flow are shown in Figure 34b. The calculated recovery efficiency of the first cycle remains the same when a hydraulic gradient of 1 or 2‰ is applied compared to the situation without ambient groundwater flow. The recovery efficiency decreases in subsequent cycles as compared to the situation without ambient groundwater flow, because of an increase of downstream leakage of fresh water under the flow barrier, but the relative decrease is much smaller than for recovery approach 1. When a hydraulic gradient of 5‰ is applied, the stored volume is not recoverable in the first cycle, but the recovery efficiency increases in subsequent cycles.

The calculated recovery efficiencies for simulations with recovery drains and ambient groundwater flow are shown in Figure 34c. The configuration of the recovery drains is the same as in Figure 33a. A hydraulic gradient of 1 and 2‰ results in a decrease in recovery efficiency in the fifth cycle from 80% to 75% and 57% respectively, compared to the situation without ambient groundwater flow. When a hydraulic gradient of 5‰ is applied, the stored volume drifts along with ambient groundwater and the recovery efficiency is zero. Optimization is possible when shallow recovery wells are applied, and the well positions are biased toward the down-gradient direction to recapture fresh water that has moved away from the central well.
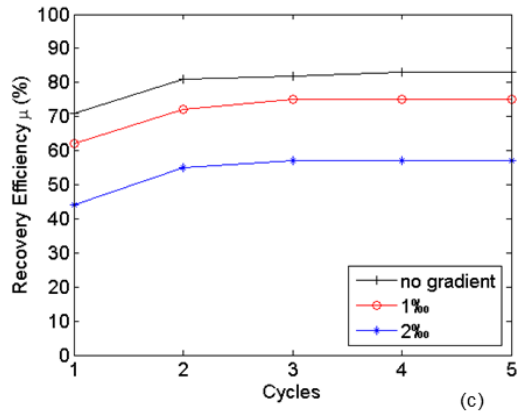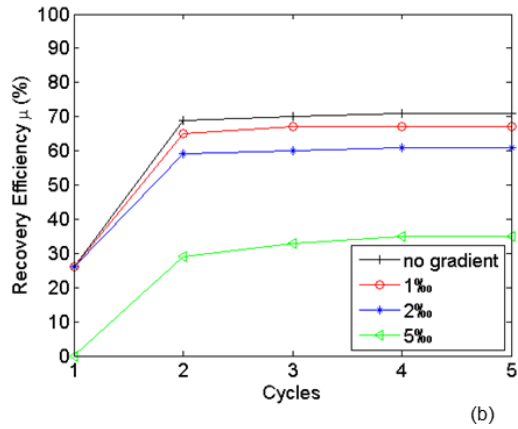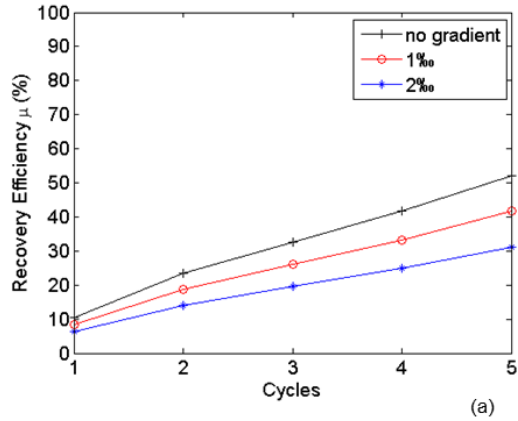
Figure 34: Calculated recovery efficiency in successive cycles for different rates of ambient flow. The labels indicate the piezometric gradient of the ambient flow. a) Recovery approach 1 upper screen same well where $Q_s=2\,Q_f$, b) recovery approach 2 upper screen same well with barriers where $Q_s=Q_f$, and c) recovery approach 3 circular recovery drains or shallow recovery wells where $\sum Q_s=Q_f$.

4.7.2 Effect of interruptions of saltwater pumping

Saltwater extraction may be interrupted during power outages and maintenance, which may cause the fresh water to float upward to the top of the aquifer. Such an interruption during the storage phase may affect the recovery efficiency of recovery approaches 1 and 3. The recovery efficiency of recovery approach 2 is not affected by an interruption during the storage phase, as the freshwater cone is horizontally bounded by vertical barriers and saltwater extraction is not necessary during storage.

The effect of interruption of saltwater pumping during storage in the first cycle on the recovery efficiency of recovery approach 1 with $Q_s=2Q_f$ is shown in Table 5. Numerical simulations show that the timing of the interruption of saltwater pumping during the storage period is important. It is possible to restore the freshwater cone after an interruption of 10 d at the beginning and in the middle of the storage period. When saltwater pumping is interrupted 10 d before the start of the recovery period, there is not enough time to restore the freshwater cone, which results in a lower recovery efficiency.

Table 5
Effect of interruption of saltwater pumping
Cycle 1 Recovery approach 1 $Q_s=2Q_f$

Interruption	Recovery efficiency (%)
No interruption	10
Day 1-10 of the storage phase	10
Day 40-50 of the storage phase	9
Day 80-90 of the storage phase	5

Numerical simulations show that the recovery efficiency via recovery drains is the same after an interruption of saltwater pumping of 10 d during the storage phase as compared to a situation without interruption of saltwater pumping.

4.8 Conclusions

A new operational paradigm for small-scale ASR in saline aquifers was presented. The main feature of the new paradigm is that freshwater storage is combined with saltwater extraction from below the freshwater cone. The saltwater extraction counteracts the buoyancy due to the density difference between fresh water and salt water, thus reducing the upward flow of fresh water. The method is especially useful in situations where the continuous flow of salt water can be used for desalination purposes. As an example, the

operational paradigm was applied for the seasonal storage of fresh water produced by desalination plants in a tourist resort.

An analytical Dupuit solution was presented to compute the saltwater discharge which is required to store a given volume of fresh water. The analytical solution defines the relation between the stored volume of fresh water, the saltwater extraction, and the maximum radius of the freshwater cone.

Numerical modelling was carried out to determine how the stored fresh water can be recovered. Three recovery approaches were examined. In recovery approach 1, fresh water is recovered from the upper screen. The recovery efficiency increases in successive cycles. Acceptable recovery efficiencies are obtained for larger saltwater extractions during freshwater recovery. The downsides of this approach, however, are firstly that a large amount of salt water must be processed which probably exceeds the capacity of the desalination plant and secondly that the storage is vulnerable for ambient groundwater flow and interruptions in saltwater pumping.

In recovery approach 2, flow barriers surrounding the well obstruct the freshwater cone from expanding radially, and saltwater extraction is not necessary during the storage phase. The recovery efficiency reaches a limit in successive cycles due to the maximum storage capacity between the barriers defined by their radius and depth. A disadvantage of this approach is that fresh water leaking under the barriers is unrecoverable. Leakage can be largely prevented when the optimal distance between the barriers and the depth of the barriers for an intended volume is determined by numerical modelling. Advantages of the application of flow barriers around the well are firstly that the flow barriers protect the freshwater cone from ambient flow and secondly that the system is not affected by an interruption of saltwater pumping.

In recovery approach 3, fresh water is extracted over a larger areal extent of the freshwater cone by several circular recovery drains or shallow recovery wells. The recovery efficiency may be reduced by ambient groundwater flow and by interruptions in saltwater extraction during the storage phase. It is concluded that recovery approach 2 is the most effective of the three recovery approaches.

CHAPTER 5 DISTRIBUTION OF GRAIN SIZE AND RESULTING HYDRAULIC CONDUCTIVITY IN LAND RECLAMATIONS

This chapter is based on:
Van Ginkel, M., T.N. Olsthoorn *Distribution of grain size and resulting hydraulic conductivity in land reclamations constructed by bottom dumping, rainbowing and pipeline discharge*, Water Resources Management, 2019
Some changes have been made in the introduction and in the section headings for reasons of consistency

5.1 Chapter introduction

The previous chapters focussed on preferable physical properties and operational conditions of land reclamations for freshwater storage and recovery. Besides the preferred physical and operational conditions, one should also consider what is creatable within current dredging practice. It appears that little is known about the aquifer properties that can be created. Dredging techniques have been studied intensively, but these studies have mainly focussed on geotechnical aspects that are related to bearing capacity, settlement and risk of liquefaction and have not considered properties such as the hydraulic conductivity. In this chapter, the distribution of grain size and resulting hydraulic conductivity of land reclamations are considered that are constructed by a combination of bottom dumping, rainbowing and discharging the sand-water mixture by pipeline.

Section 5.2 presents the rationale for the study and Section 5.2 and Section 5.3 provide generic background information on the placement methods used in the construction of land reclamations. Pumping tests are commonly applied to determine the hydraulic characteristics of the subsurface. However, pumping tests were not available for this study because land reclamations have been barely studied hydraulically. Therefore, grain-size distribution curves and cone-penetration tests were considered of study area D2 in Maasvlakte II, the Netherlands. These data are supplemented with the geotechnical data of the four other land reclamations that could be found in the literature. The data is presented in Section 5.4.

Section 5.5 analyses the sedimentation from a sand-water mixture as a result of bottom dumping. The analysis provides insight in the grain sorting as it varies from place to place in the bottom-dumped fill. The structure of the obtained porous media is validated by comparison with semi-variograms of cone-penetration tests. In Section 5.6 and Section 5.7, similar analyses are executed for rainbowing and pipeline discharge, respectively. Finally, the consequences for the hydraulic conductivity of land reclamations are synthesized in Section 5.8. It is found that all placement methods lead to some degree of heterogeneity, so that the hydraulic conductivity in land reclamations is not fully constant and this is important to consider when designing water storage in future land reclamations.

5.2 Geohydrological properties of land reclamations

Urban expansions in seaward direction by means of land reclamations occur worldwide in highly urbanised coastal areas for residential, industrial and recreational development, and for ports and airports. Fresh water often already is a critical resource in these coastal areas, because of overexploitation due to urbanisation, economic development and climate change (e.g., Loucks 2017; Koop et al. 2017). Fresh water from the mainland is, therefore, often not available for urban development on the reclamation. Hence, it is important to arrange freshwater supply on the new land by means of desalination or rainwater collection, storage and reuse. Van Ginkel (2015) pointed out that land reclamations have potential for the managed storage of fresh water in the subsurface of the reclamation for later recovery and use analogous to a freshwater lens, as can be found under natural islands in the ocean (e.g., Stoeckl et al. 2016). Such systems are otherwise known as Aquifer Storage Recovery (ASR; Pyne 1995) and can provide a robust, effective and cost-efficient solution to manage freshwater resources (e.g., Zuurbier et al. 2016).

Figure 35 presents the minimum and maximum grain-size distribution curves of reclamations constructed in the Netherlands, the United Arab Emirates, Malaysia, and China. These reclamations consist of fine to coarse sand. The corresponding porosity and hydraulic conductivity values are, therefore, likely to be moderate to high. At first sight, these conductivities seem to make these land reclamations suitable for the development of a natural freshwater lens or the artificial storage of fresh water for later recovery and use. Such systems are otherwise known as aquifer storage recovery (ASR; Pyne 1995). Van Ginkel (2015) has pointed out that ASR in land reclamations has large potential for fresh water supply.

In the literature, the hydraulic conductivity in land reclamations is generally considered fairly homogeneous compared to natural soils in which layering, and anisotropy are ubiquitous. Jiao et al. (2001; 2006) and Huizer et al. (2017), for instance, applied a constant porosity and conductivity for the land reclamation when they studied the increase of the freshwater volume under adjacent old land caused by land reclamations in Hong Kong, China and along the Dutch North Sea coast.
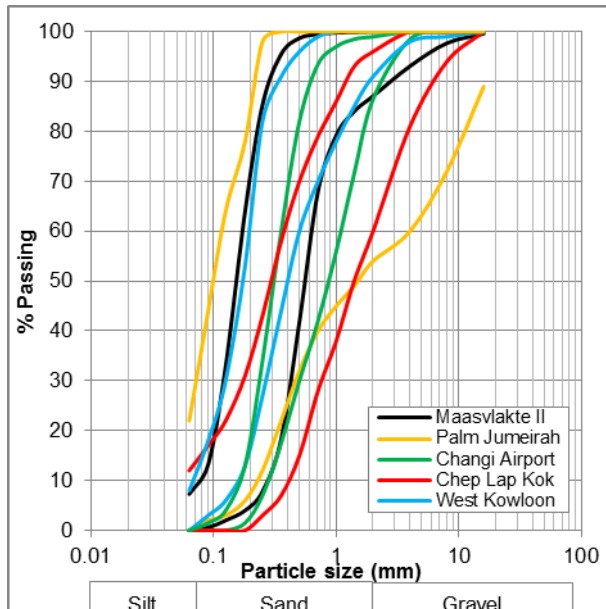
Figure 35: The minimum and maximum grain-size distribution curves of samples taken from the Maasvlakte II, Rotterdam, the Netherlands, Palm Jumeirah, Dubai, the United Arab Emirates (Lees et al. 2013), Changi Airport, Singapore, Malaysia (Chua et al. 2007), Chep Lap Kok, Hong Kong, China (Lee 2001), West Kowloon, Hong Kong, China (Lee et al. 1999).

However, several geotechnical scientists, including Sladen and Hewitt (1989), Lee et al. (1999), Lee (2001), Chang et al. (2006) and Chua et al. (2007), analysed the results of cone-penetration tests taken on land reclamations that were constructed using different placement methods. They concluded that the grain sorting and the degree of compaction differed per placement method. Since each land reclamation is constructed with material originating from a single source area, these differences are attributed to the sedimentation characteristics pertaining to each placement method. Which implies that different placement methods also cause different hydraulic properties within land reclamations. This is because porosity is determined by the degree of sorting and compaction. Hydraulic conductivity also depends on grain characteristics (Bear 1972) which more profoundly determines the difference in hydraulic properties between land reclamations because of different source areas.

Chua et al. (2007), in Singapore, obtained different values for hydraulic conductivity and groundwater flow velocity at different depths within a land reclamation that was constructed by bottom dumping, rainbowing and

pipeline discharge. Hydraulic conductivity values between 10 and 94 m/d were obtained with slug tests, a repacked sand column test, a step-drawdown test and grain-size analyses. No other studies that specifically address the hydraulic properties of land reclamations were found in the literature.

Average conductivity values may be sufficient to determine external hydrological effects of land reclamations. However, more detailed information is required if land reclamations are to be considered for water storage as part of their freshwater supply (Van Ginkel 2015). The objective of this paper, therefore, is to investigate the distribution of grain size and the resulting hydraulic conductivity of land reclamations that are constructed by the most commonly applied placement methods, which are bottom dumping, rainbowing and discharging the sand-water mixture by pipeline.

5.3 Placement methods used in the construction of land reclamations

The construction of land reclamations involves a number of consecutive phases (Van 't Hoff and Van der Kolff 2012). Firstly, the fill material is dredged, secondly, this material is transported to the reclamation site, thirdly, the fill material is placed, and lastly, if necessary, ground improvement of the fill material is applied. Land reclamations are often constructed using so-called Trailing Suction Hopper Dredgers (TSHD), which are vessels equipped with devices to loosen sand at the seabed, mix it with process water and suck the sand-water mixture into the vessel. Process water is spilled overboard to allow filling the TSHD to its maximum capacity. Because the overflowing water caries along fines, the content of fines in the TSHD is lower than at the borrow area (Van Rhee 2002). Once filled, the TSHD sails to the reclamation site and discharges the sand-water mixture by bottom dumping, rainbowing or via floating pipelines. The hopper capacity of TSHDs varies between 4000 m^3 and 35.000 m^3 of which the larger ones are used for land reclamations (Van 't Hoff and Van der Kolff 2012). Table 6 lists the characteristics of TSHDs currently operated by the Dutch dredging companies Van Oord and Boskalis (2018).

Table 6	
Characteristics of Trailing Suction Hopper Dredgers	
Hopper capacity	4.000-35.000 m3
Draught	7-14 m
Length over all	100-230 m
Breadth	20-32 m
Discharge pipeline diameter	1 m

The placement methods, namely bottom dumping, rainbowing and discharging by floating pipelines, are often executed in sequence. Bottom dumping is the quickest placement method but can only be applied when there is sufficient water depth (Figure 36a). The sand-water mixture falls through the water column by opening the bottom doors or splitting the hull of the TSHD. A TSHD with a typical capacity of 20.000 m^3 can unload by bottom dumping in approximately 5 minutes. Dumps are deposited in a random pattern until the water depth becomes too shallow for the TSHD.

Rainbowing consists of high-velocity pumping of the sand-water mixture above seawater level, which is done from a nozzle on board of the TSHD onto the reclamation site (Figure 36b). This method is usually applied until the reclamation rises above sea level. A 20.000 m^3 TSHD can unload by rainbowing in approximately 60 minutes. Above sea level, the sand-water mixture is discharged to the reclamation site by floating pipelines, where bulldozers guide the flow of the sand-water mixture by setting up bunds (Figure 36c). In this process, the bulldozers also compact the sand.

According to Morgenstern and Kupper (1988), these are the most commonly applied placement methods for hydraulic filling. Other placement methods are known (Van 't Hoff and van der Kolff 2012). One of them is pumping through a spreader or diffuser which is often used to attain an equal spreading on top of a soft seafloor. However, no data could be found of land reclamations constructed by those other placement methods, so these were not included in this study.
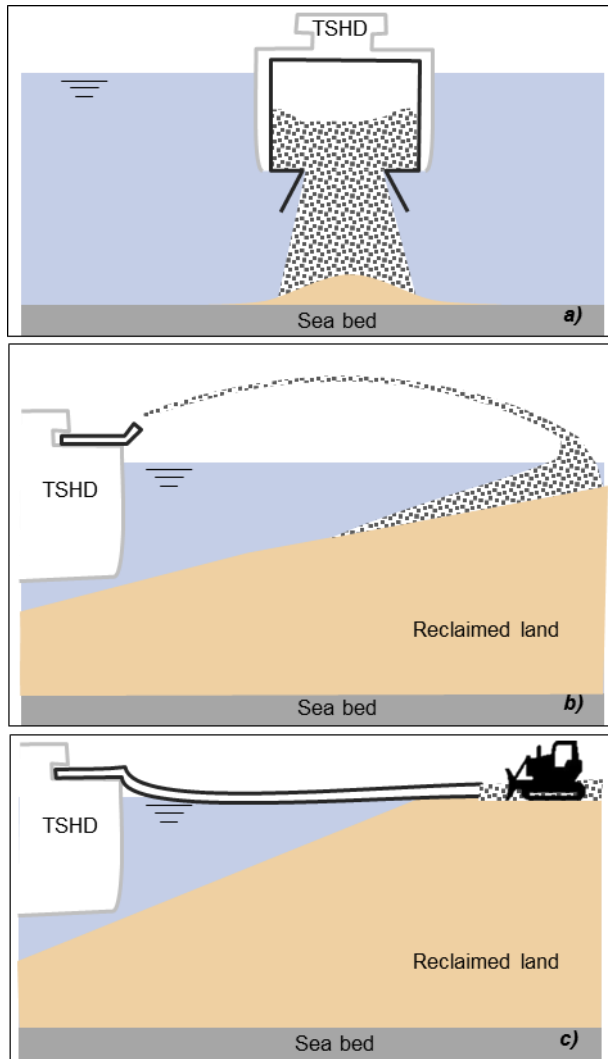
Figure 36: Placement methods: a) bottom dumping, b) rainbowing, and c) pipeline discharge.

5.4 Data case study and reference cases

5.4.1 Case study Area D2 Maasvlakte II, the Netherlands

Maasvlakte II is a large-scale, 2000 ha, expansion of the port of Rotterdam in the Netherlands that was constructed from 2008 to 2013. Figure 37 presents the location of Maasvlakte II in the Netherlands and study area D2 in the southern part of Maasvlakte II. The placement methods and depths as applied in study area D2 are essentially the same as elsewhere in the Maasvlakte II. Bottom dumping was applied until -7 m mean sea level (MSL), followed by rainbowing to bring the reclamation up to MSL. Fill material above this level was placed by pipelines to achieve the final elevation of +5.35 m MSL.
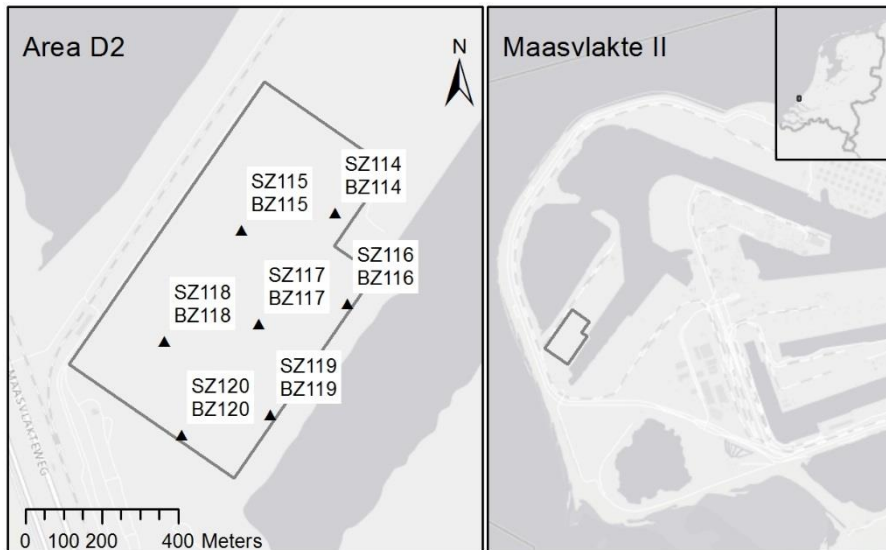
Figure 37: Location of study area D2 at Maasvlakte II, the Netherlands.

Maasvlakte II is constructed of quartz sand of marine origin (Vessies 2012). The black lines in Figure 35 present the outer ranges of the grain-size distribution. In study area D2 soil samples were taken at a total of seven borehole locations, as presented in Figure 37. The soil samples were taken every 2 m depth, up to 10 m below ground level, and the sieve curves of the soil samples were determined. Figure 38 shows D_{10} and D_{50} of the soil samples and indicates which placement method was adopted at which depth.
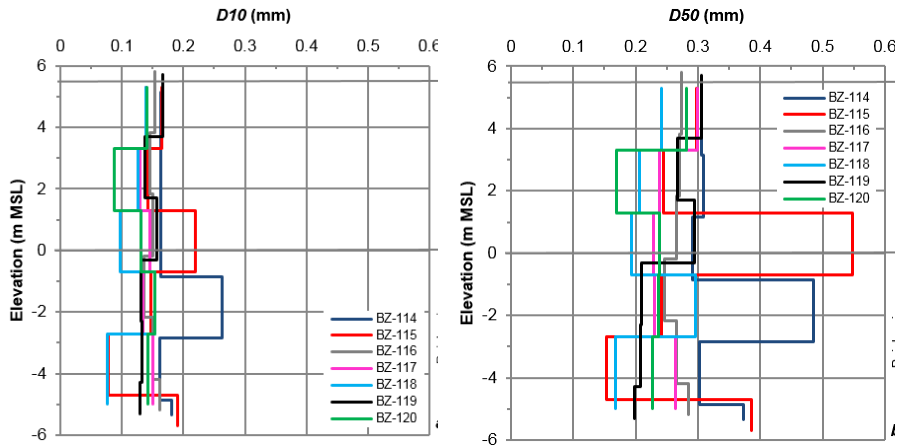
Figure 38 a) D10 (mm) and b) D50 (mm) over depth of the soil samples taken at Maasvlakte II-study area D2.

Seven cone-penetration tests (CPTs) were taken in the study area. Figure 39 shows the CPTs and indicates which placement method was adopted at which depth. The cone-penetration resistance, q_c, varies from 5 to 25 MPa in sands under MSL (Robertson 1989). A low penetration resistance in combination with a high friction ratio generally indicates finer sand, and a higher penetration resistance indicates coarser sand. The CPTs show the composition of the sand across the depth in more detail than the sieve curves, because the soil samples are disturbed. The CPTs, therefore, provide a more detailed picture of the grain-size distribution than the soil samples.
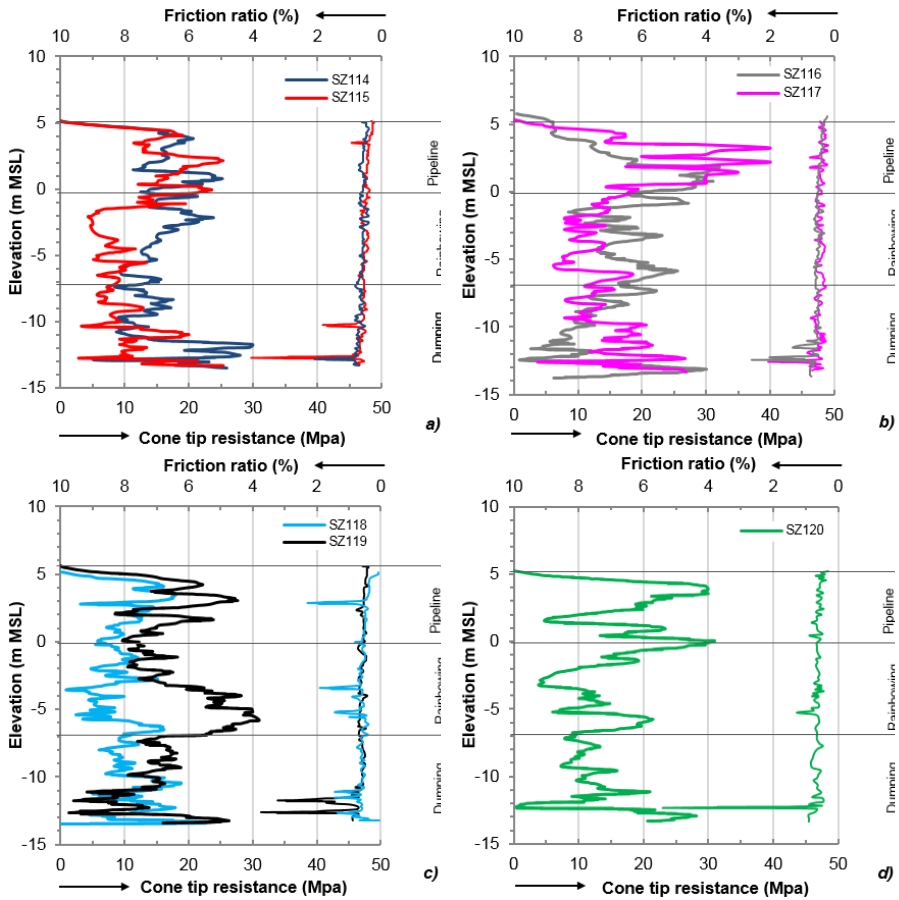
Figure 39: Cone-tip resistance (left lines) and friction ratio (right lines) at Maasvlakte II-study area D2.

5.4.2 Data reference cases Palm Jumeirah, Changi Airport, Chep Lap Kok and West Kowloon

Data of Maasvlakte II-study area D2 has been supplemented with the grain-size distribution curves and cone-penetration tests that were previously presented in the work of Lees et al. (2013), Chua et al. (2007), Lee (2001) and Lee et al. (1999). They studied land reclamations that were constructed in the United Arab Emirates, Malaysia, and China, respectively. These land reclamations were also constructed by a combination of bottom dumping, rainbowing and pipeline discharge. Dimensions and construction details of these land reclamations can be found in the references. To the authors' knowledge, no other geotechnical data on land reclamations is available in the literature. The available studies all investigated the details and data of one land

reclamation; this paper, however, considers all these site-specific details and data in combination.

Figure 35 presents the outer ranges of the grain-size distribution of the considered reference cases. Quartz sand of marine origin was used at Changi Airport (Chua et al. 2007), Chep Lap Kok (Lee 2001) and West Kowloon (Lee et al. 1999). Shelly carbonate sand was used at Palm Jumeirah (Lees et al. 2013). Shells are very angular and typically have a wider grain-size distribution than quartz grains, which is mainly due to crushing during construction (Lees et al. 2013). Figure 40 shows the CPTs of the reference cases and indicates which placement method was adopted at which depth.
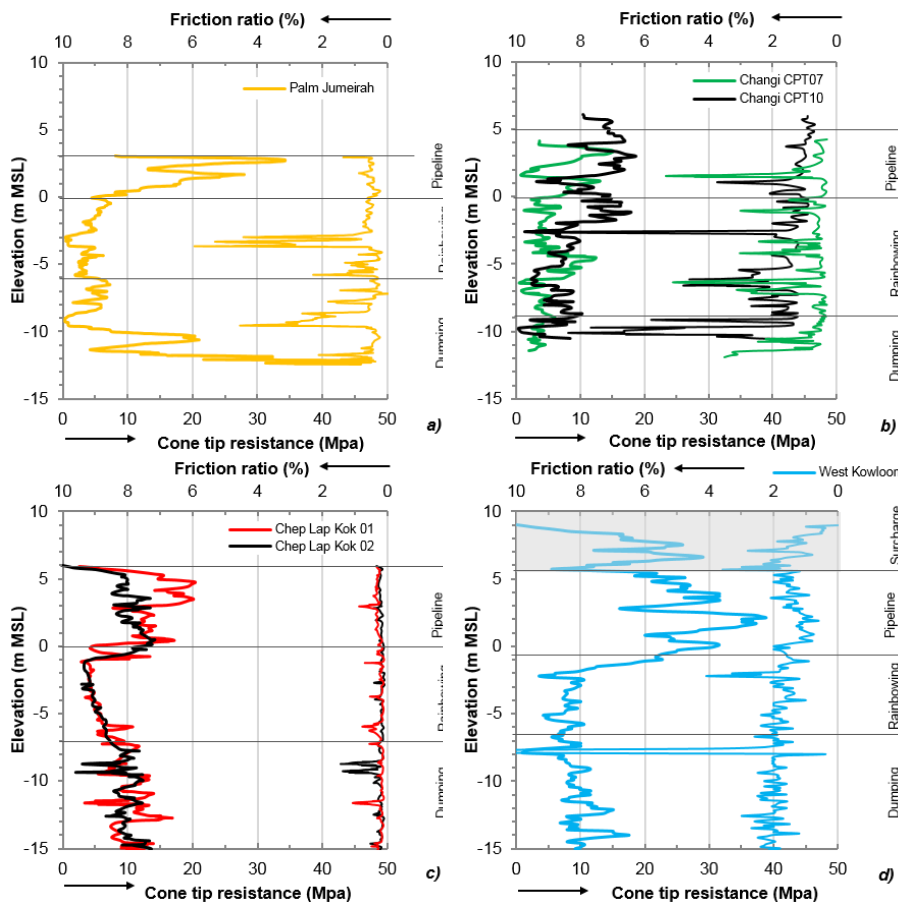
Figure 40: Cone-tip resistance (left lines) and friction ratio (right lines) at a) Palm Jumeirah (Lees et al. 2013), b) Changi Airport (Chua et al. 2007), c) Chep Lap Kok (Lee 2001) and d) West Kowloon (Lee et al. 1999).

5.5 Bottom dumping

5.5.1 Sedimentation process and resulting structure of the porous medium

Stokes's law expresses the terminal settling velocity of a single grain in a fluid (e.g., Selley 2000; Van Rhee 2002):

$$w_0 = \sqrt{\frac{4g\Delta D}{3C_D}} \tag{24}$$

Where w_o [L/T] is the terminal settling velocity of a single grain, D [L] is the diameter of the grain, g [L/T²] is the gravitational acceleration, Δ is the specific density defined as $\Delta = (\rho_g - \rho_f)/\rho_f$, where ρ_g and ρ_f [M/L³] are the density of the grain and fluid respectively, and C_D [-] is the drag coefficient. The drag coefficient depends on the Reynolds number Re [-]:

$$Re = wD\rho_f/\mu \tag{25}$$

Where μ [M/LT] is the dynamic viscosity of the fluid. In the laminar flow regime, where Re<1, the drag coefficient is $C_D = 24/Re$ which leads to an explicit relation for the terminal velocity:

$$w_0 = \frac{\Delta g}{18\nu}D^2 \tag{26}$$

The drag coefficient is $C_D = 24/Re + 3/\sqrt{Re} + 0.34$ for the transitional regime, where 1<Re<2000, and the terminal settling velocity can be computed by iteration of C_D with Eq. 24. For turbulent flow, where Re>2000, the drag coefficient is C_D=0.4 and the terminal velocity is:

$$w_0 = 1.8\sqrt{\Delta g D} \tag{27}$$

The ambient seawater is, in principle, displaced sideways during settling of the sand-water mixture, allowing the mixture to descent as a single mass (Figure 41). However, some seawater will probably escape upward through irregularities in the sand-water mixture; random volcanos of seawater will likely develop spontaneously in the sand-water mixture where seawater starts to flow through the mixture. The Reynolds number of the sand-water mixture

lies in the turbulent regime. Turbulent eddies occur around the mixture keeping fine material in suspension. However, the bulk of the sand-water mixture will quickly arrive at the seafloor.
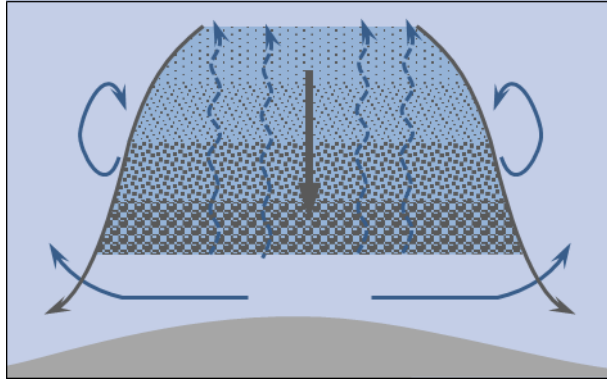

Figure 41: Settling sand-water mixture and displacement of ambient seawater.

Segregation has already developed during loading and transportation inside the TSHD. Research on sedimentation in TSHDs has been carried out by Van Rhee (2002). Based on measurements of the particle-size distribution, the concentration and the velocity in the TSHD, Van Rhee deduces that the incoming sand-water mixture flows towards the bottom of the TSHD while forming an erosion crater and a density current. Sedimentation takes place from this current from which the largest grains settle first. This leads to a segregated sand bed in the TSHD, with the coarsest grains at the bottom and the finest material remaining in suspension and flowing overboard.

Segregation of the grains also occurs within the settling sand-water mixture, where the larger grains tend to settle faster than the smaller grains according to Stokes's law. Complete segregation can only occur in infinite deep water. However, land reclamations are typically constructed in the coastal zone where water depth is limited to a few tens of meters maximum, because of which it is unlikely that the mixture fully segregates. In addition, the settling velocity of the grains is hindered according to a well-known formula by Richardson and Zaki (1954):

$$w_s = w_0(1 - C)^\alpha \tag{28}$$

Where w_s [L/T] is the settling velocity of grains, a=4 and the concentration is $C = (\rho_m - \rho_f)/(\rho_g - \rho_f)$, where ρ_m [kg/m³] is the density of the sand-water mixture.

The computed hindered-settling velocity as function of the grain diameter is shown in Figure 42 for a sand-water mixture concentration of 0, 35 and 50%. The concentrations of 35 and 50% correspond to a density of the sand-water mixture of 1600 and 1800 kg/m³, respectively. These mixture densities are practical values. Hindered settling is caused by a) the return flow created by the settling grains, b) the increased mixture density which reduces the driving buoyancy force, c) the increased viscosity of the fluid, and d) collision between particles (De Wit 2015). The initial concentration is reduced by entrainment of ambient water during the settling process, which reduces the hindered-settling effect.
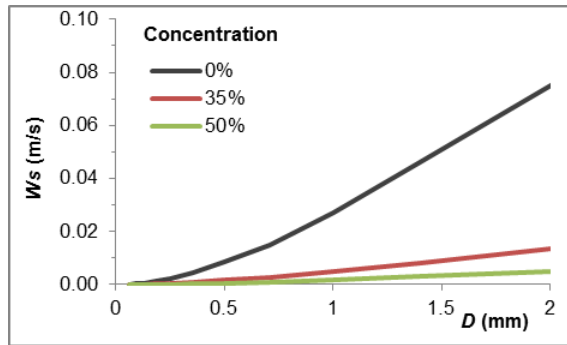
Figure 42: Hindered-settling velocity ws in a sand-water mixture (viscosity 13·10-3 kg/ms) as function of the grain diameter D for 0, 35 and 50% concentration.

The sand-water mixture flows radially outward as soon as it hits the seafloor and the velocity decreases significantly due to the divergence of the flow lines. The turbulence in the sand-water mixture decreases accordingly, causing the mixture to come to a nearly abrupt standstill during which sand falls out of suspension. Redistribution takes place only when the angle of the dumped fill becomes more than the angle of repose, which cause sand slides along the slope.

A distinct segregation mark between two bottom-dumped layers can be observed in the typical section of a vibrocore sample as presented in Lee (2001) and Shen and Lee (1995) taken from the bottom-dumped fill at Chep Lap Kok. Based on examination of the sample, Lee found that the grain-size distribution

of the coarser grains corresponds closely to the upper bound of the possible range of the Chep Lap Kok sand, whereas that of the finer grains is close to the lower bound of the Chep Lap Kok sand.

Lee (2001) represented the shape of each dump as a trapezium and suggested that dumps are randomly distributed. The model of Lee was slightly modified in this study. Figure 43 was made by assuming that each dump has the shape of the normal probability density function (pdf), which, therefore, reaches from $-\infty$ to $+\infty$. Its central location is the position of the TSHD and its volume equals that of the vessel. The thickness of each dump at any location is, therefore, given by the pdf times the volume. In this model, the sieve curve of Maasvlakte II-study area D2 is assumed to be segregated completely within each dump. Therefore, the grains in each dump are distributed upward from coarse to fine in accordance to the sieve curve. This is true at any x-coordinate for every dump. Subsequent dumps are added, so that the upper and lower boundary of each dump is according to the sequence of dumping. The THSD is placed randomly across the reclamation site for the first dumps. And later, the TSHD is placed just above the location with the maximum distance between the elevation of the dump and the target elevation. This fills the reclamation to a uniform height. Pure random dumping will never give the desired end shape.
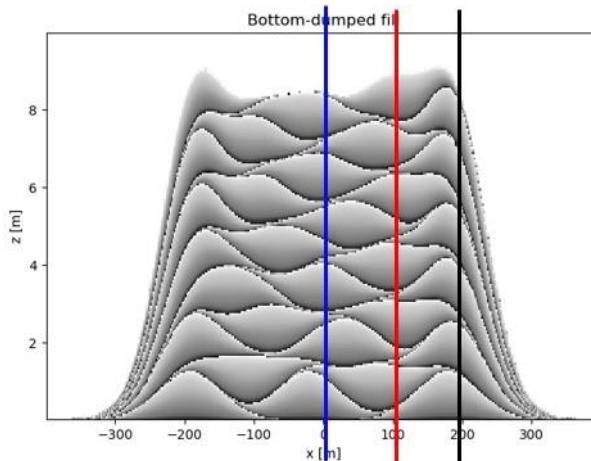
Figure 43: Cross-section of a bottom-dumped fill model in which the shading reflects the structure of the porous medium. A darker colour indicates a coarser grain size.

As Figure 43 suggests for an ideal fully-segregated dump, a bottom-dumped fill will consist of thin, elongated lenses of circa 1 to 2 m height and several tens of meters wide with a characteristic vertical grain-size distribution. The occurrence of such lenses in a bottom-dumped fill may be investigated by means of semi-variograms. The semi-variance $\gamma(h)$ is half the average squared difference between points separated at a certain lag distance h (Matheron 1963).

Figure 44 presents the semi-variograms of vertical cross-sections through the bottom-dumped fill model at x=0, 100 and 200 m. The semi-variance fluctuates periodically with lag distance. The periodic structure is most apparent at x=200 m, showing a sinusoidal semi-variance with a period of 1,5 m lag distance. According to Pyrcz and Deutsch (2003), a periodic semi-variance indicates regularly clustered lenses or strata of higher and lower grain size in the bottom-dumped fill. Figure 43 also shows that the characteristic distance between dumps at x=200 m repeats every 1.5 m. At x=0 and 100 m the periodic structure is more distorted because the stacking of the dumps is less uniform, as also appears from Figure 43.
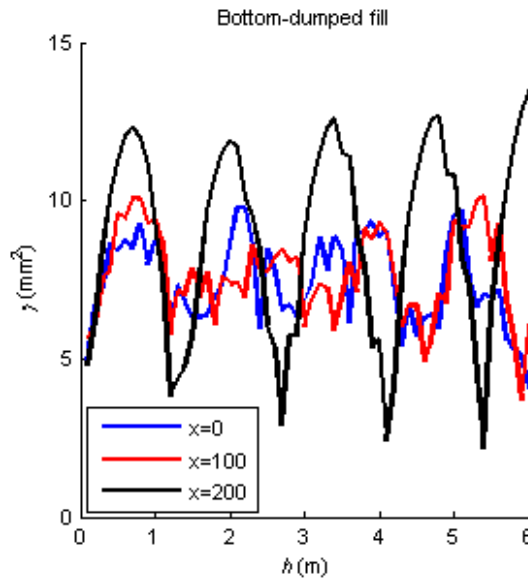
Figure 44: Semi-variogram of bottom-dumped fill model.

5.5.2 Data analysis

The occurrence of lenses in existing bottom-dumped fills may be investigated by means of semi-variograms of the cone-tip resistance registered by cone-penetration tests (CPTs) done shortly after construction. Figure 45a and b present the semi-variograms of the bottom-dumped fills of the CPTs of Figure 39 and Figure 40. Similar to Figure 44, these semi-variograms exhibit a periodic structure which now indicates regularly clustered lenses or strata of higher and lower resistance of the cone-penetration in the bottom-dumped fill.
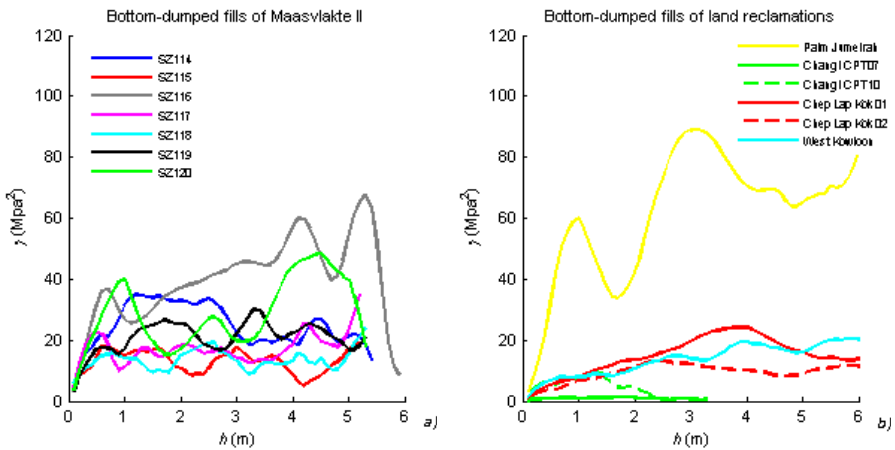
Figure 45: Semi-variogram of CPTs of bottom-dumped fills, a) Maasvlakte II-study area D2 and b) the other land reclamations.

How should these CPTs be interpreted in terms of conductivities while CPTs are known to reflect the relative density? Several researchers, such as Baldi et al. (1986) and Lunne and Christofferson (1983), established correlations between the cone tip resistance q_c, the vertical effective stress σ_v' and the relative density D_r:

$$D_r = \frac{1}{C_2} ln \left(\frac{q_c}{C_0 (\sigma_v')^{C_1}} \right) \tag{29}$$

Where C_0, C_1 and C_2 are parameters correlated in calibration chamber tests for specific sands. The relative density relates the in situ density ρ_d to the minimum and maximum reference density values $\rho_{d,min}$ and $\rho_{d,max}$ and these are inversely related to the minimum and maximum porosity n_{min} and n_{max} (Van 't Hoff and Van der Kolff 2012):

$$D_r = \frac{\rho_d - \rho_{d,min}}{\rho_{d,max} - \rho_{d,min}} 100\% = \frac{n_{max} - n}{n_{max} - n_{min}} 100\% \tag{30}$$

The semi-variograms of the CPTs thus provide insight in the variation of porosity. Higher porosities are linked to more uniform grain size distributions and/or lower compaction. The more uniform grain size distributions are finer because coming from the same borrow area, the coarse grains have been sorted out.

So it is plausible that the peaks in the CPTs correlate with the better mixed material at the bottom of each dump that consists of a mixture of coarser and finer grains. The relatively low values in the CPTs correlate with the more well-sorted, i.e. finer, material at the tops and slopes of dumps.

For the seven CPTs of the Maasvlakte II, the characteristic distance between lenses is about 1.5 m. The semi-variograms for West Kowloon and Palm Jumeirah for the bottom-dumped fills show a similar periodicity. The much larger variance of Palm Jumeirah compared to the other land reclamations can be attributed to the larger gradation in grain-size caused by the broken shells that characterizes this fill material (Miedema and Ramsdell 2011; Lees et al. 2013). The periodicity of the semi-variograms of Chep Lap Kok 01 and 02 is approximately 2 m. Based on this periodicity, it is assumed that larger TSHDs were used for this land reclamation. The bottom-dumped fill in Changi is not thick enough to recognise periodicity.

5.6 Rainbowing

5.6.1 Sedimentation process and resulting structure of the porous medium

In the land reclamations considered in this study, rainbowing up to sea level was applied on top of the bottom-dumped fill. The sand-water mixture is fluidized and mixed on board the TSHD to obtain pumpability. The sand-water mixture that is then sprayed through the nozzle is well mixed, in contrast to dumping. The diameter of the nozzle is up to 1 m. The sand-water mixture flies through the air as a compact jet up to 150 m distance (Van 't Hoff and Van der Kolff 2012). The composition of the mixture hardly changes in the air and its diameter is enlarged by air entrainment (Vessies 2012).

The velocity of the sand-water mixture is immediately reduced upon reaching the sea surface. Some segregation will occur during settling. The sand-water mixture starts building up a fill which grows as rainbowing continues at the same location. As the fill grows, the sand-water mixture flows more and more as a density current over its slopes. The slopes tend to maintain a certain angle of repose, so that the fill keeps the same shape while growing. The density current, equally called turbidity current, is driven by gravity, i.e. the density difference between the sand-water mixture and seawater (Middleton 1993). Density currents can transport material over large distances; in 1929 for example, a 7.2-magnitude earthquake-induced turbidity current running off the continental shelf near Newfoundland, Canada, broke 12 trans-Atlantic cables 1000 km out into the abyssal plain (Heezing and Ewing 1952).

While rushing down the slope, turbulent eddies generated by the density current entrain seawater into the mixture (Huppert and Simpson 1980, Hallworth et al. 1993). With increasing distance from the top, the driving density difference is thus reduced by dilution. Near the top, where the sand concentration in the density current is high, settling is most hindered, which results in a less segregated deposit along the upper part of the slope (Lowe 1982). The mixture is more diluted further down, so settling is less hindered, resulting in a more segregated deposit.

Figure 46 shows the hypothetical structure of the porous medium resulting from rainbowing. The increased segregation downslope, results in a finer and more uniform particle-size distribution with distance from the top of the fill. Because the same processes operate during the total build-up of the fill, the grain size tends to remain constant for a fixed distance to the fill centre. This implies that the grain-size distribution is uniform in cylinders centred around the axis of the fill, i.e. constant along vertical lines.
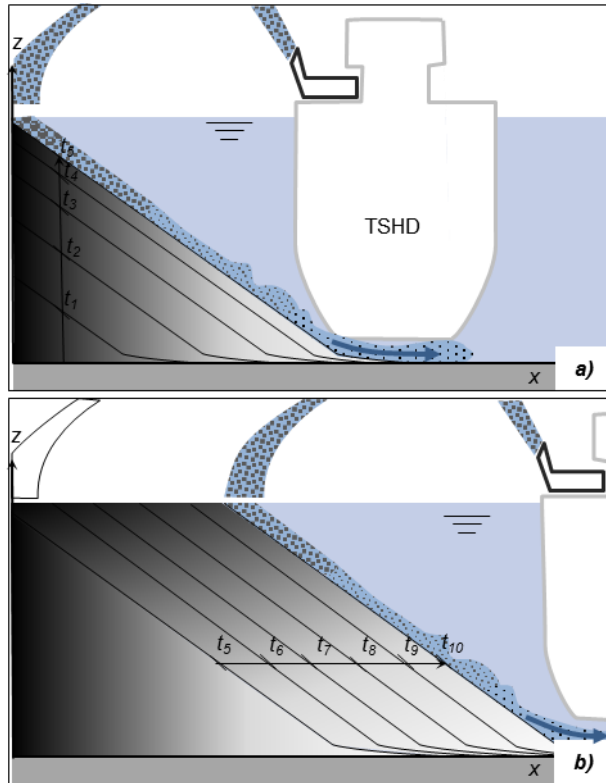
Figure 46: a) Cross-section of a rainbow-discharged fill over time (starting at t1 to t5) in which the shading reflects the structure of the porous medium and b) the build-out over time (starting at t5 to t10). A darker colour indicates a well-mixed material consisting of coarser and finer grains and a lighter colour indicates more well-sorted material dominated by finer grains.

The impact of the plunging jet will, of course, scour a depression in the top of the fill when it approaches sea level within a few meters. However, the amount of material that is thus spread out over the slopes is small and is, therefore, further neglected. Once the fill has reached sea level, the TSHD withdraws in seaward direction. The fill then builds out seaward (Figure 46b). The grain size remains constant at the same distance from the top of the forward moving slope. This implies that the grain-size distribution will be constant horizontally, refining in downward direction.

The finest grains will always accumulate at the sea floor in front of the toe of the slope and are buried under the advancing slope. Fines still in suspension will settle after each interruption of the rainbowing process. This is expected

to cause up to a few cm-thick layer of fines marking the slope at rainbowing interruptions, however, no evidence could be found in the literature.

5.6.2 Data analysis

The geotechnical scholars (e.g., Lee 2001; Lee et al. 1999) concluded from the CPTs that the q_c profiles for rainbow-discharged fills are generally much smoother than for bottom-dumped and pipeline-discharged fills. That implies that rainbow-discharged fills are more homogenous. The increase in average q_c over depth is less than for bottom-dumped fills (Lee 2001).
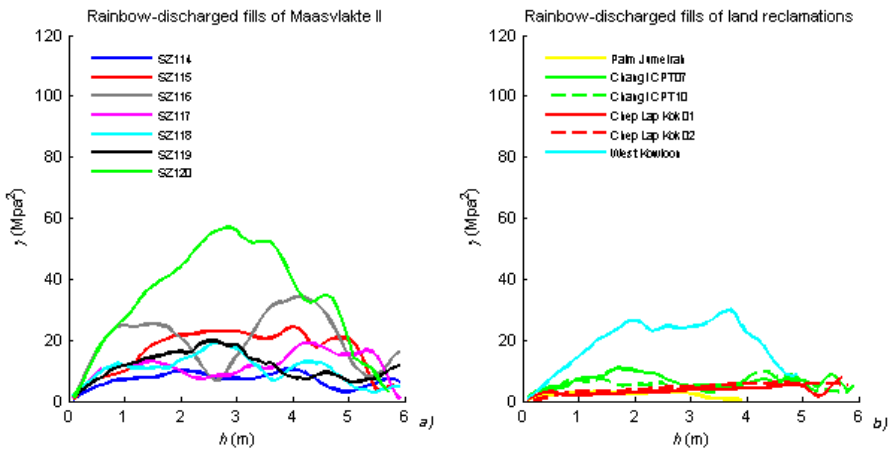
Figure 47: Semi-variogram of CPTs of rainbow-discharged fills, a) Maasvlakte II-study area D2 and b) the other land reclamations.

Figure 47 presents the semi-variograms of the CPTs for the rainbow-discharged fills. The variance in Maasvlakte II and West Kowloon is comparable to the variance for bottom-dumped fills, in contrast to the other rainbow-discharged fills which show a lower variance than in Figure 45. Periodic structures are not apparent. It is assumed that the higher variance in Maasvlakte II and West Kowloon compared to Chep Lap Kok and Changi Airport is caused by the higher amount of fine grains in these sands (Figure 35); which caused more segregation during rainbowing and, moreover, more settling of finer material during interruptions in the rainbowing process. The relatively low variance in the rainbow-discharged fill at Palm Jumeirah can be attributed to the shells in the density current that cause more hindered settling due to which less segregation took place.

5.7 Pipeline discharge

5.7.1 Sedimentation process and resulting structure of the porous medium

The part of the land reclamations above sea level is generally placed by pipeline. The fluidized sand-water mixture is pumped through floating pipelines to the reclamation site. Bulldozers first construct small containment bunds at a certain mutual distance. These bunds guide the flow of the sand-water mixture as the space between these bunds is filled by the pipeline discharge. While constructing the bunds, the bulldozers also compact the sand.

Figure 48 shows the hypothetical structure of the porous medium resulting from pipeline discharge. At the pipeline outflow, the sand-water mixture forms a scour hole. The sand-water mixture flows over the edge of the scour hole. While the diameter of the pipeline is about the same as the diameter of the rainbow nozzle, the pumping rate is much lower. The degree of turbulence is so low that coarse grains settle directly near the pipeline (Mastbergen and Bezuijen 1988). Finer grains are transported along the slope and the finest grains accumulate at the toe (Figure 48a). Bulldozers level the area in front of the pipeline outflow and fill the scour hole.

After a certain elevation is reached, the next (circa 12 m) pipe section is connected and the filling process is continued (Figure 48b). The segregation of grains along the slope is similar to that happening under water during rainbowing. This implies that the grain-size distribution will be constant horizontally and will refine in downward direction. As is the case with rainbowing, the finest grains accumulate in front of the toe of the slope and are then buried as the slope advances. This creates a band of fine grains at the bottom. Fine material also accumulates before the bunds.
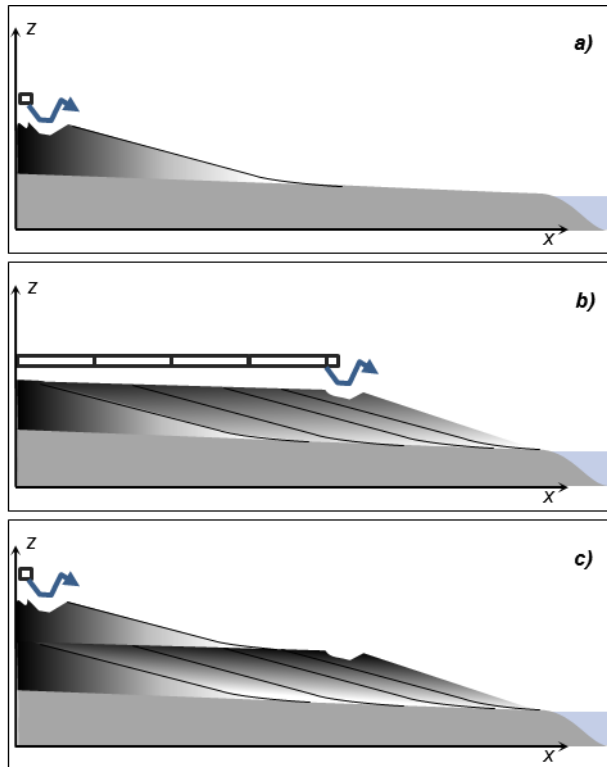
Figure 48: Cross-section of a pipeline-discharged fill above water in which the shading reflects the structure of the porous medium, a) one section, b) several sections that coincide with the extension of the pipeline, and c) second lift. A darker colour indicates well-mixed material consisting of coarser and finer grains and a lighter colour indicates more well-sorted material dominated by finer grains.

Once the end of the fill area is reached, the filling process may be repeated to create a following lift (Figure 48c). When the required elevation level is reached, the pipeline is moved to the next strip. As a result, the structure of the porous medium of a pipeline-discharged fill consists of stacked lifts similar to the so-called para-sequences of natural marine deposits (Coe 2002) in which each lift refines from top to bottom. These lifts may be recognised in a drilling by the band of fine material that vertically separates them, but these bands may be too thin to be recognized in a CPT.

5.7.2 Data analysis

Lee (1999), Lee et al. (2001) and Lees et al. (2013) concluded that the cone-tip resistance of sand fills formed by subaerial-placement methods (i.e. above water, as defined by Morgenstern and Kupper (1988)) is substantially higher

than that of sand fills formed by subaqueous placement. They explain this higher compaction of subaerial placements by noting that a sand fill above water is subjected to downward seepage, which results in a void ratio lower than that of subaqueous deposition. The compaction is further increased by the levelling operations of the bulldozers and the impact of other construction traffic.

Figure 49 presents the semi-variograms of the available CPTs of the pipeline-discharged fills. The variance is higher than that of the other placement methods shown in Figure 45 and Figure 47. All semi-variograms of the pipeline-discharged fills exhibit a periodic structure. This periodicity strongly suggests that several lifts were applied; the periodicity is consistent with a general lift thickness of circa 1 to 2 m.
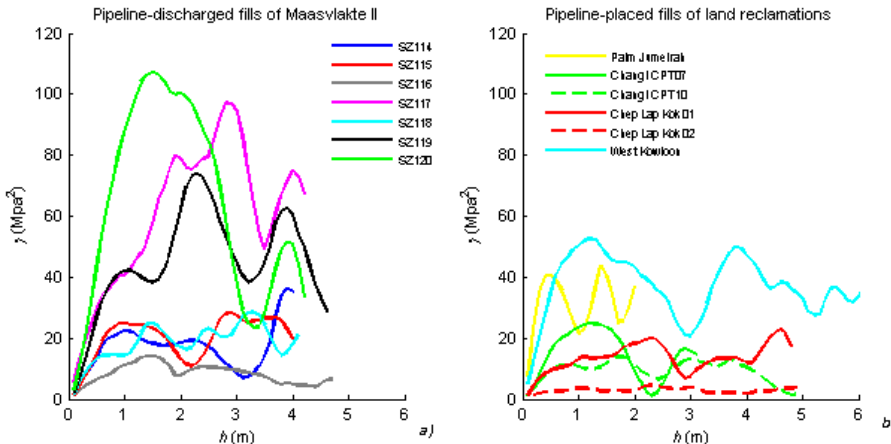
Figure 49: Semi-variogram of CPTs of pipeline-discharged fills, a) Maasvlakte II-study area D2 and b) the other land reclamations.

5.8 Consequences for the hydraulic conductivity of land reclamations

At the size of a representative elementary volume (Bear 1972), i.e. circa 20 grain diameters, the conductivity is essentially expressed by the Carman-Kozeny relation:

$$K = \frac{\rho g}{\mu} \frac{1}{CS_0^2} \frac{n^3}{(1-n)^2} D_{eff}^2 \qquad (31)$$

Where $\rho g/\mu$ is the unit weight/viscosity of water, n [-] is porosity, D_{eff} [L] is the effective grain diameter usually taken to be equal to D_{10}, and S_o [1/L] is the specific surface. C is an empirical coefficient to correct for grain ordering and grain shape to match laboratory measurements for permeability with actual porosity and effective grain diameter. C is usually taken to be equal to 5.

With a given grain size distribution, porosity is the only unknown in estimating conductivity. Porosity in in the range of 35% to 40% in most unconsolidated sediments in the Netherlands (Olsthoorn 1977), but could be somewhat higher in freshly reclaimed land, especially where the grain-size distribution is more uniform.

The difference in conductivity between sands with equal grain-size distribution but a porosity of 35% and 40% respectively, is a factor 1.75. However, the difference in conductivity due to different effective grain diameters D_{10} of the two extreme sieve curves from Figure 35 is about 4 in the Maasvlakte II study area D2, about 2 in Changi Airport and even more at the three other reclamation sites discussed in this thesis.

As conductivity is proportional to the effective grain diameter squared, it follows that the effect of the effective grain size by far outweighs that of porosity. This is also the case with segregation of the grains, which can be illustrated by splitting the sieve curve in a lower part containing the finer grains and an upper part containing the denser ones (Figure 50).
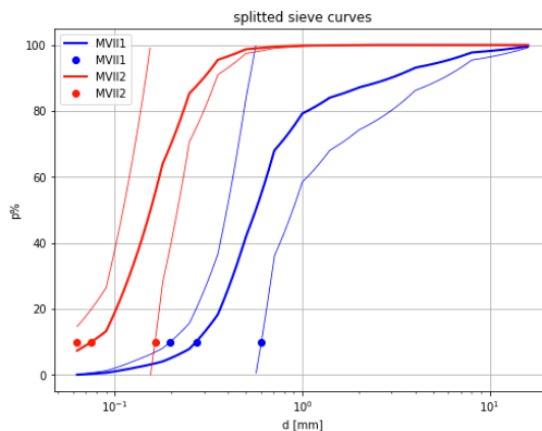
Figure 50: The two extreme sieve curves for Maasvlakte II original (thick line) and split in their lower and upper halves to illustrate the effect of segregation, which makes the curves steeper and shifts the effective D_{10} away from the original value (thick line).

This segregation makes both sieve curves more uniform, i.e. steeper, but at the same time, the D_{10} of the lower curve is reduced relative to the original, and that of the upper curve has increased. According to Carman Kozeny, this implies that the conductivity of the lower curve is reduced and that of the upper curve in increased relative to the original mixture. It is likely that the more uniform fine sand will have highest porosity, but this porosity effect may only partly compensate its lower effective grain diameter.

In conclusion, the CPTs reveal zones of higher and lower relative density, i.e. of lower and higher porosity, rather than conductivity. However, the coarser sand will remain better mixed when placed and, therefore, has the highest relative density. Due to the outweighing of the effective grain diameter over the porosity effect on conductivity, it is most plausible that the higher CPT values correspond to higher conductivity in land reclamations. Consequently, the grain-size distributions as illustrated in Figure 43, Figure 46 and Figure 48 mimic the conductivity.

It is noted that in case the relative density of the fill mass after deposition and/or the underlying soil does not meet the required design criteria, ground improvement techniques are applied to improve the properties of the fill and/or subsoil. According to Van 't Hoff and van der Kolff (2012) ground improvement is typically carried out to: 1) prevent excessive settlements of the surface, 2) improve the shear strength of the fill and/or subsoil to ensure sufficient bearing capacity and stability of the slopes, 3) increase the relative density of the fill mass and/or the subsoil to prevent liquefaction and 4) to improve the soil permeability. Porosity may decrease by circa 5% because of adequate soil improvement techniques that increase the relative density of the fill. Ground improvement was not considered in this thesis, because the available data was without soil improvement.

5.9 Consequences for subsurface freshwater storage in land reclamations

Using Eq. 31, and taking D_{10} of the actual soil samples of the rainbow-discharged part of the fill of Maasvlakte II study area D2, which are depicted in Figure 38a, the conductivity would fluctuate between 2 and 24 m/d, which is an order of magnitude, an effect that goes unseen if only average values are considered and which is important for the subsurface storage and recovery of fresh water. The recovery efficiency of these systems

can be impacted by differences in dispersion and preferential flows resulting from the applied placement methods. As such, the recovery efficiency is expected to be lowest for bottom-dumped fills in which the sand has a wide grain-size distribution. They show the largest grain-size variation on small vertical scales, because of the irregular stacking of lenses in each of which the grain size coarsens downward. The recovery efficiency is expected to be highest in rainbow-discharged fills, because they are composed of well-mixed material where the grain size smoothly coarsens upward over the total thickness of the fill.

Despite the small variations that may cause variations in dispersion in preferential flow; the porosity and hydraulic conductivity of land reclamations that are constructed of sand by bottom dumping, rainbowing and pipeline discharge are comparable to natural dunes and the heterogeneity is more predictable than that of natural soils. Disturbances, such as clay layers, do not occur, because only sand is used for the construction of the land reclamation. Moreover, the content of fine material in land reclamations is lower than in the so-called borrow areas, which is due to the overflowing water during loading of the TSHD carrying along fines, and because fines are partly transported beyond the reclamation site during placement. In conclusion, land reclamations that are constructed of sand by bottom dumping, rainbowing and pipeline discharge are, therefore, suitable for subsurface storage and recovery of fresh water.

It is noted that land reclamations are typically constructed in coastal zones of limited depth of at most a few tens of meters. The potential storage zone is, therefore, restricted, unless the sea floor itself is highly conductive. The thickness of the potential storage zone may be further restricted where land reclamations are constructed by a sequence of placement methods, because a layer of finer grains is expected to be present at the bottom of the rainbow-discharged fill and at the bottom of the pipeline-discharged fill.

It is also noted that a band of fine material will be present along the edges of pipeline-placed fills wherever closing bunds were applied. Such bund-formed elongated bands of fine material may have an advantage for the formation of a freshwater lens. On the other hand, parallel bunds bounding strips of land that mark phases in the construction of the reclamation, result in some degree of compartmentation. The location of these bunds may be derived from the

documentations regarding the phasing of the construction of the land reclamation.

5.10 Conclusions

The structures of the porous media were investigated resulting from three placement methods, i.e. bottom dumping, rainbowing and discharging the sand-water mixture by pipeline. The results were compared with the data of a study area at Maasvlakte II, the Netherlands, and four other land reclamations. It was found that all placement methods result in some degree of heterogeneity in the structure of the porous medium. Therefore, the hydraulic conductivity in land reclamations is not constant, even though the heterogeneity is more predictable than that of natural soils.

A bottom-dumped fill consists of a random distribution of stacked thin, elongated lenses that are about 1 to 2 m high and several tens of meters wide, in which the resulting hydraulic conductivity must decrease from the centre of the lens to its outer edges because of the obtained grain-size distribution. The resulting hydraulic conductivity in a rainbow-discharged fill must increase from the bottom to the top of the fill for the same reason. A rainbow-discharged fill will be interspersed with sloping layers of low conductivity caused by interruptions of the rainbowing process. A pipeline-discharged fill consists of stacked lifts of about 1 m thickness, in which the hydraulic conductivity should likewise increase from the bottom to the top.

The degree of segregation caused by a specific placement method still depends on site-specific circumstances, such as settling depth, grain-size distribution and angularity resulting from grain type. It is impossible to separate these three parameters from a single CPT. Therefore, to verify the hydraulic properties in a specific land reclamation in which the exact placements are not known, (undisturbed) soil samples and pumping tests at different depths and places are deemed indispensable.

These outcomes imply that the hydraulic conductivities of land reclamations that are constructed of sand by bottom dumping, rainbowing and pipeline discharge make these new lands suitable for subsurface storage and recovery of fresh water. However, if land reclamations are considered for Aquifer Storage Recovery (ASR), the recovery efficiency of these systems can be

impacted by differences in dispersion and preferential flows resulting from the applied placement methods.

Future research may focus on validation by means of pumping tests. For a specific land reclamation in which the placement method, the volume, the dumping time and the grain-size distribution per dump are known, a numerical groundwater model can be made based on the structure of the porous media as presented in this chapter. This model can then be validated by means of a pumping test.

CHAPTER 6 CONCLUSIONS AND FUTURE PROSPECTS

6.1 Conclusions

The aim of this thesis is to examine how the subsurface of land reclamations can be optimally designed, created and operated for freshwater storage and recovery. For this purpose, it was studied how the aquifer properties, subsurface constructions and well placement and operation can be jointly optimized to maximize freshwater recovery efficiency. The internal structure of the porous media of land reclamations were studied to determine heterogeneity and the hydraulic conductivity that is created within current dredging practice.

The conclusion of this dissertation is that land reclamations that are constructed of sand by bottom dumping, rainbowing and pipeline discharge are generally suitable for subsurface storage and recovery of fresh water. It was shown that mixing and density stratification of fresh water stored in saline aquifers can successfully be controlled by the application of flow barriers or the construction of horizontal layering in the soil structure, and by combining freshwater storage with saltwater extraction during operation.

The main scientific findings of this dissertation are:

a) Three concepts have been identified that allow managing the mixing and density stratification occurring along with freshwater storage and recovery in saline aquifers in land reclamations:
    1. The properties of these man-made aquifers that reduce mixing and buoyancy and preferential flow.
    2. Vertical flow barriers of limited depth preventing the volume of fresh water from expanding radially, speeding up the formation of the freshwater stock.
    3. Saltwater extraction from below the freshwater stock, preventing the freshwater volume from floating up by counteracting buoyancy.

b) Insight has been given in the internal structure of the porous media and its hydraulic properties of different land reclamations constructed by the most commonly applied placement methods, i.e., bottom dumping, rainbowing and pipeline discharge.

This thesis focusses on land reclamations that are designed from scratch and constructed in the ocean, which implies that the properties of the man-made

aquifer are part of the design and, therefore, can be optimized for freshwater storage and recovery. It is noted that the new concepts for freshwater storage and recovery that are presented in this thesis, i.e. by means of flow barriers and in combination with saltwater extraction, are also applicable in natural brackish or saline aquifers to increase the freshwater recovery efficiency.

6.1.1 Flow barriers

When fresh water is infiltrated between flow barriers that partly penetrate a saline aquifer, the density difference between the two water types causes the lighter fresh water to float on top of denser saline groundwater; the mixing zone separates the two fluids (Figure 51). Fresh water is preferably recovered by horizontal wells in a layer of gravel at the top of the aquifer or directly extracted by vegetation. A geotextile between the layer of gravel and the underlying sand prevents fines from being washed into the gravel layer. Fluctuations in flow velocity may be counteracted by spatially adjusting the grain-size distribution within the storage area or the thickness of the layer of gravel at the time of construction.
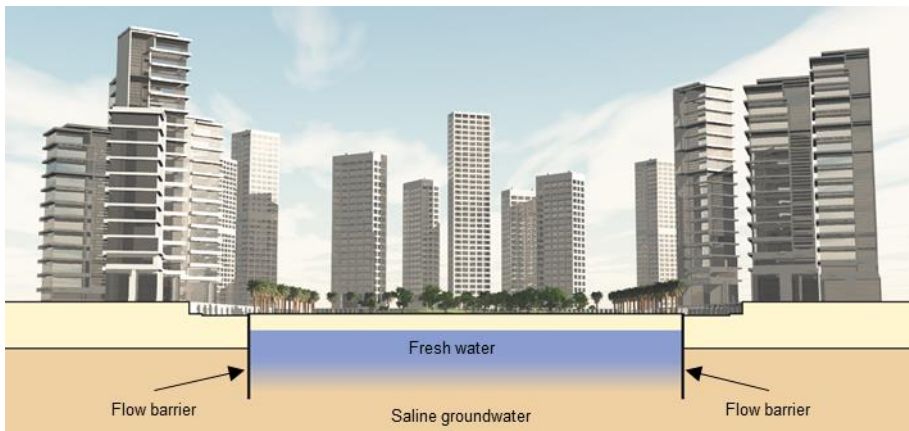
Figure 51: Artist impression of freshwater storage and recovery between flow barriers in a saline aquifer.

The effect of flow barriers on the groundwater flow and on mixing between fresh and saline water was studied by numerical modelling experiments. Freshwater recovery rates on the order of 65% in the first cycle rising to as much as 90% in following cycles were achievable for the studied configurations. It was shown that larger density differences and higher conductivity values reduce the inclination of the interface and increase the storage capacity. It was also shown that larger ratios of the distance between

the flow barriers and their depth, and between their depth and the thickness of the aquifer impact the recovery. A gravel layer at the bottom of the storage zone results in more uniform vertical head gradients in this zone, which enhances recovery efficiency.

6.1.2 Horizontal layering

No geotechnical data could be found about land reclamations constructed by thin horizontal layers which however could be favourable for freshwater storage. This is because a low vertical conductivity while maintaining a normal to high horizontal conductivity limits both mixing and buoyancy. Contrary to the most commonly applied placement methods, i.e., bottom dumping, rainbowing and pipeline discharge, a build-up of land reclamations by successive thin layers is sometimes applied on clayey ocean floors for geotechnical reasons, e.g., in Jakarta Bay. However, thin-layer placement methods are more time consuming and expensive than reclaiming land in a standard fashion. In such highly vertical anisotropic aquifers, fresh water is preferably recovered by vertical wells that are protected against in-wash of fine grains by means of a gravel pack enhanced by a geotextile envelope.

6.1.3 Combination with saltwater extraction

Saltwater extraction from below the freshwater stock counteracts the density-induced buoyancy of the freshwater volume (Figure 52). This storage concept is especially useful in situations where a continuous saltwater extraction is maintained for desalination, as is often a primary source of drinking water on land reclamations as well as resorts along desert coasts, e.g., the Red Sea coast of Egypt.
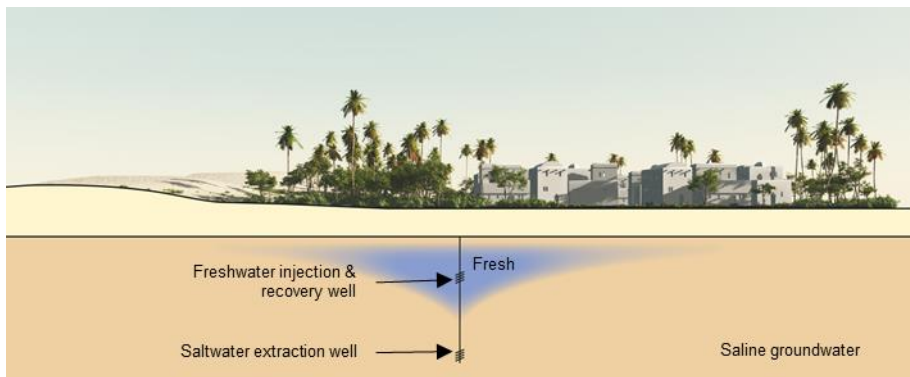
Figure 52: Artist impression of freshwater storage in combination with saltwater extraction from below the freshwater cone.

An analytical Dupuit solution was presented for the steady flow of salt water toward a well with a volume of fresh water floating on top of the cone of depression. This solution gives the required saltwater discharge to keep a given volume of fresh water in place. Numerical simulations showed that freshwater recovery rates of up to 70% in the first cycle increasing to 80% in subsequent ones are achievable when salt water is extracted at high rates, flow barriers are applied at a distance from the well, or when several freshwater recovery drains are used. The impact of ambient flow and interruptions of saltwater pumping on the recovery were quantified.

6.1.4 Hydraulic properties of land reclamations

Although an aquifer with optimal properties for freshwater storage can readily be designed, in the end, the freshwater recovery efficiency will always be affected by both the properties of the material in the borrow area, i.e. the location where the sand was mined, and by the placement methods and their spatial configuration as applied during construction of the reclamation.

The structure of the porous media and their resulting hydraulic conductivity were deduced from the data of five land reclamations, which were constructed of marine sediment by a combination of bottom dumping, rainbowing and pipeline discharge. It was found that these three most commonly applied placement methods all lead to some degree of heterogeneity, which precludes that the hydraulic conductivity in land reclamations is uniform. This is a consequence of the extent of segregation of grains pertaining to each placement method. Segregation even varies within a specific placement method due to site-specific circumstances such as settling depth, grain-size distribution and grain angularity.

These outcomes imply that the freshwater recovery efficiency in land reclamations can be impacted by differences in dispersion and by preferential flows resulting from the applied placement methods. However, even though heterogeneity exists in land reclamations, it is still more predictable than that of natural soils and, moreover, disturbances, such as clay layers, do not occur because only sand is used. As such, it is concluded that land reclamations constructed of marine sediment by means of bottom dumping, rainbowing and pipeline discharge are suitable for freshwater storage and recovery.

6.3 Further research perspectives

This research was a first attempt to determine the opportunities that the design, construction and operation of land reclamations for urban expansion could provide to optimize their subsurface for freshwater storage and recovery. This section suggests several directions for further research, which were encountered during this study and are mainly related to field experiments, other dredging techniques, water quality and site-specific conditions.

6.3.1 Field experiments

This research is based on theoretical and analytical considerations, numerical modelling and laboratory experiments. Although these research methods provide a good insight in the behaviour and sensitivities of fresh and saline groundwater, field experiments in future studies are valuable to verify the theory.

6.3.2 Land reclamation data

Land reclamations have been barely studied hydraulically. The study of Chua et al. (2007) was the only study found in the scientific literature into the hydraulic aspects of a land reclamation. Because no other hydraulic data on land reclamations were available, the analysis of the structure of the porous media and their resulting hydraulic conductivity in Chapter 5 is based on geotechnical data, i.e. sieve curves and cone penetration tests (CPT). The degree of segregation caused by a specific placement method still depends on site-specific circumstances, such as settling depth, grain-size distribution and grain angularity. It is impossible to separate these three parameters from a single CPT. Therefore, to verify the hydraulic properties in a specific land reclamation in which the exact placements are not known, (undisturbed) soil samples and pumping tests at different depths and places are deemed indispensable.

The structure of the obtained porous media as presented in Chapter 5 is validated by comparison with semi-variograms of cone-penetration tests. Future research may focus on validation by means of pumping tests. For a specific land reclamation in which the placement method, the volume, the dumping time and the grain size distribution per dump are known, a numerical groundwater model can be made based on the structure of the porous media as presented in Chapter 5. This model can then be validated by means of a pumping test.

It was surprisingly difficult to get geotechnical data of existing land reclamations suitable for scientific research. Fortunately, the Port of Rotterdam provided data of the Maasvlakte II, which could be supplemented with geotechnical data of four other land reclamations from the literature. However, a high volume of information must be available for each land reclamation, because the quality control and monitoring programme for each project implies, among other things, measurement of the as-placed volumes and grain-size distributions, area-wide cone-penetration tests and soil samples.

This high volume of geotechnical data, would provide insight in the structure of the porous media of land reclamations on a worldwide scale, which would allow to determine the potential for freshwater storage and recovery on these new lands. A technique applicable to each land reclamation would be to construct area-wide semi-variograms. Such semi-variograms would provide this insight:
1. By integrating cone-penetration tests of many different locations within a single land reclamation and separately for each dredging technique;
2. By comparing different land reclamations in which the same technique was applied;
3. By building up experience, allowing to extract porous media properties directly from the shape and properties of the semi-variograms.

This insight might also be relevant for deducing bearing capacity and risk of liquefaction and for improving the general operations of dredging practice.

Bottom dumping, rainbowing and pipeline discharge that were analysed in Chapter 5 are the most commonly applied placement methods. Pumping through a spreader or diffuser is another placement method, which is often used to attain an equal spreading on top of a soft sea floor. Chapter 2 explains that land reclamations constructed by a build-up by subsequent thin layers, will theoretically have a high vertical anisotropy, which is favourable for subsurface freshwater storage and recovery. However, no (geotechnical) data were available about this placement technique, so that the hydraulic conductivity of artificial aquifers constructed by this technique has yet to be researched.

6.3.3 Water quality
Land reclamations are constructed of marine sediment that is extracted at the surface of the sea floor in the so-called borrow area. It is not expected that

these recent deposits contain pyrite and, therefore, no risk of arsenic is anticipated, also because the dredging technique and placement method provide a lot of oxygen that would likely oxidize the pyrite. However, this is a point of further research.

Reactive transport controls on the chemical water quality during freshwater storage and recovery were not assessed in this thesis, because there is currently no data available. In land reclamations in which subsurface freshwater storage and recovery will be applied, proper soil analysis, modelling and monitoring of water quality must, of course, be carried out.

6.3.4 Site-specific conditions

The storage capacity and the freshwater recovery efficiency partly depend on the resistance of the sea floor. For a specific land reclamation, site-specific soil samples and cone-penetration tests of the sea floor are, therefore, required. The infiltration and controlled recovery of the fresh water given these site-specific circumstances can then be worked out by means of numerical modelling.

6.3.5 Costs and benefits

This research focused on freshwater storage and recovery in the subsurface of land reclamations from a hydrological point of view. An analysis of the costs and benefits of subsurface storage compared to other forms of freshwater supply must be made for each specific land reclamation. Regarding the costs, the costs for the land use and maintenance should also be considered in addition to the investment costs. For the benefits, attention should also be paid to material use, energy consumption and CO_2 reduction and the natural, ecological and landscape values of alternatives for freshwater supply.

6.3 Future prospects

Although there are no examples of application yet, the results presented in this dissertation enable to determine the conditions for site-specific designs. Consider a to-be-constructed land reclamation off the coast of a megacity that is constructed of marine sediment by means of bottom dumping, rainbowing and pipeline discharge. How would we then design the subsurface for freshwater storage and recovery?

Given the concepts developed in this thesis, it is recommended to apply a combination of freshwater storage between flow barriers and saltwater

extraction from below the stored volume to create a recoverable freshwater volume in this man-made subsurface. This combination was modelled as recovery approach 2 in Chapter 4. These concepts are recommended first, since normal placement methods can then be applied. Further research can be executed later into techniques to construct high vertical anisotropy. As shown in Figure 11 in Chapter 4, flow barriers lead to significantly improved recovery efficiencies and a faster growth of the freshwater volume, because they prevent radial expansion of the stored freshwater volume. In probably most future cases, fresh water cannot be supplied from the mainland. Desalination is, therefore, presumably the only feasible freshwater resource for this land reclamation. This will even be more often the case in the initial stages in which the freshwater stock is built up. Given the concept in Chapter 4, it is recommended to use saltwater extraction wells inside the flow-barrier compartments instead of beach wells to obtain salt water for desalination.

Figure 53, Figure 54, Figure 55 and Figure 56 present artist impressions of the development of the freshwater lens over time in combination with flow barriers and saltwater extraction. Figure 53 presents the initial situation in which all groundwater is saline, barriers are installed and salt water is extracted with a groundwater well for desalination purposes.
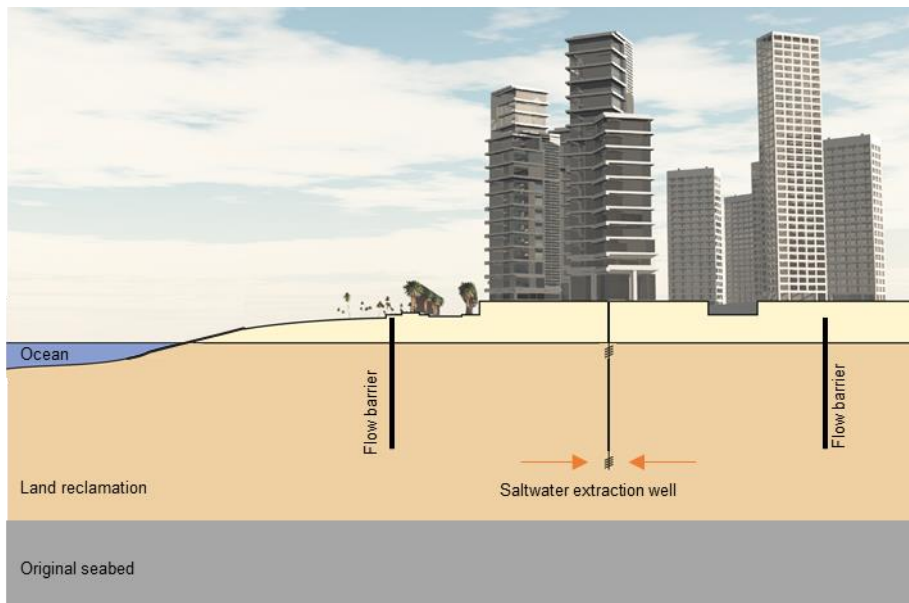
Figure 53: Initial situation: a land reclamation with flow barriers and saline groundwater extraction.

A numerical groundwater model can be made with the structures of the porous media resulting from the applied placement methods that are presented in Chapter 5. This model will be based on the spatial distribution of the applied placement methods, their volume, location and dumping times and grain-size distributions as well as the properties of the sea floor below the land fill. This model is used to design the depth of the flow barriers in relation to their mutual distance and the saltwater extraction used to counteract buoyancy.

Flow barriers can be applied along the outside of the land reclamation or to create a number of compartments within the land reclamation used for different purposes; e.g. for park irrigation, drinking water, emergency storage, etcetera. Flow barriers might be constructed during reclamation by special placement; e.g. elongated bands of fine material will be present along the edges of rainbow-discharged and pipeline-placed fills wherever closing bunds were applied. But it seems more practical for reasons of construction speed and geotechnics to construct them afterwards, e.g. by vertically placed high-density poly-ethylene (HDPE)-foils, sheet piles or clay walls. Biomineralization (Pham et al. 2018; Pham et al. 2016) and podsolization (Zhou et al. 2018; Laumann et al. 2018; Laumann et al. 2016) are recent scientific developments to construct flow barriers, which use natural processes for in situ reduction of permeability.

Figure 54 presents the second stage in which fresh water from different sources starts to be infiltrated. Infiltration may be done naturally using ponds or gravel beds and actively by means of wells. Depending on the climate and the above-ground functions, freshwater resources for the subsurface storage can be rainwater, piped water, desalinated water or treated wastewater. Especially if several subsurface compartments are designed.
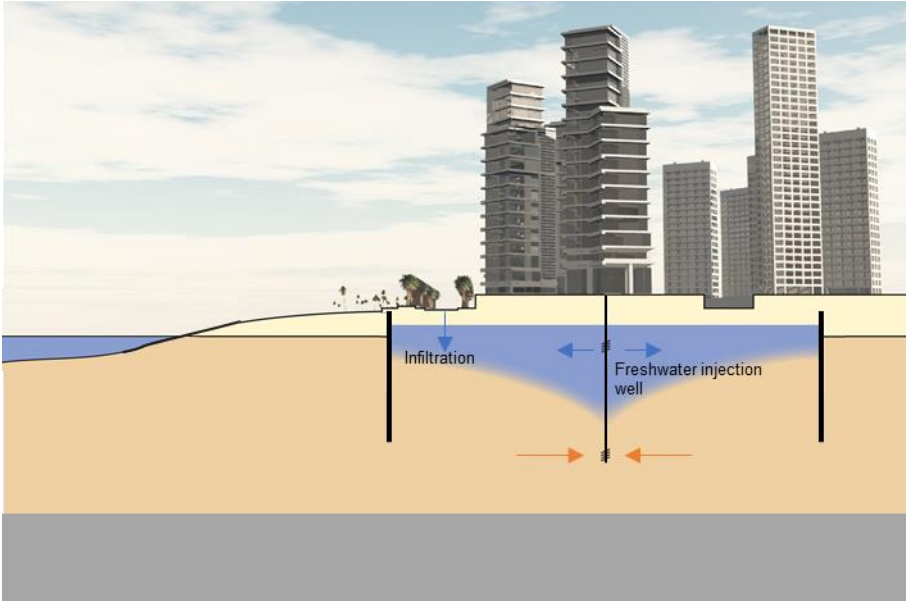
Figure 54: Second stage, freshwater volume starts to grow and saline groundwater extraction continues to produce water for desalination.

Rainwater can often be a source of fresh water, but then the urban storm-water system must be designed to recharge the subsurface and not discharge it readily into the ocean as is normally done. Due to the slow infiltration in respect to the, often, intense surface runoff, temporal storage above ground should be maximized. For this purpose, drainage infiltration and transport (DIT)-systems can be used, which not only transport and discharge storm water, but also retain and infiltrate part of it. Retention and infiltration can also be achieved by wadi-like facilities in green areas, by infiltration basements or by gravel layers under buildings and roads.

It should go without saying, that drainage water from potentially contaminated surfaces should be treated appropriately, e.g. by passing through a settlement pond, an oil separator and/or a helophyte filter, prior to infiltration. Piped water, like desalinated water, water from the mainland and treated wastewater, would preferably be injected via horizontal and/or vertical injection wells.

The time required to fill the storage volume to its design capacity depends on the available water resources and the capacity of the infiltration facilities. In tropical and moderate climates with considerable precipitation, the potential

growth of the freshwater volume is likely largest during the construction phase when the reclamation is still unpaved. This emphasizes the importance to incorporate freshwater storage already in the design of the land reclamation, so that its freshwater supply be fully utilized. Another advantage is that gravel packs around wells and under infiltration facilities can be far more easily realised during construction works of the land reclamation. This also applies to the construction of the infiltration facilities, i.e. the infiltration basements, infiltration ponds, storm water attenuation and infiltration crates and wadis. And this is also evident for horizontal wells and can thus reduce the costs of construction as well as the risk of malfunctioning during later operation.

The freshwater volume develops over time. Figure 55 presents the third stage in which vegetation reaches the fresh groundwater and the freshwater volume starts to freshen the saltwater extraction well, which results in less energy consumption for the desalination.
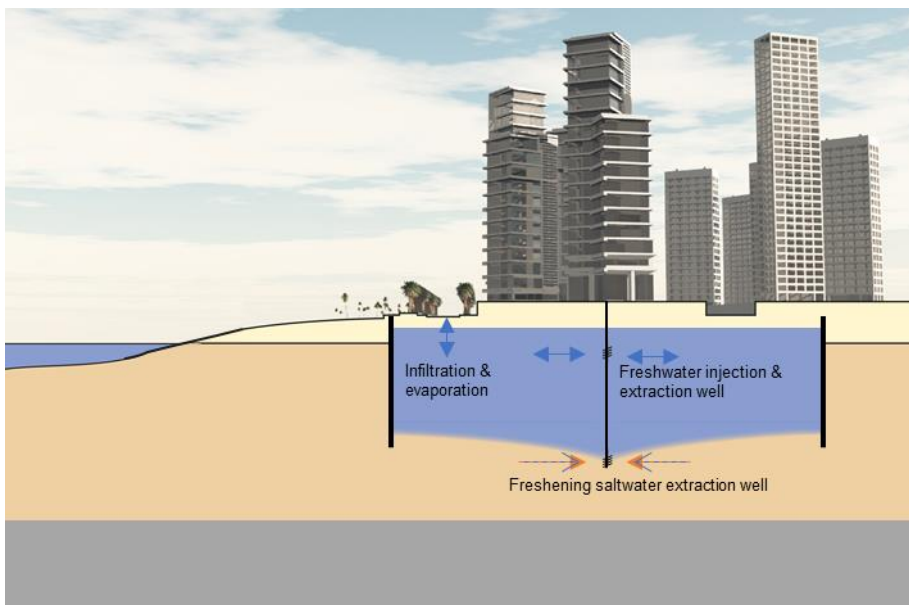
Figure 55: Third stage, freshening of the saltwater extraction well and vegetation using fresh groundwater.

Fresh water in the subsurface is vulnerable to above-ground spills and contamination. Therefore, the ownership of the stored fresh water in the subsurface should be stipulated and regulations for above-ground use and groundwater protection zones are crucial to prevent contamination. Pollution

of the rainwater runoff can be prevented by 1) regulations for i.e. car-washing and dog-outlet areas and 2) by the choice of materials used in the above-ground architecture; i.e. stainless steel instead of weathering-sensitive metals such as zinc and copper.

Ownership and regulation can be simplified when location-specific storage is applied, which can be achieved by compartmentalization of the subsurface by means of flow barriers. Monitored supported enforcement is required to ensure that the regulations are respected. Adequate real-time sensoring also allows predictive control over the stored freshwater volumes and yields data necessary to analyse operational problems when they occur.

Figure 56 presents a final stage in which the freshwater volume has grown so far that fresh water escapes under the barriers and the volume partly extends into the sea floor. This situation requires a surplus of fresh water. In cases without such a surplus, the situation in Figure 55 applies. This is optimized in actual cases by designing the size of the subsurface storage in relation to the available water resources.
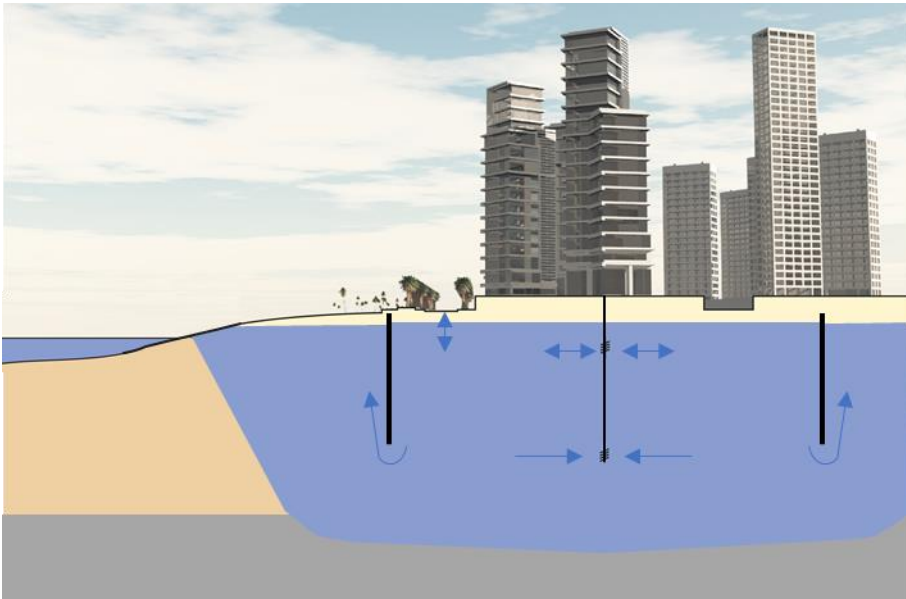
Figure 56: Final stage, a freshwater lens has developed and the salinity in the extraction well is minimized.

A successful implementation of freshwater storage in the subsurface of land reclamations not only requires linking dredging and water engineers, but especially raising awareness of its benefits among spatial developers and their consultants. Only when this happens, subsurface freshwater storage will be incorporated in the specifications of to be designed land reclamations. This incorporation is a precondition for dredging and water engineers to cooperate in designing site-specific solutions for freshwater storage in the subsurface of future land reclamations.

ABOUT THE AUTHOR

Marloes van Ginkel was born on the 3rd of December 1982. She grew up in Borne, the Netherlands, and she attended High School (VWO) at Twickel College in Hengelo. She studied Civil Engineering at Delft University of Technology and graduated in 2007.

During her studies, Marloes became interested in groundwater and nature's way to make life possible in pure saline environments like oceanic islands by the simple combination of natural density difference between fresh and salt water, gravity and Darcy's Law. In 2005, for her BSc thesis, she investigated the possibilities to increase the freshwater stock in the subsurface of the Dutch Wadden Island Ameland for the drinking water company Vitens, with the aim of using this stock to bridge high freshwater demands in the touristic summer season.

Figure 57: Marloes in Egypt

For her MSc thesis, she went to the Red Sea coast of Egypt to investigate the possibilities to create freshwater stocks in the purely saline coastal subsurface using freshwater from reverse osmosis installations, with the aim of improving the efficiency of RO installations by providing a subsurface stock of fresh water that can be used to bridge demand fluctuations and production interruptions. She introduced a new idea to keep the subsurface stock in place by the same mechanisms that create a natural interface between fresh and salt water in an oceanic island environment, but in a reverse way. She showed that the

freshwater stock can be kept in place by means of saltwater extraction below the injected freshwater volume, which causes the interface to dip down to the centre and allows brackish water to be removed naturally. This idea seems specifically applicable for touristic, coastal, desert like environments where even the subsurface is completely saline and desalination is the only possibility to produce drinking water. She carried out field measurements in several RO plants in resorts along the Red Sea coast in Egypt and worked out the idea by modelling to quantify the possibilities and limits. The research was executed in cooperation with Smidt Groundwater, Van Essen Instruments and Darwish Consultants.

Marloes started her professional career at Royal HaskoningDHV in February 2008 as water resources consultant. She has been involved in many water supply and drought studies, climate change adaptation and water resources management projects, offshore wind farm development, carbon capture and storage, gas exploration, land reclamations, and industrial, port and urban development, both in the Netherlands and abroad.

While working on the drainage design of a land reclamation project off the coast of Nigeria, Marloes became fascinated by the opportunities that the construction of new lands for urban expansion could offer to optimize their subsurface for freshwater storage and recovery, using the same physical mechanisms as were mentioned above, to sustain their freshwater supply. She discussed this idea with professor Theo Olsthoorn and they concluded that the opportunities of this new field were well worth to be properly investigated. Therefore, guided by curiosity, Marloes started her part-time PhD research at Delft University of Technology in July 2011 while also continuing to work as a water resources consultant at Royal HaskoningDHV.

Even before she officially started her PhD trajectory, she presented her ideas for the Red Sea coast at the International Conference on Managed Aquifer Recharge in Abu Dhabi, in 2010, and presented it also at the University of Muscat in a one-day conference in Oman guided by professor Kacimov, who later cited the paper presented in Chapter 4.

She realized that a large improvement of the recovery efficiency of the fresh water would be reached by adding a subsurface flow barrier to prevent the expansion of the outer ring of the freshwater stock beyond recoverable reach. This was worked out by modelling, and experimentally tested in a sand-tank in

the laboratory by TU Delft-student Bas des Tombe for his Minor project, who, for his BSc thesis in 2013, also studied how flow barriers could prevent the salinization of an irrigation well in the Mekong Delta in Vietnam.

She was invited by Clifford Voss, editor-in-chief of Hydrogeology Journal, to write an essay on her idea to utilize the opportunities of land reclamations to design an artificial aquifer with properties that are optimal for subsurface freshwater storage and recovery in a saline environment. The option to create an aquifer with desired properties, completely reverses the normal state-of-affairs where the physical conditions are given, and the design of the freshwater storage has to be adapted to them.

Marloes became involved in the design of one of the new islands to be created in the Jakarta Bay, Indonesia, where the client was interested in the possibilities of subsurface storage and recovery of fresh water for irrigation of the island's future golf course. TU Delft-student Marianne Tijs was invited to design the subsurface of the new island for the purpose of freshwater storage, which she did for her MSc thesis in 2014.

Marloes noticed that the hydraulic properties of land reclamations had nowhere been investigated yet may be crucial for the recoverability of the fresh water through their impact on mixing of fresh and salt water in the subsurface through dispersion and preferential flow paths. She realized that it was necessary to gain insight in dredging technology and sedimentation processes to allow understanding of the internal structure of the porous medium that makes up the land reclamation. Several dredging engineers gladly shared their knowledge about dredging practices. The Port of Rotterdam offered access to the geotechnical data of Maasvlakte II, which she extended with data from the literature of Palm Jumeirah in Dubai, Singapore airport, Hong Kong airport and Hong Kong harbour.

After finalization of her PhD research, she expects to help design and realize sustainable freshwater storage and recovery systems in new land reclamations in the North Sea and elsewhere. She expects that for these to-be-constructed new lands, several ideas of this dissertation can be combined, like the barriers and the saltwater extraction below the freshwater stock that she originally worked out for desalination plants in Egypt.

Peer reviewed articles

Van Ginkel, M., T.N. Olsthoorn. 2019. Distribution of grain size and resulting hydraulic conductivity in land reclamations constructed by bottom dumping, rainbowing and pipeline discharge. Water Resources Management 33: 993, doi: 10.1007/s11269-018-2158-3.

Van Ginkel, M., B. des Tombe, T.N. Olsthoorn, M. Bakker. 2016. Small-scale ASR between flow barriers in a saline aquifer. Groundwater 54-6, 840-850, doi: 10.1111/gwat.12427.

Van Ginkel, M. 2015. Aquifer design for freshwater storage and recovery in artificial islands and coastal expansions. Hydrogeology Journal 23: 615-618, doi: 10.1007/s10040-015-1245-2.

Van Ginkel, M., T.N. Olsthoorn, M. Bakker. 2014. A new operational paradigm for small-scale ASR in saline aquifers. Groundwater 52: 685-693, doi: 10.1111/gwat.12113.

Conference papers and oral presentations

Van Ginkel, M., T.N. Olsthoorn, M.L. Tijs. 2014. Guiding Principles for fresh water lens development, exploitation and maintenance in artificial islands. Salt Water Intrusion Meeting23, Husum, Germany.

Van Ginkel, M., T.N. Olsthoorn 2013. Fresh Water Storage in Land Reclamations; an Integrated Approach in an Early Design Phase. 8th International Symposium on Managed Aquifer Recharge, Beijing, China.

Des Tombe, B.F., M. van Ginkel, T.N. Olsthoorn. 2011. Aquifer Storage Recovery, the Storage Tank Method, Can the Storage Tank Method increase the Recovery Efficiency? Salt Water Intrusion Meeting22, Buzíos, Brazil.

Van Ginkel, M., T.N. Olsthoorn, B. des Tombe. 2011. Using Density Difference to store freshwater in saline aquifers. Salt Water Intrusion Meeting22, Buzíos, Brazil.

Van Ginkel, M., T.N. Olsthoorn, E. Smidt, R. Darwish, S. Rashwan. 2010. Fresh Storage Saline Extraction (FSSE) wells, feasibility of freshwater storage in saline aquifer with a focus on the Red Sea coast, Egypt. 7th International Symposium on Managed Aquifer Recharge, Abu Dhabi, United Arab Emirates.

ACKNOWLEDGEMENT

REFERENCES

Aliewi, A.S., R. Mackay, A. Jayyousi, K. Nasereddin, A. Mushtaha, A. Yaqubi. 2001. Numerical simulation of the movement of saltwater under skimming and scavenger pumping in the Pleistocene aquifer of Gaza and Jericho areas, Palestine. *Transport in Porous Media* 43: 195-212.

Ali, G., M.N. Ashgar, M. Latif, Z. Hussain. 2004. Optimizing operation strategies of scavenger wells in lower Indus Basin of Pakistan. *Agricultural Water Management* 66: 239-249.

Anwar, H.O. 1983. The Effect of a Subsurface Barrier on the Conservation of Freshwater in Coastal Aquifers. *Water Resources Research* 17(10):1257-1265.

Asghar, M.N., S.A. Prathapar, M.S. Shafique. 2002. Extracting relatively-fresh groundwater from aquifers underlain by salty groundwater. *Agricultural Water Management* 52: 119-137.

Bakker, M., G.H.P. Oude Essink, C.D. Langevin. 2004. The Rotating Movement of Three Immiscible Fluids – a Benchmark Problem, *Journal of Hydrology* 287:270-278.

Bakker, M. 2010. Radial Dupuit interface flow to assess the aquifer storage and recovery potential of saltwater aquifers. *Hydrogeology Journal* 18: 107-115.

Bear, J. 1979. *Hydraulics of Groundwater*, Dover Publications, INC., Mineola, New York (edition 2007).

Bear, J. 1972. *Dynamics of Fluids in Porous Media*. Dover, New York, NY.

Boskalis. 2018. *Factsheet Equipment Boskalis*, https://boskalis.com/about-us/fleet-and-equipment.html. Cited 1 March 2018.

Bregman, M., J. Hollander. 2014. *Fresh water storage in a coastal expansion in the North Sea*. Minor Thesis, Delft University of Technology, January 2014, Delft, the Netherlands.

Cederstrom, D.J. 1947. *Artificial recharge of a brackish water well*, Vol. 14, No. 14. Virginia Chamber Commerce, Richmond, pp 31-73.

Chang, M.F., G. Yu, Y.M. Na, V. Choa. 2006. Evaluation of relative density profiles of sand fill at a reclaimed site. *Canadian Geotechnical Journal* 43:903–914.

Chua, L.H.C., E.Y.M. Lo, D.L. Freyberg, E.B. Shuy, T.T. Lim, S.K. Tan, M. Ngonidzashe (2007) Hydrostratigraphy and geochemistry at a coastal sandfill in Singapore. *Hydrogeology Journal* 15:1591-1604.

Coe, A.L. 2002. *The Sedimentary Record of Sea Level Change*. Cambridge University Press, ISBN 0521538424, 287 pp, Cambridge, New York, USA.

Dagan, G., A. Fiori, I. Jankovic. 2013. Upscaling of Flow in Heterogeneous Porous Formations: Critical Examination and Issues of Principle. *Advances in Water Resources* 51:67-85.

De Josselin De Jong, G. 1960. Singularity Distributions for the Analysis of Multiple Fluid Flow through Porous Media. *Journal of Geophysical Research* 65: 3739-3758.

De Louw, P.G.B., S. Eeman, B. Siemon, B.R. Voortman, J. Gunnink, E.S. van Baaren, G.H.P. Oude Essink. 2011. Shallow rainwater lenses in deltaic areas with saline seepage. *Hydrology and Earth System Sciences* 15: 3659-3678.

De Louw, P.G.B, S. Eeman, G.H.P. Oude Essink, E. Vermue, V.E.A. Post. 2013. Rainwater lens dynamics and mixing between infiltrating rainwater and upward saline groundwater seepage beneath a tile-drained agricultural field. *Journal of Hydrology* 501: 133-145.

Des Tombe, B.F., M. van Ginkel, T.N. Olsthoorn. 2011. Aquifer Storage Recovery, the Storage Tank Method, Can the Storage Tank Method increase the Recovery Efficiency? In G. Cardoso da Silva Jr & D. Montenegro (Eds.), *Proceedings Salt Water Intrusion Meeting 22*, Buzíos, Brazil.

Des Tombe, B.F. 2013. *Finding a feasible solution to prevent salinization of the well, Bà Ria Vung Tàu, Vietnam*. BSc. Thesis, Delft University of Technology, June 17, 2013, Delft, the Netherlands.

De Wit, L. 2015. *3D CFD modelling of overflow dredging plumes*. PhD. thesis, Delft University of Technology, January 14, 2015. ISBN 9789461864086, 178 pp, Delft, the Netherlands.

Dillon, P., P. Pavelic, S. Toze, S. Rinck-Pfeiffer, R. Martin, A. Knapton, D. Pidsley. 2006. Role of aquifer storage in water reuse. *Desalination* 188: 123-134.

Drabbe, J. and W. Badon Ghijben. 1889. Nota in verband met de voorgenomen putboring nabij Amsterdam. *Tijdschrift van het Koninklijk Instituut van Ingenieurs* 1888-1889: 8-22.

Eeman, S., A. Leijnse, P.A.C. Raats, S.E.A.T.M. van der Zee. 2011. Analysis of the Thickness of a Fresh Water Lens and of the Transition Zone between this Lens and Upwelling Saline Water. *Advances in Water Resources* 34:291-302.

Eeman, S., E.A.T.M. van der Zee, A Leijnse, P.G.B. de Louw, C. Maas. 2012. Response to recharge variation of thin rainwater lenses and their mixing zone with underlying saline groundwater. *Hydrology and Earth System Sciences* 16: 3535-3549.

Esmail, O.J., O.K. Kimbler. 1967. Investigation of the technical feasibility of storing freshwater in saline aquifers. *Water Resources Research* 3, No. 3: 686-695.

Fiori, A., I. Jankovic. 2012. On Preferential Flow, Channeling and Connectivity in Heterogeneous Porous Formations. *Mathematical Geosciences* 44:133-145.

Hallworth, M.A., J.C. Phillips, H.E. Huppert, R.S.J. Sparks. 1993. Entrainment in turbulent gravity currents. *Nature* 362:829-831.

Heezing, B.C., M. Ewing. 1952. Turbidity currents and submarine slumps, and the 1929 Grand Banks earthquake. *American Journal of Science* 250:849-873.

Herzberg, B. 1901. Die Wasserversorgung einiger Nordseebäder. *Journal für Gasbeleuchtung und verwandte Beleuchtungsarten sowie für Wasserversorgung* 44: 815-819, 841-844.

Huizer, S., G.H.P. Oude Essink, M.F.P. Bierkens. 2017. Fresh groundwater resources in a large sand replenishment. *Hydrology and Earth System Sciences* 20:3149-3166.

Huppert, H.E., J.E. Simpson. 1980. The slumping of gravity currents. *Journal of Fluid Mechanics* 99(4):785-799.

Intergovernmental panel on climate change. 2013. *IPCC Fifth Assessment Report*: Climate Change 2013.

Jiao, J.J., S. Nandy, H. Li. 2001. Analytical studies on the impact of land reclamation on groundwater flow. *Groundwater* 39 (6):912-920.

Jiao, J.J., X.S. Wang, S. Nandy. 2006. Preliminary assessment of the impacts of deep foundations and land reclamation on groundwater flow in a coastal area in Hong Kong, China. *Hydrogeology Journal* 14:100-114.

Kaleris, V.K., A.I. Ziogas. 2013. The effect of cutoff walls on saltwater intrusion and groundwater extraction in coastal aquifers. *Journal of Hydrology* 476:370-383.

Koop, S.H.A., C.J. van Leeuwen. 2017. The challenges of water, waste and climate change in cities. *Environment Development and Sustainability* 19: 385-418.

Kumar, A., O.K. Kimbler. 1970. Effect of dispersion, gravitational segregation, and formation stratification on the recovery of freshwater stored in saline aquifers. *Water Resources Research* 6, No. 6: 1689-1700.

Langevin, C.D., D.T. Thorne, Jr., A.M. Dausman, M.C. Sukop, W. Guo. 2008. *SEAWAT Version 4: A Computer Program for Simulation of Multi-Species Solute and Heat Transport: U.S. Geological Survey Techniques and Methods Book 6*, Chapter A22, 39 p.

Laumann, S., J. Zhou, T. Heimovaara. 2018. Laboratory investigations on the interaction between aluminum and organic matter and its impact on soil permeability. *Geophysical Research Abstracts of the 20th EGU General Assembly*, Vienna, Austria, 8-13 April 2018. EGU2018-14762.

Laumann, S., J. Zhou, T. Heimovaara. 2016. Aluminum-organic matter precipitation as a geoengineering tool for in situ permeability reduction in a porous media. *Abstract 26th Goldschmidt Conference – Yokohama*, 26 Jun-1Jul 2016, Japan, p1689.

Lee, K.M., C.K. Shen, D.H.K. Leung, J.K. Mitchell. 1999. Effects of Placement Method on Geotechnical Behavior of Hydraulic Fill Sands. *Journal of Geotechnical and Geoenvironmental Engineering* 125(10):832-846.

Lee, K.M. 2001. Influence of placement method on the cone penetration resistance of hydraulically placed sand fills. *Canadian Geotechnical Journal* 38:592-607.

Lees A., D.A. King, S. Mimms. 2013. Palm Jumeirah, Dubai: cone penetrometer testing data from the carbonate sand fill. *In Proceedings of the Institution of Civil Engineers Geotechnical Engineering* 166(3):253-267.

Loucks, D.P. (2017) Managing water as a critical component of a changing world. *Water Resources Management* 31:2905.

Lowe, D.R. 1982. Sediment gravity flows: II. Depositional models with special reference to the deposits of high density turbidity currents. *Journal of Sediment Research* 52(1):279-297.

Lowry, C.S., M.P. Anderson. 2006. An assessment of aquifer storage recovery using ground water flow models. *Groundwater* 44, No. 5: 661-667.

Luyun, R. Jr., K. Momii, K. Nakagawa. 2011. Effects of Recharge Wells and Flow Barriers on Seawater Intrusion. *Groundwater* 49(2):239-249.

Maliva, R.G., W. Guo, T.M. Missimer. 2006. Aquifer storage and recovery: recent hydrogeological advances and system performance. *Water Environment Research* 78(13), 2428-2435.

Maliva R.G., T.M. Missimer. 2010. *Aquifer Storage and Recovery and Managed Aquifer Recharge Using Wells: Planning, Hydrogeology, Design and Operation. Methods in Water Resources Evaluation Series No. 2*. Houston: Schlumberger Water Services.

Mastbergen, D.R., A. Bezuijen. 1988. *Het storten van zand onder water 5: Zand Waterstromingen, Verslag experimentele vervolgstudie middelgrof zand (The dumping of sand under water 5: Sand water mixture flows. Report experimental follow-up study medium sand)* Tech. Rep. Bagt. 420/Z261/CO 294750, Grondmechanica Delft, WL|Delft Hydraulics, the Netherlands.

Matheron, G. 1963. Principles of Geostatistics. *Economic Geology* 58(8):1246-1266.

Merkens, J.L., L. Reimann, J. Hinkel, A.T. Vafeidis. 2016. Gridded population projections for the coastal zone under the Shared Socioeconomic Pathways. *Global and Planetary Change* 145: 57-66.

Merritt, M.L. 1986. Recovering freshwater stored in saline limestone aquifers. *Groundwater* 24, No. 4: 516-529.

Middleton, G.V. 1993. Sediment deposition from turbidity currents. *Annual Review of Earth and Planetary Sciences* 21:89-114.

Miedema, S.A., R.C. Ramsdell. 2011. Hydraulic transport of sand/shell mixtures in relation with the critical velocity. *Terra et Aqua 122*. International Association of Dredging Companies, The Hague, The Netherlands.

Misut P.E., C.I. Voss. 2007. Freshwater-Saltwater Transition Zone Movement during Aquifer Storage and Recovery Cycles in Brooklyn and Queens, New York City, USA. *Journal of Hydrology* 337: 87-103.

Morgenstern, N.R., A.A.G. Kupper. 1988. Hydraulic fill structures a perspective. In *Proceedings of the ASCE Conference on Hydraulic Fill Structures*, Fort Collins, Colorado, pp. 1–31.

Neuman, B., A.T. Vafeidis, J. Zimmermann, R.J. Nicholis. 2015. Future coastal population growth and exposure to sea-level rise and coastal flooding – a global assessment. *PLoS ONE* 10:3.

Olsthoorn, T.N. 1977. In Nederlandse zandformaties zijn het doorstroomde en het totale porievolume aan elkaar gelijk. *H_2O* 10(5): 118-122.

Olsthoorn, T.N. 2013. http://code.google.com/p/mflab.

Olver, F.W.J., D.W. Lozier, R.F. Boisvert, C.W. Clark, editors. 2010. *NIST Handbook of Mathematical Functions*. Cambridge University Press, New York, NY. Print companion to NIST Digital Library of Mathematical Functions. http://dlmf.nist.gov/, Release 1.0.5 of 2012-10-01 (http://dlmf.nist.gov/7.2.E5).

Pennink, J.M.K. 1915. *Grondwater Stroombanen (motions of groundwater – results of researches made in the years 1904 and 1905, into the form of lines of flow for sub-soil water motion in pure sand)*. Stadsdrukkery Amsterdam, the Netherlands, 151 pp.

Pham, V.P., L.A. van Paassen, W.R.L. van der Star, T.J. Heimovaara. 2018. Evaluating strategies to improve process efficiency of denitrification-based MICP. *Journal of Geotechnical and Geoenvironmental Engineering* 144(8).

Pham, V., A. Nakano, W.R.L. van der Star, T. Heimovaara, L. van Paassen. 2016. Applying MICP by denitrification in soils: a process analysis. *Environmental Geotechnics* 5(2): 79-93.

Pyne, R.D.G. 1995. *Aquifer Storage Recovery: A Guide to Groundwater Recharge through Wells*. ASR Press 2nd edition (2005), ISBN 0977433706, 608 pp, Gainesville, Florida USA.

Pyrcz, M.J., C.V. Deutsch. 2003. The Whole Story on the Hole Effect. *Newsletter Geostatistical Association Australasia* 18:3-5.

Richardson, J.F., W.N. Zaki. 1954. *Sedimentation and fluidisation: Part I.* Transactions of the American Institute of Chemical Engineers 32:35-53.

Robertson, P.K. 1989. Soil classification using the cone penetration test. *Canadian Geotechnical Journal* 27:151-158.

Saeed, M.M., M. Ashraf. 2005. Feasible design and operational guidelines for skimming wells in the Indus Basin, Pakistan. *Agricultural Water Management* 74: 165-188.

Selley, R.C. 2000. *Applied Sedimentology*. Academic Press 2nd edition, ISBN 978-0-12-636375-3, 523 pp. London, United Kingdom.

Shen, C.K., K.M. Lee. 1995. *Hydraulic fill performance in Hong Kong. GEO Rep. 40.* Geotechnical Engineering Office, Civil Engineering Department, Government of the Hong Kong Special Administrative Region, Hong Kong.

Sladen, J.A., K.J. Hewitt. 1989. Influence of placement method on the in situ density of hydraulic sand fills. *Canadian Geotechnical Journal* 26:453-466.

Stoeckl, L., M. Walther, T. Graf. 2016. A new numerical benchmark of a freshwater lens. *Water Resources Research* 52: 2474-2489.

Stoeckl, L., G. Houben. 2012. Flow Dynamics and Age Stratification of Freshwater Lenses: Experiments and Modeling. *Journal of Hydrology* 458-459: 9 15.

Sufi, A.B., M. Latif, G.V. Skogerboe. 1998. Simulating skimming well techniques for sustainable exploitation of groundwater. *Irrigation and Drainage Systems* 12: 203-226.

Tijs, M.L. 2014. *Subsurface Freshwater Storage & Recovery in Artificial Islands, case study of Pluit City Land Reclamation Jakarta, Indonesia.* Master's thesis, Delft University of Technology, Civil Engineering, 128 pp, Delft, the Netherlands.

United Nations. 2010. *UN Atlas of the Oceans*. United Nations, Rome, Italy.

Van Ginkel, M., B. des Tombe, T.N. Olsthoorn, M. Bakker. 2016. Small-scale ASR between flow barriers in a saline aquifer. *Groundwater* 54-6, 840-850.

Van Ginkel, M. 2015. Aquifer design for freshwater storage and recovery in artificial islands and coastal expansions. *Hydrogeology Journal* 23: 615-618.

Van Ginkel, M., T.N. Olsthoorn, M. Bakker. 2014. A New Operational Paradigm for Small-Scale ASR in Saline Aquifers. *Groundwater* 52: 685-693.

Van Ginkel, M., T.N. Olsthoorn, E. Smidt, R. Darwish, S. Rashwan. 2010. Fresh Storage Saline Extraction (FSSE) wells, feasibility of freshwater storage in saline aquifer with a focus on the Red Sea coast, Egypt. *In 7th Annual International Symposium on Managed Aquifer Recharge*, 9 to 13 October 2010, Abu Dhabi. 7th Annual International Symposium on Managed Aquifer Recharge.

Van Oord. 2018. *Factsheet Trailing Suction Hopper Dredgers Van Oord*: https://www.vanoord.com/activities/trailing-suction-hopper-dredger. Cited 1 March 2018.

Van Rhee, C. 2002. *On the sedimentation process in a Trailing Suction Hopper Dredger.* Ph.D. thesis, Delft University of Technology, December 3, 2002, 246 pp, Delft, the Netherlands.

Van t Hoff, J., A.N. Van der Kolff. 2012. *Hydraulic Fill Manual*. CRC Press/Balkema Taylor & Francis Group 1e edition (2012). ISBN 9780415698443, 642 pp, Leiden, the Netherlands.

Vessies, W.C.N. 2012. *Relative Density Differences of a Sand Fill*. Master's thesis, Delft University of Technology, Civil Engineering, 260 pp, Delft, the Netherlands.

Verruijt, A. 1971. Steady Dispersion across an Interface in a Porous Medium. *Journal of Hydrology* 14:337-347.

Ward, J.D., C.T. Simmons, P.J. Dillon, P. Pavelic. 2009. Integrated assessment of lateral flow, density effects and dispersion in aquifer storage and recovery. *Journal of Hydrology* 370: 83-99.

Ward, J.D., C.T. Simmons, P.J. Dillon. 2008. Variable-density modeling of multiple-cycle aquifer storage and recovery (ASR): importance of anisotropy and layered heterogeneity in brackish aquifers. *Journal of Hydrology* 356: 93-105.

Ward, J.D., C.T. Simmons, P.J. Dillon. 2007. A theoretical analysis of mixed convection in aquifer storage and recovery: how important are density effects? *Journal of Hydrology* 343, No. 3-4: 169-186.

Zhou, J., S. Laumann, T. Heimovaara. 2018. In situ precipitation of aluminum and organic matter as a geo-engineering tool to reduce soil permeability: a field test. *Geophysical Research Abstracts of the 20th EGU General Assembly*, Vienna, Austria, 8-13 April 2018. EGU2018-14628.

Zuurbier, K.G., W.J. Zaadnoordijk, P.J. Stuyfzand. 2014. How Multiple Partially Penetrating Wells improve the Freshwater Recovery of Coastal Aquifer Storage and Recovery (ASR) Systems: A Field and Modeling Study. *Journal of Hydrology* 509:430-441.

Zuurbier, K.G., J.W. Kooiman, M.M.A. Groen, B. Maas, P.J. Stuyfzand. 2015. Enabling Successful Aquifer Storage and Recovery of Freshwater Using Horizontal

Directional Drilled Wells in Coastal Aquifers. *Journal of Hydrologic Engineering* 20:3.

Zuurbier, K.G., K.J. Raat, M. Paalman, A.T. Oosterhof, P.J. Stuyfzand. 2017. How subsurface water technologies (SWT) can provide robust, effective and cost-efficient solutions for freshwater management in coastal zones. *Water Resources Management* 31:671-687.